

論文 / 著書情報
Article / Book Information

題目(和文)	光合成生物におけるモノガラクトシルジアシルグリセロール合成経路の進化とその機能についての研究
Title(English)	Studies on evolution and functions of monogalactosyldiacylglycerol synthesis pathways in phototrophs
著者(和文)	湯澤優一
Author(English)	Yuichi Yuzawa
出典(和文)	学位:博士(理学), 学位授与機関:東京工業大学, 報告番号:甲第8635号, 授与年月日:2012年3月26日, 学位の種別:課程博士, 審査員:太田 啓之
Citation(English)	Degree:Doctor (Science), Conferring organization: Tokyo Institute of Technology, Report number:甲第8635号, Conferred date:2012/3/26, Degree Type:Course doctor, Examiner:
学位種別(和文)	博士論文
Type(English)	Doctoral Thesis

**Studies on Evolution and Functions of
Monogalactosyldiacylglycerol Synthesis Pathways in Phototrophs**

A Doctoral Dissertation

Yuichi Yuzawa

Graduate School of Bioscience and Biotechnology,

Tokyo Institute of Technology

2011



Contents

Chapter I	General Introduction	1
	References	8
Chapter II	The analyses for the plant-type pathway for MGDG synthesis	
	Introduction	14
II-1	Comprehensive phylogenetic analysis of MGDG synthase homologs	
	Results and Discussion	16
	Materials and Methods	38
	References	43
II-2	The estimation of divergence point type A and B MGDG synthases	
	Results and Discussion	48
	Materials and Methods	56
	References	58
Chapter III	The analyses for the cyanobacterial pathway for MGDG synthesis	
	Introduction	61
	Results	63
	Discussion	85
	Materials and Methods	97
	References	102
Chapter IV	General Conclusion	111
	References	115
Acknowledgments		117

Abbreviations

AtMGD1	Arabidopsis MGDG synthase 1
CsMGD	Cucumber MGDG synthase
CtMgdA	Chlorobaculum MGDG synthase
DAG	diacylglycerol
DGDG	digalactosyldiacylglycerol
DGlcDG	diglucosyldiacylglycerol
DPG	diphosphatidylglycerol
DPH	1, 6-diphenyl-1, 3, 5-hexatriene
GlcGalDG	glucosylgalactosyldiacylglycerol
Het	heterozygous line of $\Delta mglcd$
MGDG	monogalactosyldiacylglycerol
MGD	MGDG synthase
MgdA-CP	pSL1211:: <i>ctmgdA</i> / $\Delta mglcd$
MGD1-CP	pSL1211:: <i>AtMGD1</i> / $\Delta mglcd$
MGlcDG	monoglucosyldiacylglycerol
MGlcD	MGlcDG synthase
MGlcD-CP	pSL1211:: <i>mglcd</i> / $\Delta mglcd$
NPQ	non-photochemical quenching
PSI	photosystem I
PSII	photosystem II
PC	phosphatidylcholine
PE	phosphatidylethanolamine
PG	phosphatidylglycerol
PI	phosphatidylinositol
qP	photochemical quenching
RcDGlcD	<i>R. castenholzii</i> DGlcDG synthase
RcMGD	<i>R. castenholzii</i> MGDG synthase
RcMGlcD	<i>R. castenholzii</i> MGlcDG synthase
SG	sterolglucoside
SQDG	sulfoquinovosyldiacylglycerol
TLC	thin layer chromatography
UDP-Gal	uridine diphosphate galactose
UDP-Glc	uridine diphosphate glucose
UL	unknown lipid

Chapter I

General Introduction

It is generally accepted that chloroplasts evolved from a photosynthetic prokaryote that entered into an endosymbiotic relationship with a non-photosynthetic host cell (McFadden, 2001). It is also accepted that this photosynthetic prokaryote was an ancestor of the phylum *Cyanobacteria* (Nelissen et al., 1995). It is plausible, therefore, that most of the genes encoding chloroplast-localized proteins, including components of the photosynthetic machinery, are derived from this ancestral cyanobacterium (Martin et al., 2002).

Cyanobacteria and chloroplasts of higher plants share common features in many biological contexts, including photosynthesis and cell division (Wolfe et al., 1994, Osteryoung and Vierling, 1995). In addition, the lipid compositions of biological membranes (photosynthetic membranes in particular) show high degrees of similarity between cyanobacteria and chloroplasts (Fig. I-1; Joyard et al., 1998). Thylakoid membranes within a chloroplast are ~80% galactolipids, whereas the biological membranes of prokaryotic and eukaryotic cells are generally composed of phospholipids. Monogalactosyldiacylglycerol (MGDG) is the most abundant lipid in thylakoid membranes of both cyanobacteria and higher plants. Thus, it is likely that genes encoding enzymes of the galactolipid synthesis pathways were acquired in

higher plants through the endosymbiotic event.

MGDG is essential for oxygenic phototrophs. Crystal structure analyses of cyanobacteria have revealed that MGDG tightly binds to photosystem complexes, suggesting that MGDG is an important component of the photosynthetic machinery (Jordan et al., 2001, Loll et al., 2005). Furthermore, in MGDG-deficient *Arabidopsis thaliana*, photosynthetic activity is completely absent, and development arrests at the early seedling stage (Kobayashi et al., 2007). Thus, MGDG is involved in both photosynthesis and chloroplast development.

The pathways for MGDG synthesis in cyanobacteria and higher plants, however, are quite different (Fig. I-2; Sato and Murata, 1982, Awai et al., 2006). Higher plants utilize uridine diphosphate galactose (UDP-Gal) and diacylglycerol (DAG) to synthesize MGDG. In contrast, cyanobacteria first synthesize monoglucosyldiacylglycerol (MGlcDG) using uridine diphosphate glucose (UDP-Glc) and DAG, which is subsequently epimerized to produce MGDG. In addition, sequence comparison indicates that MGDG synthase (MGD) genes belong to the glycosyltransferase family 28 (GT28), whereas MGlcDG synthase (MGlcD) genes belong to the family GT2 (according to the Carbohydrate-Active Enzymes database (www.cazy.org); Shimojima et al., 1997, Dörmann and Benning, 2002, Awai et al., 2006). In *Viridiplantae* (green algae and land plants), therefore, the origin of the pathway for MGDG synthesis is not clear. In this study, as MGDG is essential for photosynthesis, I investigated the evolution and functions of both MGDG synthesis pathways which could potentially

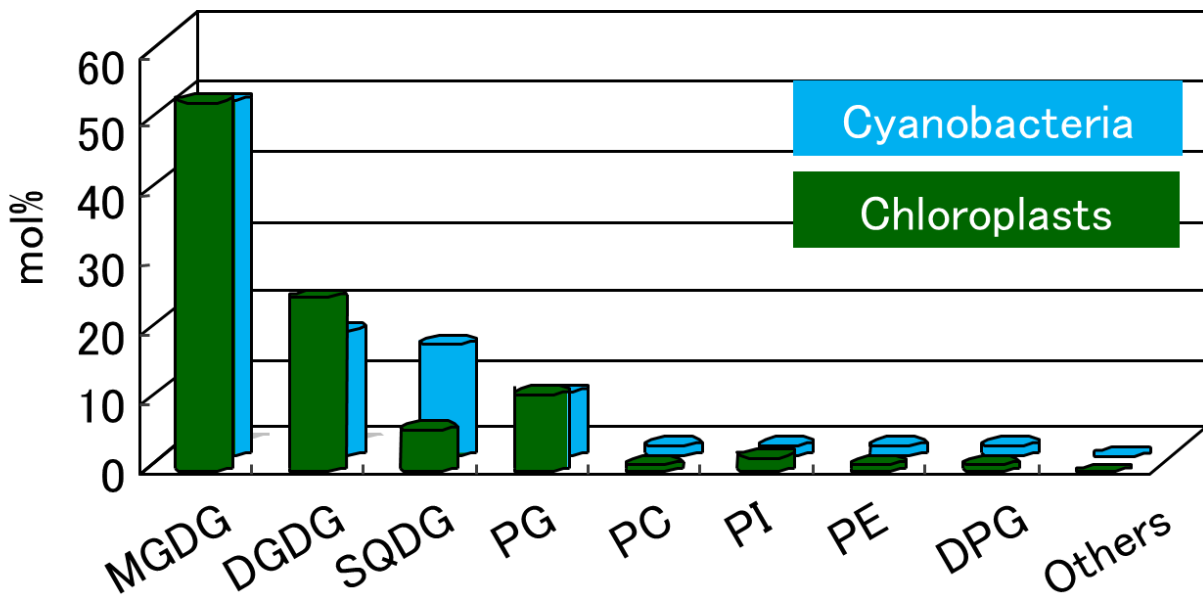


FIG. I-1. Lipid compositions of chloroplasts and cyanobacteria (Joyard et al., 1998). DGDG, digalactosyldiacylglycerol; SQDG, sulfoquinovosyldiacylglycerol; PG, phosphatidylglycerol; PC, phosphatidylcholine; PE, phosphatidylethanolamine; DPG, diphosphatidylglycerol.

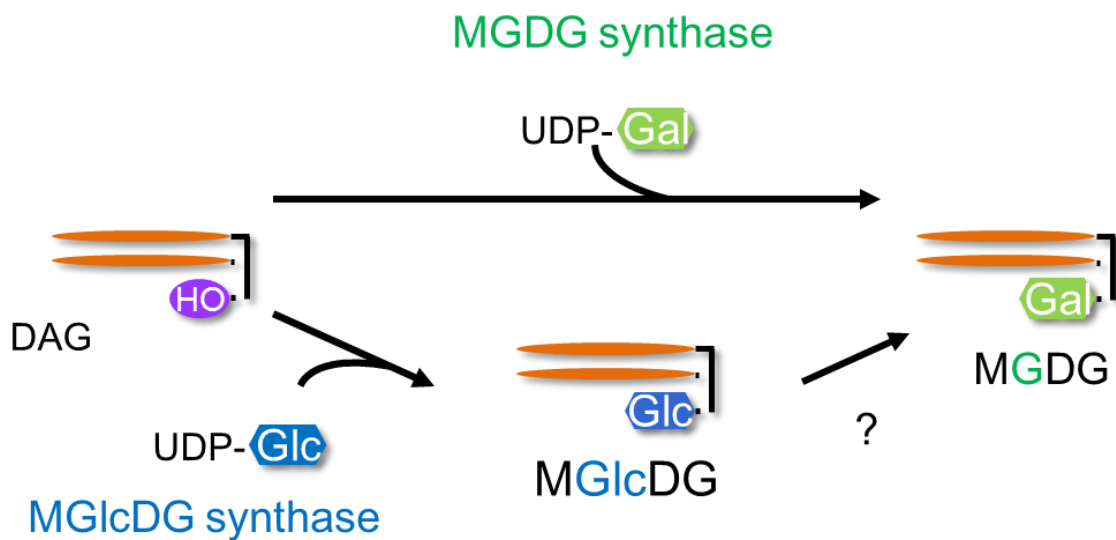


FIG. I-2. Scheme for MGDG synthesis (Sato and Murata, 1982, Awai et al., 2006). (A) In cyanobacteria, monoglucosyldiacylglycerol (MGlcDG) is synthesized from diacylglycerol (DAG) and UDP-Glucose (UDP-Glc). Then, MGlcDG is epimerized to MGDG. (B) In plants, MGDG is synthesized from DAG and UDP-Galactose (UDP-Gal) (Shimajima et al., 1997).

reveal important details concerning phototroph evolution in general.

In Chapter II-1, I investigated the plant-type pathway for MGDG synthesis. MGDG is found in some anoxygenic phototrophs as well as oxygenic phototrophs (Hözl and Dörmann, 2007). *Chloroflexi* is an anoxygenic phototrophic group of bacteria whose divergence preceded that of *Cyanobacteria* (Woese, 1987, Gupta et al., 1999, Xiong et al., 2000). The MGD homolog of *Chloroflexus aurantiacus*, a member of the phylum *Chloroflexi* (Pierson and Castenholz, 1974), belongs to the GT28 family and one of the encoded proteins has a MGDG producing activity (Hözl et al., 2005). However, phylogenetic relationship between these prokaryotic MGD homologs and higher plant MGDs had not been well established. Here, I performed comprehensive phylogenetic analyses on MGD homologs from both prokaryotic and eukaryotic organisms, and revealed that eukaryotic MGDs including *Viridiplantae*, *Rhodophyta*, and *Heterokontophyta* are monophyly and probably have a single ancestor. Moreover, I found that some of *Chloroflexi* MGD homologs are highly associated with the eukaryotic MGDs. Analyses of the sugar specificity and anomeric configuration of the sugar head groups for three MGD homologs in *Chloroflexi*, *Roseiflexus castenholzii* (Hanada et al., 2002), revealed that only one of the MGD homologs in *R. castenholzii* exhibits a genuine MGD synthase activity, suggesting a possible origin of higher plant MGDG synthases.

To understand plastid evolution, it is also important to characterize MGD gene

duplication. In *A. thaliana*, there are 2 types of MGD enzymes, type A (MGD1) and type B (MGD2 and MGD3; Fig. I-3, Awai et al., 2001). Type A MGDs reside in membranes of the inner envelope and, under normal circumstances, generate most MGDGs found in the chloroplast. In contrast, type B MGDs are found in membranes of the outer envelope and are involved in membrane remodeling under phosphate-starved conditions (Fig. I-4, Kobayashi et al., 2009a, b). MGDG synthesized in this context is converted into digalactosyldiacylglycerol (DGDG), which is used to generate cell membranes when phospholipids are not available. As type B MGDs are only found in angiosperms, this type of membrane lipid remodeling is an important characteristic of angiosperms (Andersson et al., 2003, Gaude et al., 2004, Jouhet et al., 2004, Russo et al., 2007). Under normal growth conditions, interestingly, expression of type B MGD is low in leaves but high in floral organs (Kobayashi et al., 2004). Thus, it is possible that the emergence of type B MGDs was an important step toward *Angiospermae* (angiosperm) or *Spermatophyta* (seed plant) evolution. Two types of MGDs are essential for plants to survive under low phosphate conditions, and yet a detailed analysis of MGD gene divergence has not been reported. In Chapter II-2, I present detailed data concerning MGD gene divergence. My data provide a new insight into the plastid evolution based on the biogenesis of photosynthetic membranes.

In Chapter III, I investigated the functions of MGlcDG in cyanobacteria. In order to

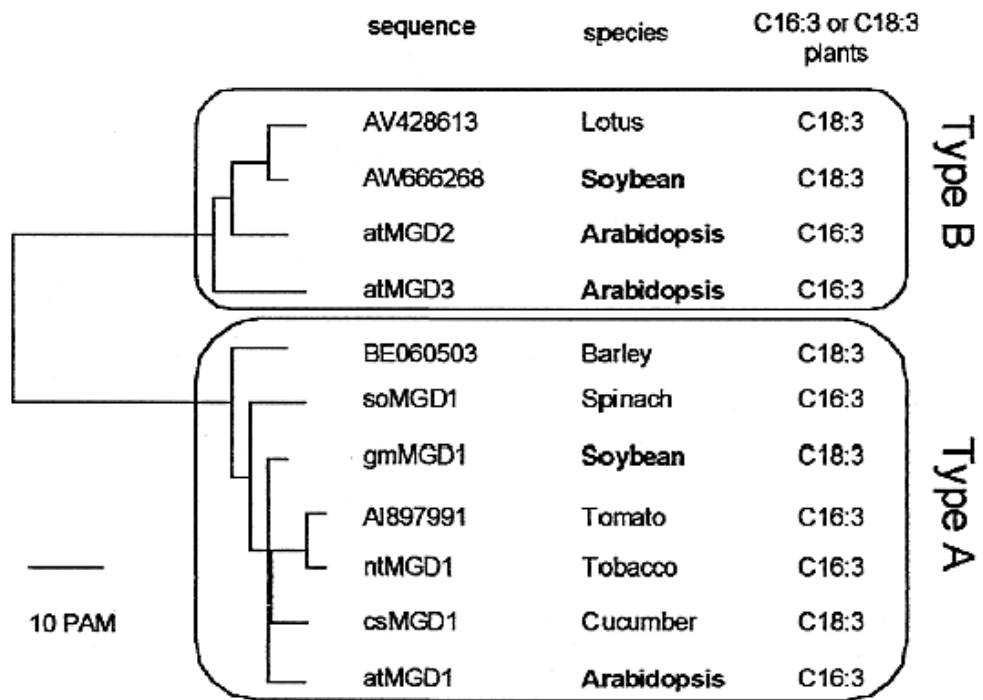


FIG. I-3. Unrooted phylogenetic tree of MGDG synthases (Awai et al., 2001).

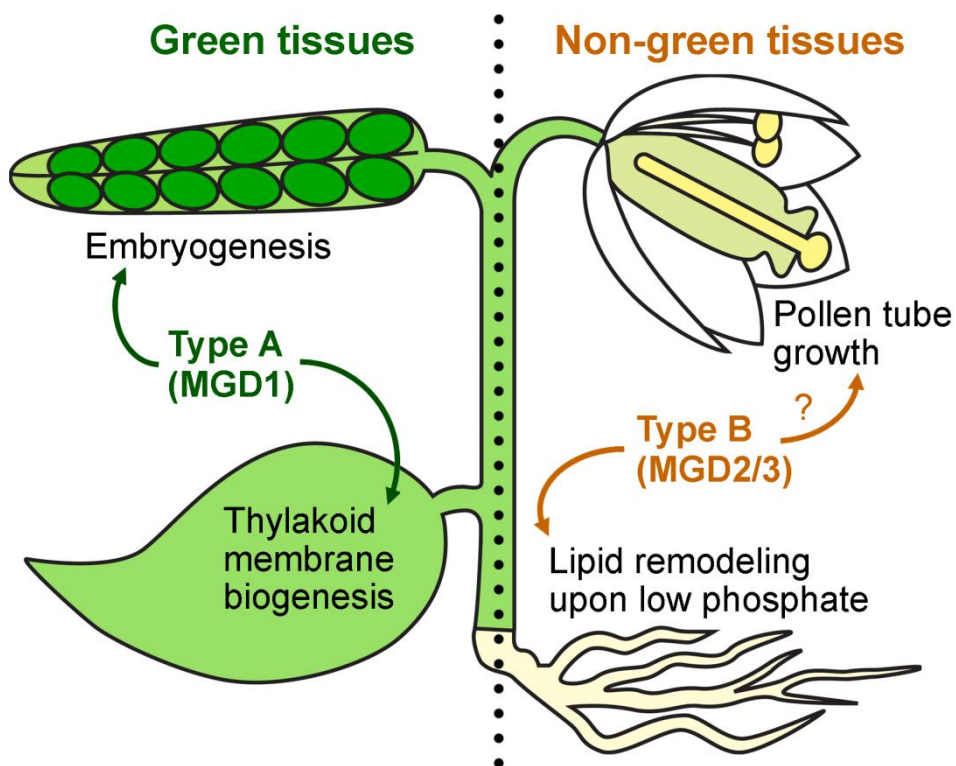


FIG. I-4. The physiological functions of Arabidopsis type A and type B MGD (Kobayashi et al., 2009b).

clarify the role of MGlcDG, I performed complementation of MGlcDG synthase (MGlcD) mutation by Arabidopsis MGDG synthase 1 (AtMGD1) in *Synechocystis* sp. PCC 6803. The complemented strain showed a significant reduction of MGlcDG synthetic activity and no accumulation of MGlcDG. In this chapter, influence of MGlcDG deficiency in *Synechocystis* was discussed.

References

- Andersson, M.X., Stridh, M.H., Larsson, K.E., Liljenberg, C., and Sandelius, A.S. 2003, Phosphate-deficient oat replaces a major portion of the plasma membrane phospholipids with the galactolipid digalactosyldiacylglycerol, *FEBS Lett.*, 537, 128–132.
- Awai, K., Kakimoto, T., Awai, C., Kaneko, T., Nakamura, Y., Takamiya, K., Wada, H., and Ohta, H. 2006, Comparative genomic analysis revealed a gene for monoglucosyldiacylglycerol synthase, an enzyme for photosynthetic membrane lipid synthesis in cyanobacteria, *Plant Physiol.*, 141, 1120–1127.
- Awai, K., Maréchal, E., Block, M.A., Brun, D., Masuda, T., Shimada, H., Takamiya, K., Ohta, H., and Joyard, J. 2001, Two types of MGDG synthase genes, found widely in both 16:3 and 18:3 plants, differentially mediate galactolipid syntheses in photosynthetic and nonphotosynthetic tissues in *Arabidopsis thaliana*, *Proc. Natl. Acad. Sci. U. S. A.*, 98, 10960–10965.
- Dörmann, P., and Benning, C. 2002, Galactolipids rule in seed plants, *Trends. Plant. Sci.*, 7, 112–118.

Gaude, N., Tippmann, H., Flemetakis, E., Katinakis, P., Udvardi, M., and Dörmann, P. 2004,

The galactolipid digalactosyldiacylglycerol accumulates in the peribacteroid membrane of nitrogen-fixing nodules of soybean and Lotus, *J. Biol. Chem.*, 279, 34624–34630.

Gupta, R.S., Mukhtar, T., and Singh, B. 1999, Evolutionary relationships among

photosynthetic prokaryotes (Heliobacterium chlorum, Chloroflexus aurantiacus,

cyanobacteria, Chlorobium tepidum and proteobacteria): implications regarding the origin of photosynthesis, *Mol. Microbiol.*, 32, 893–906.

Hanada, S., Takaichi, S., Matsuura, K., and Nakamura, K. 2002, *Roseiflexus castenholzii* gen.

nov., sp. nov., a thermophilic, filamentous, photosynthetic bacterium that lacks chlorosomes,

Int. J. Syst. Evol. Microbiol., 52, 187–193.

Hözl, G., and Dörmann, P. 2007, Structure and function of glycolipids in plants and

bacteria, *Prog. Lipid. Res.*, 46, 225–243.

Hözl, G., Zähringer, U., Warnecke, D., and Heinz, E. 2005, Glycoengineering of

cyanobacterial thylakoid membranes for future studies on the role of glycolipids in

photosynthesis, *Plant Cell Physiol.*, 46, 1766–1778.

Jordan, P., Fromme, P., Witt, H.T., Klukas, O., Saenger, W., and Krauss, N. 2001, Three-dimensional structure of cyanobacterial photosystem I at 2.5 Å resolution, *Nature*, 411, 909–917.

Jouhet, J., Maréchal, E., Baldan, B., Bligny, R., Joyard, J., and Block, M.A. 2004, Phosphate deprivation induces transfer of DGDG galactolipid from chloroplast to mitochondria, *J. Cell Biol.*, 167, 863–874.

Joyard, J., Marechal, E., Miegé, C., Block, M.A., Dorne, A.J., and Douce, R. 1998, Structure, distribution and biosynthesis of glycerolipids from higher plant chloroplasts, In *Lipid in Photosynthesis: Structure, Function and Genetics* (Siegenthaler PA and Murata N, eds), Dordrecht, Kluwer Academic Publishers, pp. 21–52.

Kobayashi, K., Awai, K., Nakamura, M., Nagatani, A., Masuda, T., and Ohta, H. 2009a, Type-B monogalactosyldiacylglycerol synthases are involved in phosphate starvation-induced lipid remodeling, and are crucial for low-phosphate adaptation, *Plant J.*, 57, 322–331.

Kobayashi, K., Awai, K., Takamiya, K., and Ohta, H. 2004, Arabidopsis type B monogalactosyldiacylglycerol synthase genes are expressed during pollen tube growth and induced by phosphate starvation, *Plant Physiol.*, 134, 640–648.

Kobayashi, K., Kondo, M., Fukuda, H., Nishimura, M., and Ohta, H. 2007, Galactolipid synthesis in chloroplast inner envelope is essential for proper thylakoid biogenesis, photosynthesis, and embryogenesis, *Proc. Natl. Acad. Sci. U. S. A.*, 104, 17216–17221.

Kobayashi, K., Nakamura, Y., and Ohta, H. 2009b, Type A and type B monogalactosyldiacylglycerol synthases are spatially and functionally separated in the plastids of higher plants, *Plant Physiol. Biochem.*, 47, 518-525.

Loll, B., Kern, J., Saenger, W., Zouni, A., and Biesiadka, J. 2005, Towards complete cofactor arrangement in the 3.0 Å resolution structure of photosystem II, *Nature*, 438, 1040–1044.

Martin, W., Rujan, T., Richly, E., Hansen, A., Cornelsen, S., Lins, T., Leister, D., Stoebe, B., Hasegawa, M., and Penny, D. 2002, Evolutionary analysis of *Arabidopsis*, cyanobacterial, and chloroplast genomes reveals plastid phylogeny and thousands of cyanobacterial genes in the nucleus, *Proc. Natl. Acad. Sci. U. S. A.*, 99, 12246–12251.

McFadden, G.I. 2001, Primary and secondary endosymbiosis and the origin of plastids, *J. Phycol.*, 37, 951–959.

Nelissen, B., Van de Peer, Y., Wilmotte, A., and De Wachter, R. 1995, An early origin of plastids within the cyanobacterial divergence is suggested by evolutionary trees based on complete 16S rRNA sequences, *Mol. Biol. Evol.*, 12, 1166–1173.

Osteryoung, K.W., and Vierling, E. 1995, Conserved cell and organelle division, *Nature*, 376, 473–474

Pierson, B.K., and Castenholz, R.W. 1974, A phototrophic gliding filamentous bacterium of hot springs, *Chloroflexus aurantiacus*, gen. and sp. nov, *Arch. Microbiol.*, 100, 5–24.

Russo, M.A., Quartacci, M.F., Izzo, R., Belligno, A., and Navari-Izzo, F. 2007, Long- and short-term phosphate deprivation in bean roots: plasma membrane lipid alterations and transient stimulation of phospholipases, *Phytochemistry*, 68, 1564–1571.

Sato, N., and Murata, N. 1982, Lipid biosynthesis in the blue-green alga, *Anabaena variabilis*

I. Lipid classes, *Biochim. Biophys. Acta.*, 710, 271–278

Shimojima, M., Ohta, H., Iwamatsu, A., Masuda, T., Shioi, Y., and Takamiya, K. 1997,

Cloning of the gene for monogalactosyldiacylglycerol synthase and its evolutionary origin,

Proc. Natl. Acad. Sci. U. S. A., 94, 333–337.

Woese, C.R. 1987, Bacterial evolution, *Microbiol. Rev.*, 51, 221–271.

Wolfe, G.R., Cunningham, F.X., Durnford, D., Green, B.R., and Gantt, E. 1994, Evidence for

a common origin of chloroplasts with light-harvesting complexes of different pigmentation,

Nature, 367, 566–568.

Xiong, J., Fischer, W.M., Inoue, K., Nakahara, M., and Bauer, C.E. 2000, Molecular evidence

for the early evolution of photosynthesis, *Science*, 289, 1724–1730.

Chapter II

The analyses for the plant-type pathway for MGDG synthesis

Introduction

The photosynthetic membranes of cyanobacteria and chloroplasts of higher plants have remarkably similar lipid composition. In particular, thylakoid membranes of both cyanobacteria and chloroplasts are composed of galactolipids, of which MGDG is the most abundant, although MGDG biosynthesis pathways are different in these organisms.

Comprehensive phylogenetic analysis revealed that MGDG synthase (MGD) homologs of filamentous anoxygenic phototrophs *Chloroflexi* have a close relationship with MGDs of *Viridiplantae* (green algae and land plants). Furthermore, analyses for the sugar specificity and anomeric configuration of the sugar head groups revealed that one of the MGD homologs exhibited a true MGDG synthetic activity. I therefore presumed that higher plant MGDs are derived from this ancestral type of MGD genes, and genes involved in membrane biogenesis and photosystems have been already functionally associated at least at the time of *Chloroflexi* divergence. As MGD gene duplication is an important event during plastid evolution, I also estimated the divergence time of type A and type B MGDs. The analysis indicated that these genes diverged ~323 million years ago, when *Spermatophyta* (seed plants) were appearing.

Galactolipid synthesis is required to produce photosynthetic membranes; based on MGD gene sequences and activities, I have proposed a novel evolutionary model that has increased our understanding of photosynthesis evolution.

II-1 Comprehensive phylogenetic analysis of MGDG synthase homologs

Results and Discussion

Evolutionary Relationship of MGD Homologs

To comprehensively understand the relationships among MGD homologs, I compared amino acid sequences of 56 MGD homologs from prokaryotes and phototrophic eukaryotes. The homologs similarly located were excluded from the phylogenetic tree. A complete list of these proteins is shown in Table II-1. My phylogenetic analyses identified monophyletic clades of *Viridiplantae*, *Rhodophyta* (red algae), and *Heterokontophyta* (heterokonts), which were clearly supported by both Bayesian inference (MrBayes) and ML analyses (Treefinder and RAxML) (Node A in Fig. II-1). My data provide compelling evidence that a single origin of MGD in a common ancestor of these groups and the pathway for MGDG synthesis is monophyletic among *Viridiplantae*, *Rhodophyta*, and *Heterokontophyta*. As indicated above, MGDs from *Heterokontophyta* formed a single group, suggesting that the common ancestor of *Heterokontophyta* acquired MGDs (Node B in Fig. II-1). This grouping was strongly supported by MrBayes, Treefinder and RAxML. Notably, *Rhodophyta* and *Heterokontophyta* formed a single group (Node C in Fig. II-1). Recent phylogenetic analyses of plastid proteins have revealed an extremely close relationship between heterokontophytes and rhodophytes. These data suggest that heterokont plastids

Table II-1. MGD Protein Sequences Used for Analysis

Classification	Species	Indication in Phylogenetic Tree	Accession Number	Database
Angiosperm	<i>Arabidopsis thaliana</i>	<i>Arabidopsis t.</i> MGD1	NP_194906	NCBI
Angiosperm	<i>Arabidopsis thaliana</i>	<i>Arabidopsis t.</i> MGD2	NP_568394	NCBI
Angiosperm	<i>Arabidopsis thaliana</i>	<i>Arabidopsis t.</i> MGD3	NP_565352	NCBI
Angiosperm	<i>Oryza sativa</i>	<i>Oryza s.</i> Type A	BAD33425	GenBank
Angiosperm	<i>Oryza sativa</i>	<i>Oryza s.</i> Type B-1	AB112060	GenBank
Angiosperm	<i>Oryza sativa</i>	<i>Oryza s.</i> Type B-2	AK064148	GenBank
Pteridophyta	<i>Selaginella moellendorffii</i>	<i>Selaginella m.</i>	XP_002973136	NCBI
Bryophyta	<i>Physcomitrella patens</i>	<i>Physcomitrella p.</i> 1	XP_001758690	NCBI
Bryophyta	<i>Physcomitrella patens</i>	<i>Physcomitrella p.</i> 2	XP_001755870	NCBI
Chlorophyta	<i>Chlamydomonas reinhardtii</i>	<i>Chlamydomonas r.</i>	AB678730	DDBJ
Chlorophyta	<i>Micromonas pusilla</i>	<i>Micromonas p.</i>	XP_003056007	NCBI
Chlorophyta	<i>Ostreococcus lucimarinus</i>	<i>Ostreococcus l.</i>	XP_001416396	NCBI
Chlorophyta	<i>Volvox carteri</i>	<i>Volvox c.</i>	XP_002948847	NCBI
Rhodophyta	<i>Cyanidioschyzon merolae</i>	<i>Cyanidioschyzon m.</i>	CM1271C	Cyanidioschyzon merolae Genome Project
Heterokontophyta	<i>Aureococcus anophagefferens</i>	<i>Aureococcus a.</i> 1	24670	A. anophagefferens Filtered Models
Heterokontophyta	<i>Aureococcus anophagefferens</i>	<i>Aureococcus a.</i> 2	1716	A. anophagefferens Filtered Models
Heterokontophyta	<i>Phaeodactylum tricornutum</i>	<i>Phaeodactylum t.</i> 1	14125	Phaeodactylum tricornutum v2.0 filtered model proteins
Heterokontophyta	<i>Phaeodactylum tricornutum</i>	<i>Phaeodactylum t.</i> 2	54168	Phaeodactylum tricornutum v2.0 filtered model proteins
Heterokontophyta	<i>Phaeodactylum tricornutum</i>	<i>Phaeodactylum t.</i> 3	XP_002176800	NCBI
Heterokontophyta	<i>Thalassiosira pseudonana</i>	<i>Thalassiosira p.</i> 1	XP_002295865	NCBI
Heterokontophyta	<i>Thalassiosira pseudonana</i>	<i>Thalassiosira p.</i> 2	XP_002293576	NCBI
Heterokontophyta	<i>Thalassiosira pseudonana</i>	<i>Thalassiosira p.</i> 3	XP_002294242	NCBI
Heterokontophyta	<i>Thalassiosira pseudonana</i>	<i>Thalassiosira p.</i> 4	118428	T. pseudonana v1.0 Filtered Models
Chloroflexi	<i>Chloflexus aggregans</i>	<i>Chloflexus ag.</i> 1	ACL26208	GenBank
Chloroflexi	<i>Chloflexus aggregans</i>	<i>Chloflexus ag.</i> 2	ACL26207	GenBank
Chloroflexi	<i>Chloflexus aggregans</i>	<i>Chloflexus ag.</i> MURG	ACL25714	GenBank
Chloroflexi	<i>Chloflexus aurantiacus</i>	<i>Chloflexus au.</i> 1	ABY33891	GenBank
Chloroflexi	<i>Chloflexus aurantiacus</i>	<i>Chloflexus au.</i> 2	ABY33892	GenBank
Chloroflexi	<i>Chloflexus aurantiacus</i>	<i>Chloflexus au.</i> MURG	ABY33993	GenBank
Chloroflexi	<i>Roseiflexus castenholzii</i>	<i>RcMGlcD</i>	ABU57307	GenBank
Chloroflexi	<i>Roseiflexus castenholzii</i>	<i>RcMGD</i>	ABU59051	GenBank
Chloroflexi	<i>Roseiflexus castenholzii</i>	<i>RcDGlcD</i>	ABU58556	GenBank
Chloroflexi	<i>Roseiflexus castenholzii</i>	<i>Roseiflexus c.</i> MURG	ABU57194	GenBank
Chloroflexi	<i>Roseiflexus sp.</i>	<i>Roseiflexus sp.</i> 1	ABQ92406	GenBank
Chloroflexi	<i>Roseiflexus sp.</i>	<i>Roseiflexus sp.</i> 2	ABQ90476	GenBank

Chloroflexi	<i>Roseiflexus</i> sp.	<i>Roseiflexus</i> sp. 3	ABQ90904	GenBank
Chloroflexi	<i>Roseiflexus</i> sp.	<i>Roseiflexus</i> sp. MURG	ABQ92140	GenBank
Chloroflexi	<i>Thermomicrobium roseum</i>	<i>Thermomicrobium</i> r.	ACM04791	GenBank
Proteobacteria	<i>Aromatoleum aromaticum</i>	<i>Aromatoleum</i> a.	CAI09308	GenBank
Proteobacteria	<i>Burkholderia</i> sp.	<i>Burkholderia</i> sp.	ABB10664	GenBank
Verrucomicrobia	<i>Methylacidiphilum inferorum</i>	<i>Methylacidiphilum</i> i.	ACD83006	GenBank
Verrucomicrobia	<i>Opitutus terrae</i>	<i>Opitutus</i> t.	ACB77287	GenBank
Cyanobacteria	<i>Gloeobacter violaceus</i>	<i>Gloeobacter</i> v.	NP_926175	NCBI
Cyanobacteria	<i>Synechococcus</i> sp.	<i>Synechococcus</i> sp.	YP_729394	NCBI
Cyanobacteria	<i>Synechocystis</i> sp. PCC 6803	<i>Synechocystis</i> sp. MURG	BAA18775	GenBank
Actinobacteria	<i>Arthrobacter aurescens</i>	<i>Arthrobacter</i> a.	ABM08975	GenBank
Actinobacteria	<i>Frankia alni</i>	<i>Frankia</i> a.	CAJ59184	GenBank
Actinobacteria	<i>Frankia</i> sp.	<i>Frankia</i> sp.	ABD09614	GenBank
Actinobacteria	<i>Streptomyces coelicolor</i>	<i>Streptomyces</i> c.	CAC13078	GenBank
Firmicutes	<i>Bacillus subtilis</i>	<i>Bacillus</i> s. 1	CAB13192	GenBank
Firmicutes	<i>Bacillus subtilis</i>	<i>Bacillus</i> s. 2	P54166	Swiss-Prot
Firmicutes	<i>Desulfotomaculum reducens</i>	<i>Desulfotomaculum</i> r.	ABO50484	GenBank
Firmicutes	<i>Hellobacterium modesticaldum</i>	<i>Hellobacterium</i> m.	ABZ84827	GenBank
Firmicutes	<i>Pelotomaculum thermopropionicum</i>	<i>Pelotomaculum</i> t.	BAF59445	GenBank
Firmicutes	<i>Staphylococcus epidermidis</i>	<i>Staphylococcus</i> e.	NP_764272	NCBI

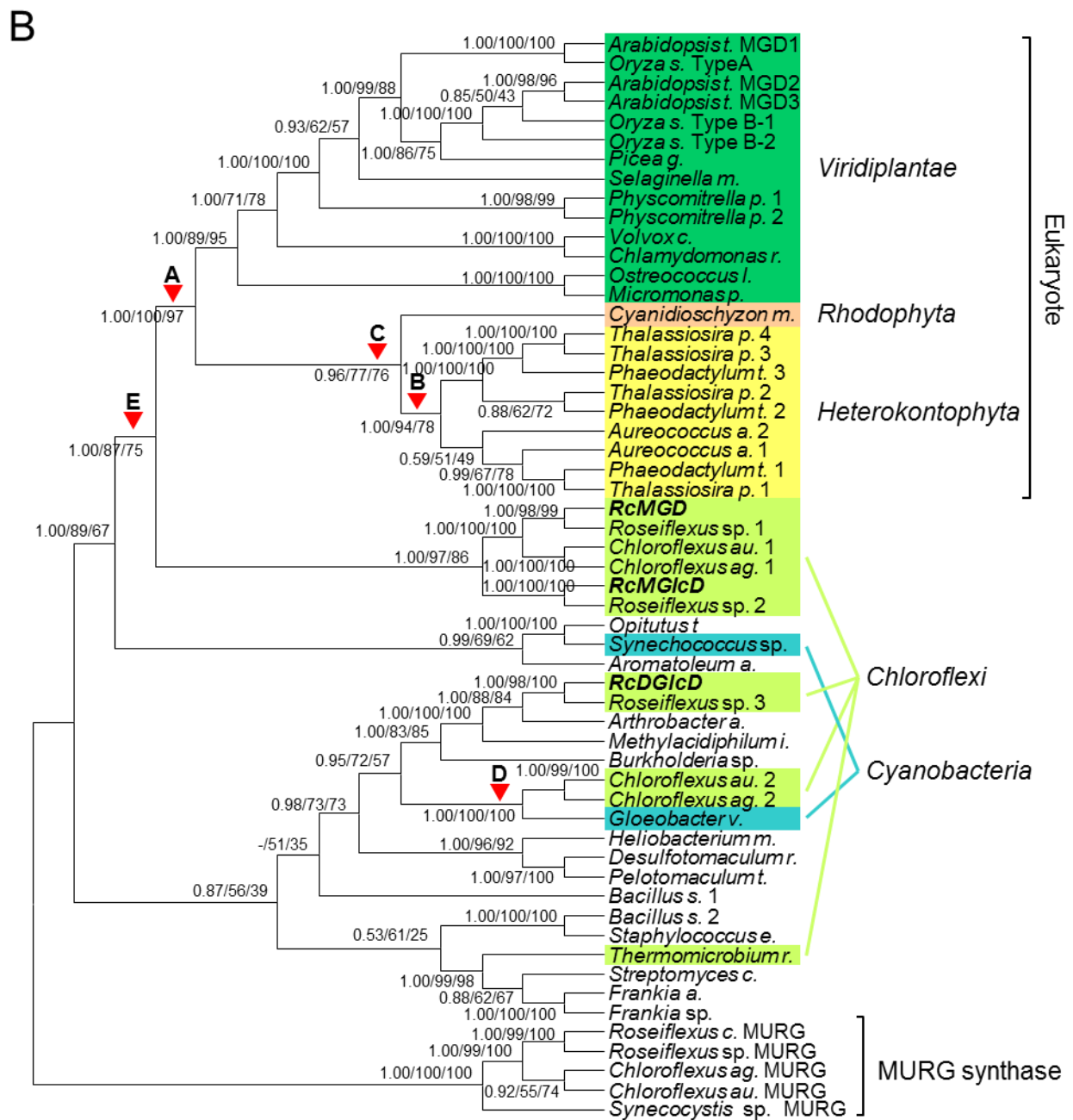
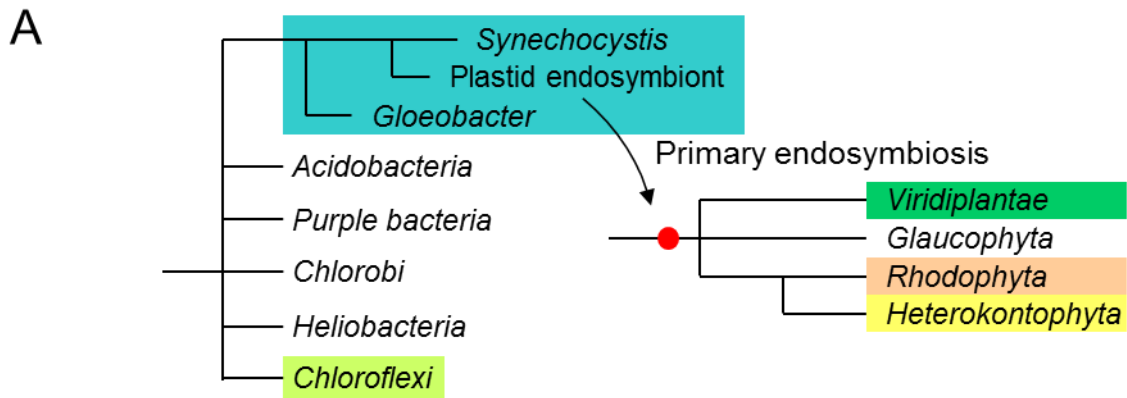


FIG. II-1. Phylogenetic relationship of MGD homologs.

(A) An accepted model of chloroplast evolution (Turner et al., 1999, Harper and Keeling, 2003, Blankenship, 2010). Each red point indicates an endosymbiotic event. (B) A phylogenetic tree of all MGD homologs from plastids and bacteria (based on amino acid sequences). To obtain MGD sequences, blastp and tblastn searches were performed using *Arabidopsis* MGD amino acid sequences as queries. Above each branch is shown: 1) the posterior probability estimated with Bayesian inference, 2) LR-ELW edge supports from Treefinder analysis, and 3) the bootstrap probability from RAxML analysis (in that order). *Viridiplantae*, *Rhodophyta*, *Heterokontophyta*, *Chloroflexi*, and *Cyanobacteria* are indicated by green, light magenta, yellow, light green, and light blue, respectively. MURG synthase genes were used as the outgroup. The original phylogenetic trees from the 3 separate analyses (Bayesian, Treefinder, and RAxML) are shown in Fig. II-S1, S2 and S3. Arrowheads indicate (A) the acquisition of MGD in plastids, (B) the acquisition of MGD homologs in *Heterokontophyta*, (C) the grouping of red algal plastids, (D) the horizontal gene transfer between *Gloeobacter* and *Chloroflexus*, and (E) the close relationship between plastids and *Chloroflexi*.

originated from endosymbiosis with *Rhodophyta* (Yoon et al., 2002, Harper and Keeling, 2003). MGDs of heterokonts were likely acquired from *Rhodophyta* through this endosymbiotic event.

Gloeobacter violaceus is one of the most ancient cyanobacterial lineages, and the *Gloeobacter* MGD homolog is a likely candidate for the origin of plastid MGDs. My phylogenetic analysis of MGDs, however, indicated that this gene formed a clade with different MGD homologs in green non-sulfur bacteria (*Chloroflexus aurantiacus* and *Chloroflexus aggregans* (Hanada et al., 1995); Node D in Fig. II-1). Since chloroplasts may be derived from ancient type of cyanobacteria, it was expected that the eukaryote MGDs may be directly evolved from a cyanobacterial MGD origin that might be acquired by the primary endosymbiotic event, although it might be lost in most of cyanobacterial species. However, here, the grouping between the *Gloeobacter* and *Chloroflexi* MGD homologs was robustly supported by MrBayes, Treefinder and RAxML (Node D in Fig. II-1). This result strongly suggests that the *G. violaceus* MGD homolog is not the origin of MGDs in *Viridiplantae* and that horizontal gene transfer may have occurred much more recently between *Gloeobacter* and *Chloroflexi*.

However, notably, other MGD homologs of *Chloroflexi* strains, *Chloroflexus* and *Roseiflexus*, were located closest to the clade of chloroplasts (Node E in Fig. II-1). *Chloroflexus au. 1*, an MGD of *C. aurantiacus*, belongs to the GT28 family and the encoded protein has a MGDG

synthetic activity (Hölzl et al., 2005). In addition, *R. castenholzii* has 3 MGD homologs that I have named RcMGD, RcMGlcD and RcDGlcD according to their functions determined (see below). These genes also belong to the GT28 family, and RcMGD and RcMGlcD form a clade with *Chloroflexus au. 1*. Although MGD homologs from *Chloroflexi* and chloroplasts were closely related phylogenetically, information regarding substrate specificity was only available for *Chloroflexus au. 1*. I have therefore examined the enzymatic properties of *Chloroflexi* MGD homologs in more detail.

Glycolipid Synthetic Activities of *R. castenholzii* MGD Homologs

To characterize the glycolipid synthetic activities of the 3 *R. castenholzii* MGD homologs, I expressed these recombinant proteins in *E. coli*. When radiolabeled UDP-Gal was used as a substrate, RcMGD was capable of synthesizing a radiolabeled lipid (Fig. II-2). I used UDP-Gal as a substrate because the proposed pathway for MGDG synthesis of higher plants utilizes UDP-Gal. Cucumber (*Cucumis sativus*) MGD1 (CsMGD) was used as a positive control for MGDG synthesis in this experiment. In contrast, RcMGD extract did not contain a radiolabeled product, when UDP-Glc was provided as a substrate, suggesting that lipid synthesis *via* RcMGD was UDP-Gal-dependent. On the other hand, the enzyme encoded by RcMGlcD synthesized MGlcDG when UDP-Glc was provided as a substrate. The MGlcDG synthase of *Synechocystis* sp. PCC 6803 (MGlcD) was used as a positive control for

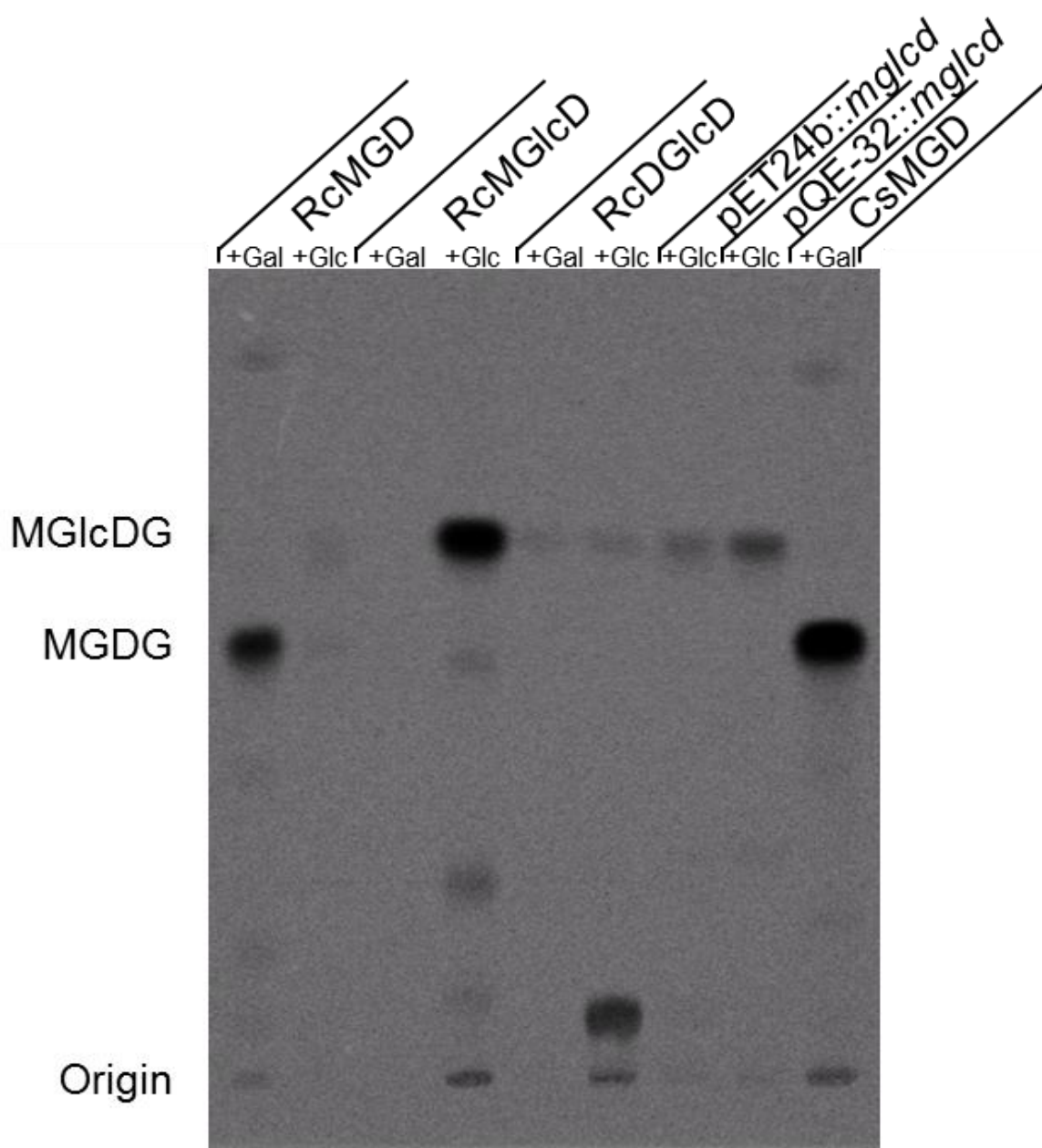


FIG. II-2. Analysis of sugar transferase activity.

Radiolabeled UDP-Gal (+Gal) or UDP-Glc (+Glc) were used as substrates. The resulting lipids were separated by TLC (chloroform-hexane-tetrahydrofuran-isopropanol-water, 50:100:1:80:2 by volume) and visualized by autoradiography. CsMGD and MGlcD (pET24b and pQE-32) were used as controls for MGDG and MGlcDG, respectively.

MGlcDG synthesis in this experiment.

Using TLC, lipids from 2 samples (RcMGD/UDP-Gal and RcMGlcD/UDP-Glc) were purified and subjected to $^1\text{H-NMR}$ analysis to reveal the sugar head groups of these lipids (Fig. II-3). In Figure I-3A and I-3B, the doublet peak indicated by the black arrow at 4.5–4.6 ppm indicates H1 of the hexose moiety of the lipid. These peaks demonstrated that the sugar head group was bound to a glycerol backbone *via* a β -anomeric configuration at the C3 position, an MGDG structure that is characteristic of land plants (Hölzl and Dörmann, 2007). Consequently, the clade in Fig. II-1, which includes *Chloroflexus* and *Roseiflexus*, represents green non-sulfur bacterial MGDG synthases. The present results indicate that MGD genes occur at least at the time of *Chloroflexi* divergence (an ancient bacterial lineage). Botté et al. has independently performed phylogenetic analysis of MGDG synthases (Botté et al., 2011). Although they indicated similar results for phylogeny of MGDG synthases, they have not included prokaryotic MGD homologs except for *Chloroflexi* in their phylogenetic analysis, and thus, phylogenetic relationship between eukaryotic and prokaryotic MGD homologs remains uncertain. My detailed analyses suggest that this ancestral type of MGD genes is the origin of higher plant MGDG synthases.

RcDGlcD synthesized a glycolipid that consisted of a number of sugars, using UDP-Glc as a substrate (Fig. II-2). The crude lipid extract from *E. coli* overexpressing RcDGlcD contained much phospholipids derived from *E. coli*. To remove phospholipids and concentrate

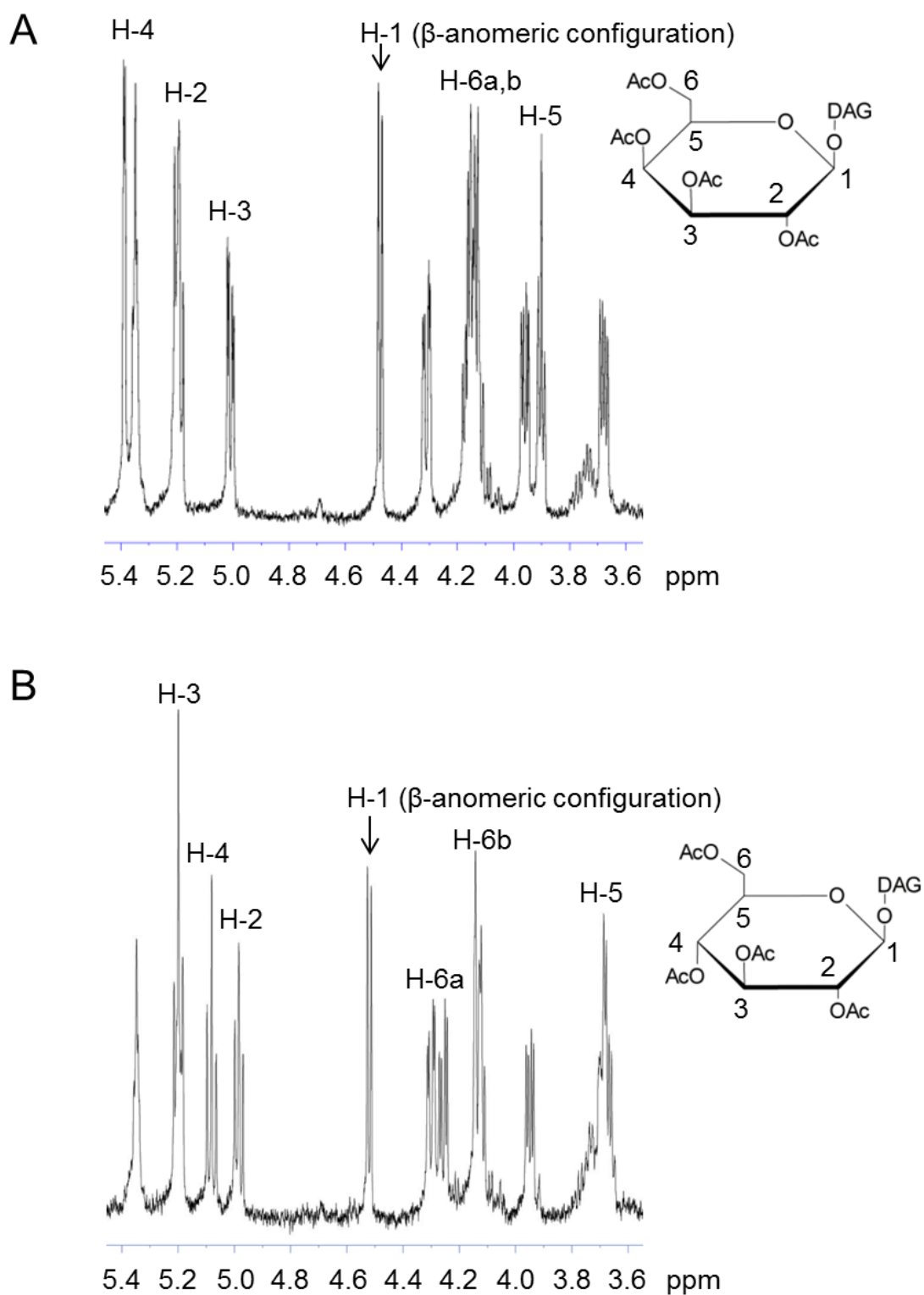


FIG. II-3. Analysis of glycolipids by $^1\text{H-NMR}$.

Each glycolipid synthesized by RcMGD and RcMGlcD was analyzed by $^1\text{H-NMR}$ at 600 MHz. (A) MGDG synthesized by RcMGD expression and (B) MGlcDG synthesized by RcMGlcD expression were isolated from *E. coli*. H-1 doublet peaks (arrows) indicate that these glycolipids formed β -anomeric configurations to the glycerol backbone.

glycolipids, the extract was purified by a silica column chromatography. The separated fractions were further developed by TLC and stained using the anthrone reagent (Fig. II-4A). The lipid mobility was associated with diglucosyldiacylglycerol (DGlcDG; Hölzl et al., 2005). ¹H-NMR analysis identified this lipid as DGlcDG. The analysis showed 2 doublet peaks H1 and H'1 (4.4-4.6 ppm) indicating 2 hexose moieties in the lipid (Fig. II-4B). The spectrum including these peaks revealed that this lipid contained 2 glucoses and these glucoses were bound to each other *via* a β-anomeric configuration. Furthermore, one of these glucoses was also bound to a glycerol backbone *via* a β-anomeric configuration. MGD gene homologs share a high degree of sequence similarity, yet sugar-donor specificity and the number of molecules involved in the reaction is clearly diverse. Detailed comparisons of MGD homolog sequences could potentially reveal novel protein domains that determine sugar-donor specificity.

Lipid analysis of *R. castenholzii*

I determined the activity of the MGD of *R. castenholzii*. Subsequently, to define whether *R. castenholzii* possesses MGDG, MGlcDG and DGlcDG or not, I analyzed the lipid composition of *R. castenholzii*. Total lipid was extracted and developed by 2D-TLC, and three glycolipids were detected by anthrone reagent (Fig. II-5A). I compared the mobility of total lipids on 2D-TLC between *A. thaliana* and *R. castenholzii* (Fig. II-6). The mobility of a *Roseiflexus* glycolipid was very similar to *Arabidopsis* MGDG. Using ¹H-NMR, I confirmed

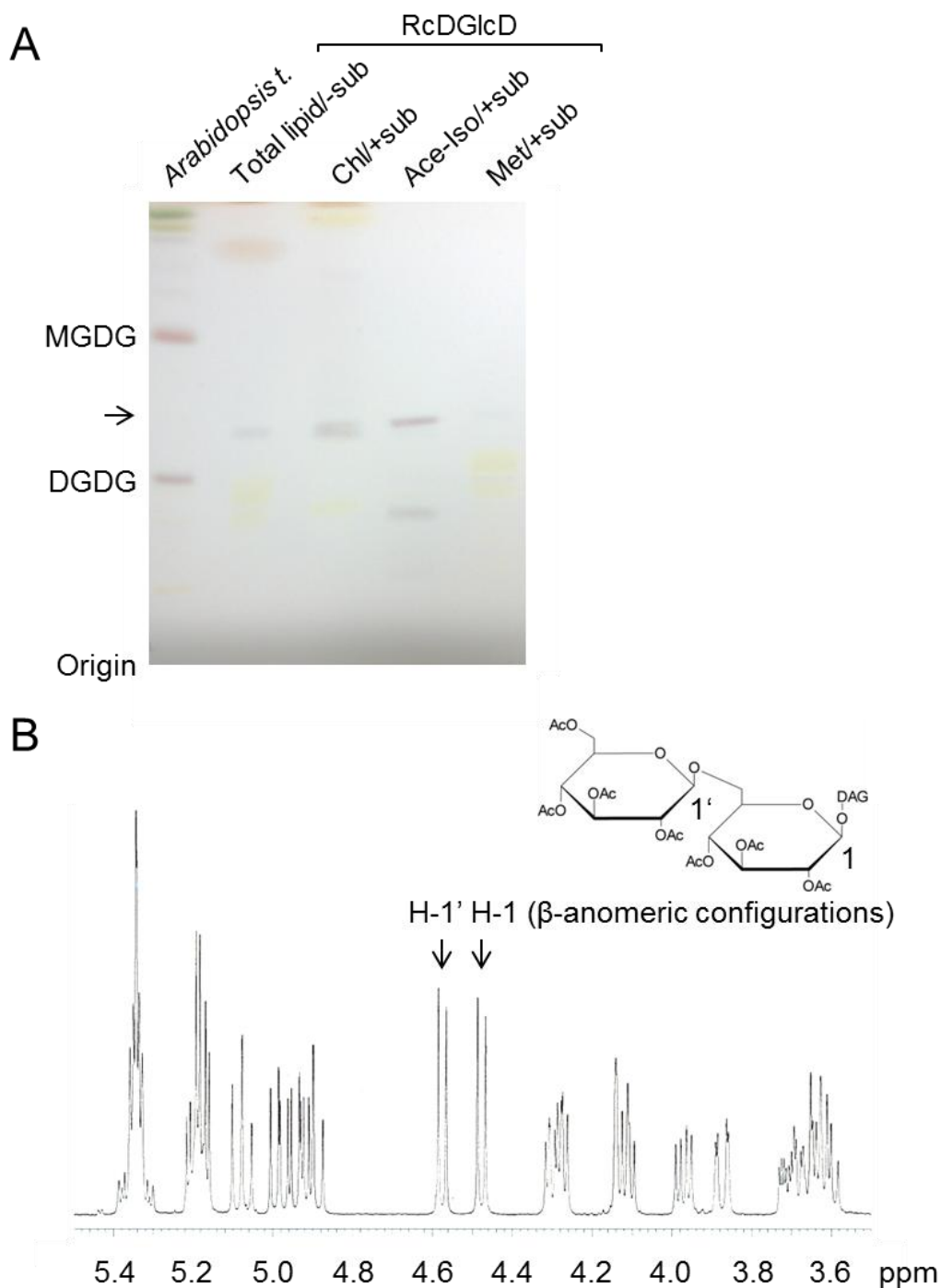


FIG. II-4. Analysis of glycolipids synthesized by RcDGlcD.

Glycolipids synthesized by RcDGlcD were analyzed by TLC (A) and $^1\text{H-NMR}$ at 400 MHz (B). (A) RcDGlcD was incubated with UDP-Glc and DAG (+sub), or without substrate (-sub). Synthesized lipids were purified by column chromatography. Fractions eluted either with chloroform (Chl), acetone-isopropanol (9:1, by volume, Ace-Iso), or methanol (Met) were developed using hexane-tetrahydrofuran-isopropanol-water (40:0.4:50:10, by volume). Glycolipids were detected by the anthrone reagent (MGDG, DGDG, and the lipid indicated by an arrow). (B) $^1\text{H-NMR}$ lipid analysis resulted in doublet H-1 peaks (arrows), indicating β -anomeric configurations.

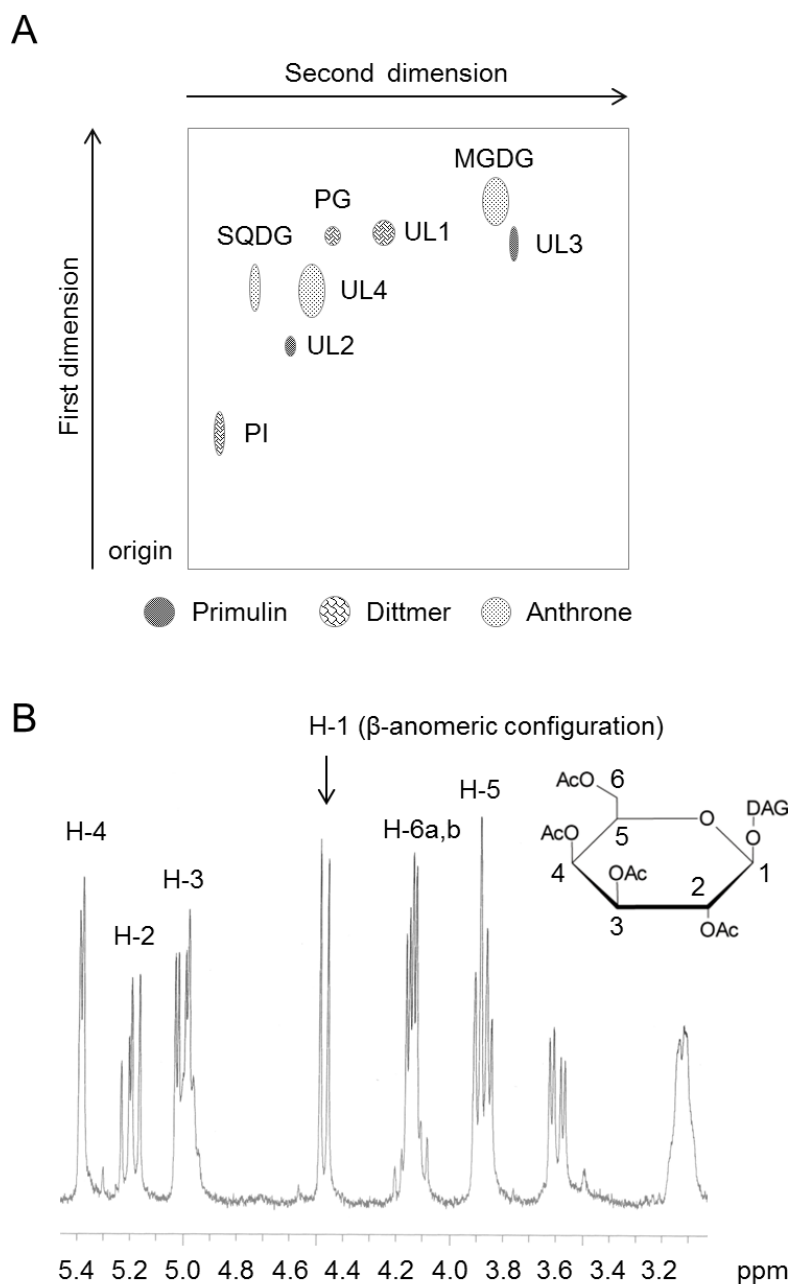


FIG. II-5. Analysis of MGDG isolated from *R. castenholzii*.

(A) Description of 2-dimensional TLC in *R. castenholzii*. The TLC analysis was performed with chloroform-methanol- 7 N ammonium hydroxide (120:80:8, by volume) in the first dimension and chloroform-methanol-acetic acid-water (170:20:15:3, by volume) in the second. The lipids were visualized by spraying with primulin reagent and viewing under ultraviolet light. The glycolipids were visualized by anthrone reagent and The phospholipids were visualized by Dittmer's reagent. PG, phosphatidylglycerol; SQDG, sulfoquinovosyldiacylglycerol; PI, phosphatidylinositol; UL, unknown lipid.

(B) MGDG isolated from *R. castenholzii* was analyzed by $^1\text{H-NMR}$ at 270 MHz. The MGDG formed a β -anomeric configuration to the glycerol backbone.

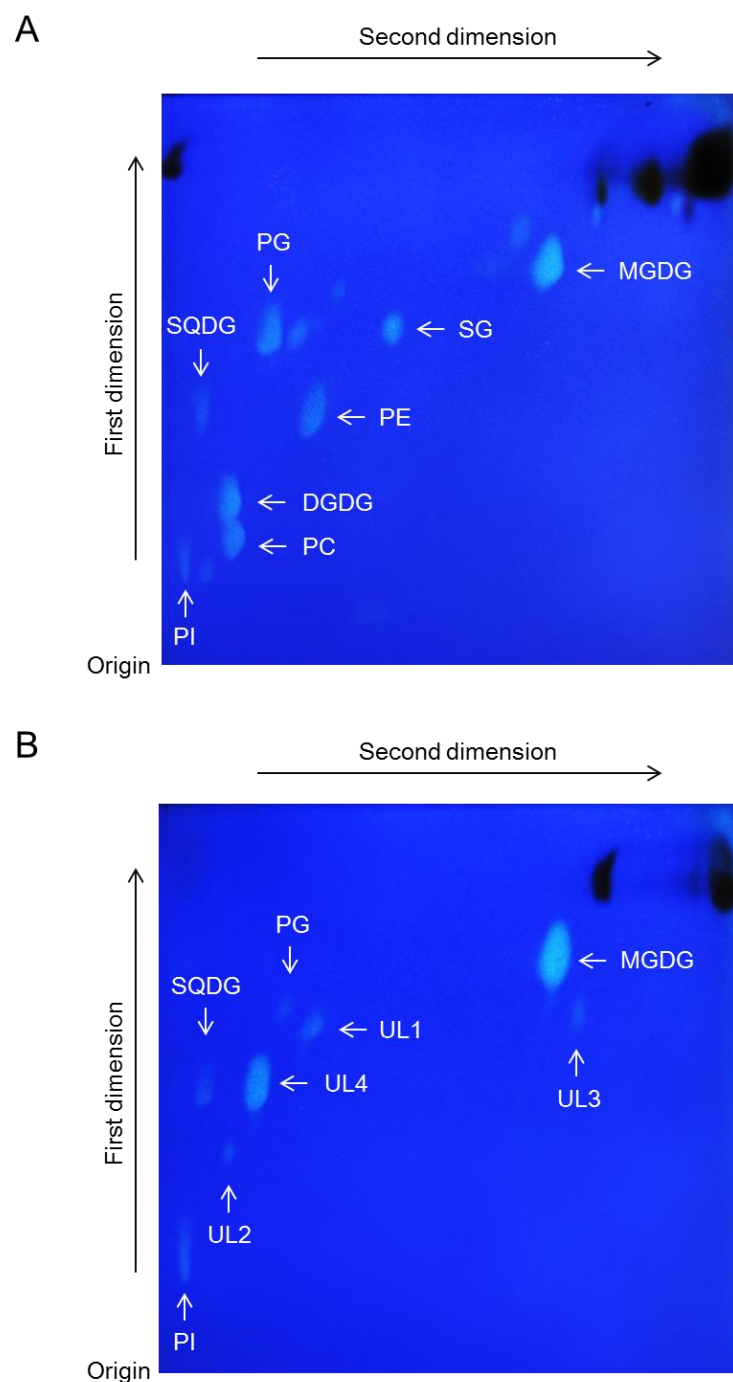


FIG. II-6. Total lipid of *A. thaliana* (A) and *R. castenholzii* (B) was developed by 2-dimensional TLC, respectively. The TLC analysis was performed with chloroform-methanol- 7 N ammonium hydroxide (120:80:8, by volume) in the first dimension and chloroform-methanol-acetic acid-water (170:20:15:3, by volume) in the second. The lipids were visualized by spraying with primulin reagent and viewing under ultraviolet light. SG, sterolglucoside; PG, phosphatidylglycerol; PE phosphatidylethanolamine; SQDG, sulfoquinovosyldiacylglycerol; PC, phosphatidylcholine; PI, phosphatidylinositol; UL, unknown lipid.

that this glycolipid was a galactolipid and formed a β -anomeric configuration to the glycerol backbone (Fig II-5B). From these results, I concluded that this glycolipid is MGDG.

Although the peak pattern derived from glycerol backbone was slightly different from MGDG synthesized by RcMGD in *E. coli*, it is probably due to the difference in fatty acid composition of DAGs as a substrate between *E. coli* and *R. castenholzii* (Table II-2). This result strongly supports that RcMGD actually functions *in vivo* to synthesize MGDG.

As indicated above, I also detected 2 other glycolipids on 2D-TLC. One of them was assumed to be sulfoquinovosyldiacylglycerol (SQDG) from the mobility on TLC. In fact, there is a homolog of Arabidopsis SQDG synthase 1 in *Roseiflexus* and the presence of SQDG in *C. aurantiacus* was reported in a previous paper (Kundsen et al., 1982). On the other hand, in another one (UL4, unknown lipid 4, in Fig. II-5A), the corresponding lipid was not existent in *A. thaliana*. This glycolipid was likely DGlcDG. However, $^1\text{H-NMR}$ analysis revealed that this lipid was not DGlcDG, although it consisted of at least 2 sugar head groups (Fig. II-S4). We could not detect MGlcDG in total lipid fraction from *Roseiflexus*. In Cyanobacteria, MGlcDG is a minor lipid, less than 1% of total lipid (Sato and Murata, 1982). Similarly, MGlcDG may not be abundant in *Roseiflexus*. Therefore, these results suggest that RcDGlcD mainly incorporates glucose to a major monoglycolipid MGDG, not MGlcDG *in vivo*.

To confirm the glucose transfer activity of RcDGlcD, I used MGDG and MGlcDG

Table II-2. Lipid and fatty acid composition in *R. castenholzii*

Lipids (mol%)	
Monogalactosyldiacylglycerol	28.6 ± 0.6
Unknown lipid 4	29.6 ± 0.8
Sulfoquinovosyldiacylglycerol	9.0 ± 0.4
Phosphatidylglycerol	4.0 ± 2.1
Phosphatidylinositol	19.6 ± 1.7
Unknown lipid 1	6.8 ± 0.2
Unknown lipid 2	1.8 ± 0.3
Unknown lipid 3	0.6 ± 0.2

Fatty acids (mol%)	16:0	16:1	18:0
Monogalactosyldiacylglycerol	72.1 ± 0.6	26.4 ± 0.7	1.6 ± 0.1
Unknown lipid 4	64.9 ± 0.7	33.3 ± 0.6	1.8 ± 0.2
Sulfoquinovosyldiacylglycerol	68.0 ± 1.0	28.8 ± 0.9	3.2 ± 0.1
Phosphatidylglycerol	74.4 ± 6.7	14.3 ± 6.6	11.3 ± 1.2
Phosphatidylinositol	57.1 ± 1.6	39.8 ± 1.7	3.1 ± 0.6
Unknown lipid 1	66.8 ± 2.0	27.0 ± 1.2	6.2 ± 1.8
Unknown lipid 2	72.0 ± 3.5	15.5 ± 2.2	12.6 ± 4.9
Unknown lipid 3	71.0 ± 10.0		29.5 ± 9.9

The values are the means ± SD of three experimental replications.

as sugar acceptors, and compared the diglycolipid producing activity (Fig. II-7). Obviously, RcDGlcD could transfer glucose to MGDG, although DGlcDG is still produced by its processive activity. When MGlcDG was used as a substrate, the band corresponding to DGlcDG was increased, confirming that RcDGlcD could also transfer glucose to MGlcDG. However, UL4 was not DGlcDG and MGDG is one of the most abundant lipids in *Roseiflexus* (Table II-2). Consequently, I presume that the main sugar acceptor of RcDGlcD *in vivo* is MGDG and UL4 is glycosylgalactosyldiacylglycerol. However, since I only utilized UDP-Gal and UDP-Glc as *in vitro* substrates (Fig. II-2), its true substrate is still uncertain, and further experiments will be needed to determine the structure of UL4.

Thylakoid membranes or membranous structures of anoxygenic photosynthetic bacteria involve complexes composed of proteins, pigments, and lipids. In particular, these types of membranes are characterized by a unique and conserved lipid composition. Genes related to the photosynthetic membrane biogenesis, therefore, have also played an important role in phototroph evolution. Recently, we reported that a distinct type of MGDG synthase belonging to GT1 family was found in the green sulfur bacterium *Chlorobacterium tepidum*, and proved to be involved in chlorosome biogenesis (Masuda et al., 2011). This work also demonstrated that MGDG is commonly important in both anoxygenic and oxygenic photosynthetic organisms, although green sulfur and non-sulfur bacteria have independently acquired different types of MGDG synthetic machineries. Given the conservation of MGD

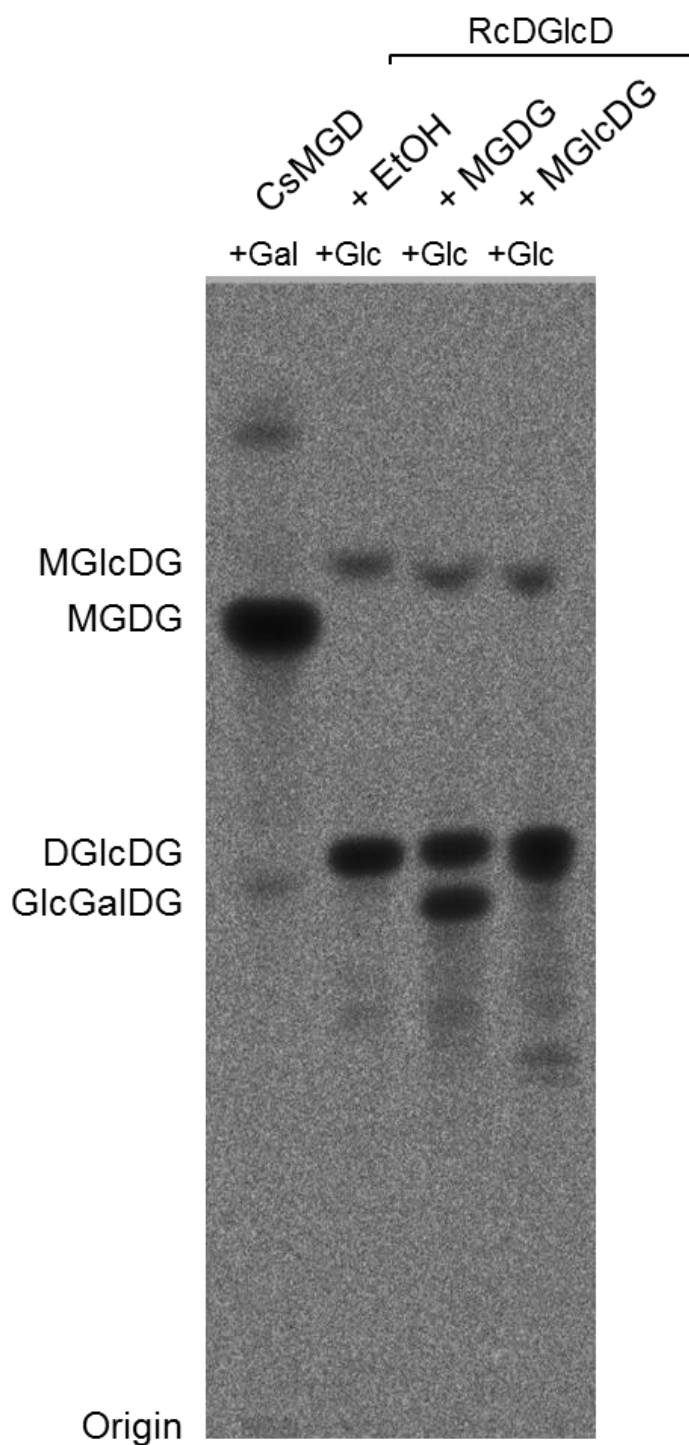


FIG. II-7. Analysis of sugar transferase activity of RcDGlcD. Radiolabeled UDP-Gal (+Gal) or UDP-Glc (+Glc) were used as substrates. Additionally, MGDG or MGlcDG eluted in EtOH were added as acceptors. The resulting lipids were separated by TLC (hexane-tetrahydrofuran-isopropanol-water, 40:0.4:50:10, by volume) and visualized by autoradiography. CsMGD was used as controls for MGDG. GlcGalDG, glucosylgalactosyldiacylglycerol.

gene families and the presence of MGDG in *Chloroflexi*, functional association between the photosystem and the membrane galactolipid MGDG was established anciently, leading to establishment of highly organized photosynthetic membranes.

My results suggested that photosynthetic eukaryote has acquired MGDG synthase gene from ancestral *Chloroflexi* in an early event, even though Cyanobacteria has a different MGDG synthesis pathway. These pathways were subsequently conserved during the course of evolution and have played important roles in chloroplast biology. Recent large scale phylogenetic analysis also revealed that considerable amount of non-cyanobacterial genomic material has contributed to the establishment of the plastid before the split of red and green algae (Suzuki and Miyagishima, 2010). Eukaryotic MGD genes may be acquired through this kind of large scale gene transfer from ancestral *Chloroflexi*.

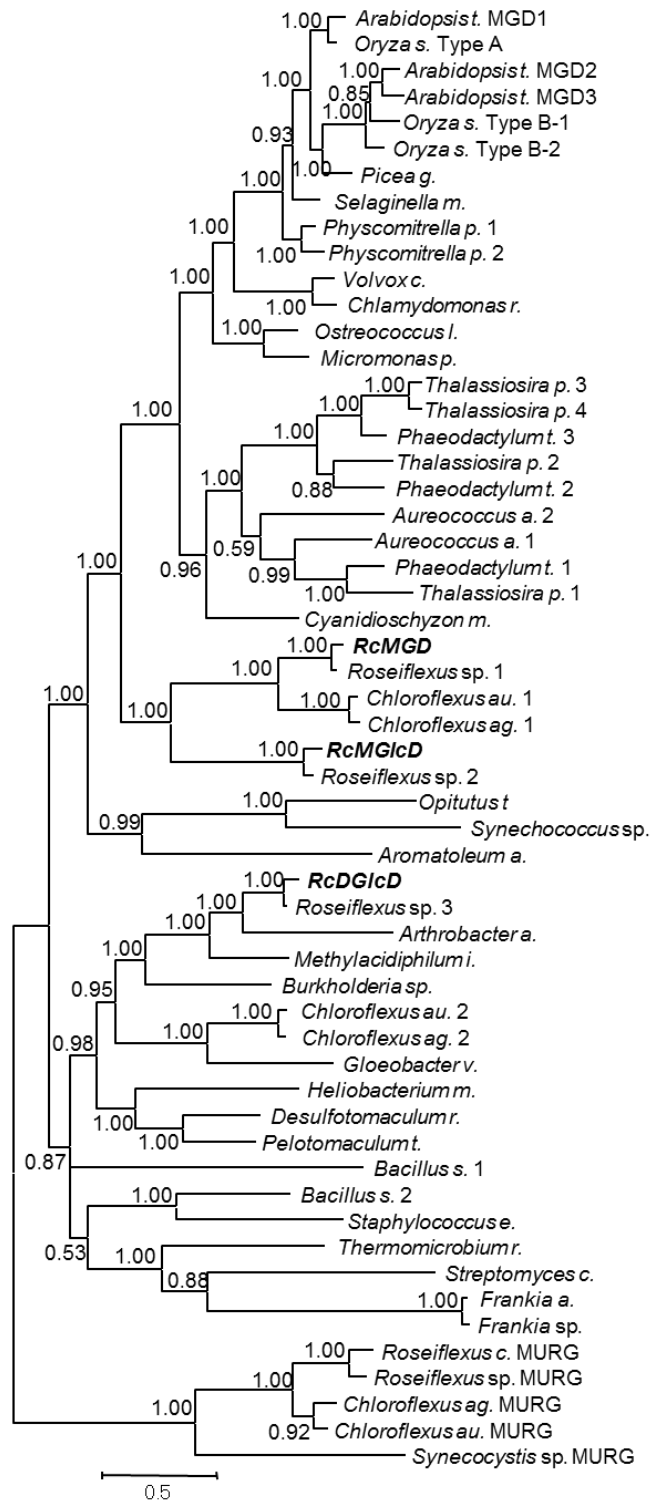


FIG. II-S1. A phylogenetic tree of the MGD amino acid dataset based on Bayesian inference under the WAG + G_4 model. MURG synthase genes were used as the outgroup. Numbers associated with individual branches represent the posterior probability.

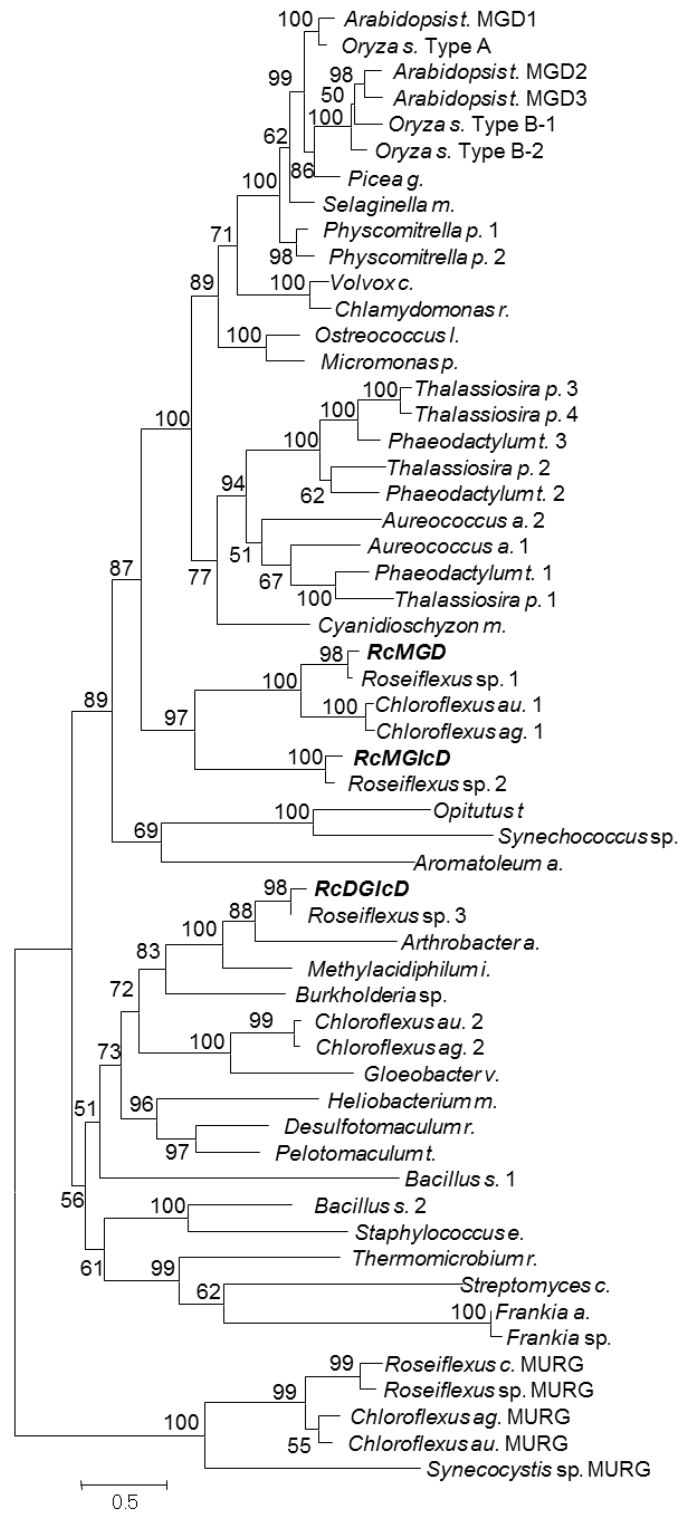


FIG. II-S2. A ML tree of the MGD amino acid dataset analyzed with Treefinder under the WAG-F + G_8 model. MURG synthase genes were used as the outgroup. Numbers associated with individual branches represent LR-ELW (expected likelihood weights by the local rearrangement) support values calculated with 10,000 replicates.

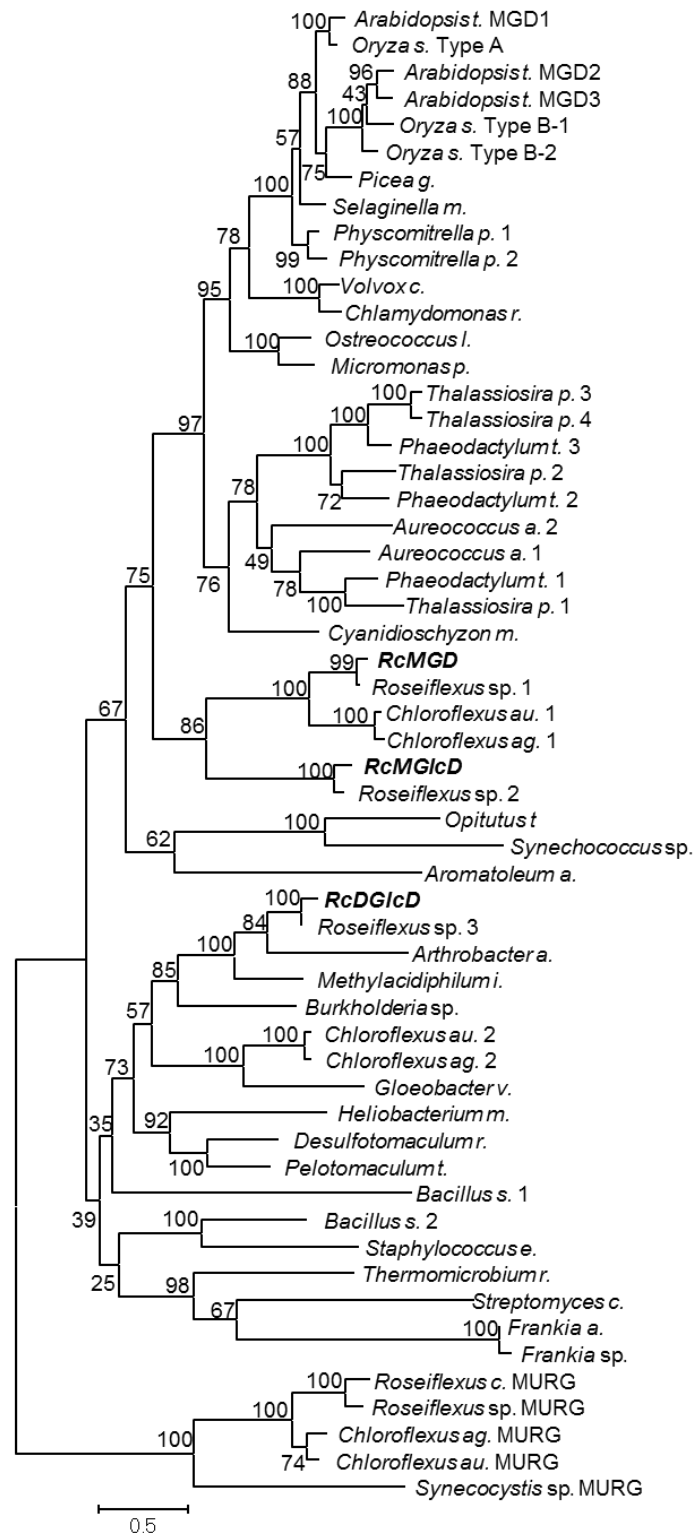


FIG. II-S3. A ML tree of the MGD amino acid dataset analyzed with RAxML under the WAG-F + G_4 model. MURG synthase genes were used as the outgroup. Numbers associated with individual branches represent bootstrap probabilities based on 1,000 bootstrap replications.

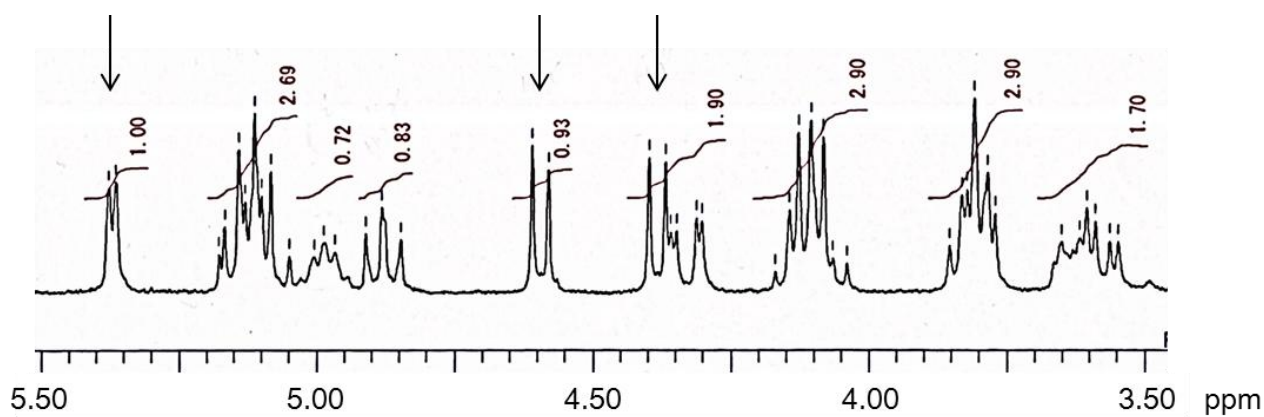


FIG. II-S4. Analysis of UL4 isolated from *R. castenholzii*.

UL4 isolated from *R. castenholzii* was analyzed by $^1\text{H-NMR}$ at 270 MHz. Arrows indicated peaks which were possible H-1 peaks of sugar head groups.

Materials and Methods

Phylogenetic Analyses

To obtain MGD gene sequences, blastp and tblastn searches were performed against the Protein (nr), GenBank, and EST databases at the National Center for Biotechnology Information website (www.ncbi.nlm.nih.gov/), using Arabidopsis MGD amino acid sequences as queries. In addition, a blastp search was conducted against genomic data at the Department of Energy Joint Genome Institute (DOE-JGI) web site (www.jgi.doe.gov/). The resulting data are listed in Table II-1.

MGD amino acid sequences were aligned using MACSIMS (Thompson et al., 2006) and MUSCLE (Edgar, 2004), followed by a partial manual correction. To refine these data for phylogenetic analysis, the 5' and 3' terminal regions of MGD gene and regions where > 15% of the species had a sequence gap were eliminated from the alignment. The refined data were then subjected to phylogenetic analyses with Bayesian inference and maximum likelihood (ML). MrBayes ver 3.1.2 (Ronquist et al., 2003) was used for Bayesian inference under the WAG + Γ_4 model. Two runs with 4 chains of Markov chain Monte Carlo (MCMC) iterations were performed for 4,000,000 generations. Trees were sampled every 100 generations, and the first 10,000 trees (1,000,000 generations) were discarded as burn-in. Treefinder ver. Oct. 2008 (Jobb et al, 2004) was used for ML analyses under the WAG-F + Γ_8 model. Approximate bootstrap supports (LR-ELW; expected likelihood weights by the local

rearrangement) were calculated with 10,000 replicates. RAxML ver. 7.0.4 (Stamatakis, 2006) was also used for ML analyses under the WAG-F + Γ_4 model with 1,000 bootstrap replications.

Expression of MGD Homologs

The genes of 3 MGD homologs from *Roseiflexus castenholzii* were amplified by PCR and cloned into the pET28a vector respectively. Vectors were transformed into BL21 (DE3) competent *Escherichia coli* (*E. coli*). Transformed cells were grown in Luria-Bertani (LB) medium at 37°C until they reached an OD₆₀₀ reading of 0.7. Protein expression was induced using 1 mM isopropyl β -D-thiogalactopyranoside for 3 h (we designated 3 genes as RcMGD, RcMGlcD, and RcDGlcD according to their functions determined).

Assay for Glycolipid Synthesis

Glycolipid synthetic activity was assayed as described Awai et al (Awai et al., 2006). Radiolabeled lipids were separated by 1-dimensional thin-layer chromatography (TLC) in chloroform-hexane-isopropanol-tetrahydrofuran-water (50:100:80:1:2, by volume) or hexane-tetrahydrofuran-isopropanol-water (40:0.4:50:10, by volume) and detected by Image Analyzer (STORM860, Molecular Dynamics, Sunnyvale, Calif. or BAS2000, FUJIX).

Isolation of Glycolipids

Cultures of *E. coli* expressing RcMGD, RcMGlcD, or RcDGlcD were centrifuged at 3,500 xg for 10 min at 4°C. Pellets were homogenized in 5 ml of 50 mM TES-KOH buffer (pH 7.0) and 125 µl of 1 M MgCl₂. The enzyme solutions were sonicated and mixed with 115 µl of 30 mM UDP-Gal or UDP-Glc. These mixtures were incubated at 37°C for 3 h and total lipids were extracted as described previously (Bligh and Dyer, 1959). Total lipids were then purified by column chromatography (InterSep SI, GL Sciences). Elution solvents included chloroform, acetone-isopropanol (9:1, by volume), and methanol. Glycolipids were collected in the acetone-toluene fraction and then isolated by 1-dimensional TLC as above or using hexane-tetrahydrofuran-isopropanol-water (40:0.4:50:10, by volume). Finally, glycolipids were eluted using chloroform-methanol (2:1, by volume).

Roseiflexus castenholzii provided from Prof. Keizo Shimada was grown as described Yamada et al (Yamada et al., 2005). Roseiflexus total lipid was also extracted as described above (Bligh and Dyer, 1959). This lipid was developed by 2-D TLC using chloroform-methanol- 7 N ammonium hydroxide (120:80:8, by volume) in the first dimension and chloroform-methanol-acetic acid-water (170:20:15:3, by volume) in the second.

Acetylation of Glycolipids

The glycolipids isolated by 1-dimensional TLC were evaporated and then eluted using 0.5 ml of pyridine and 0.25 ml of acetic acid anhydride. These mixtures were incubated overnight in the dark. Subsequently, 5 ml of toluene was added to these mixtures and evaporated. This step was repeated 3 times. Finally, acetylated lipids were dissolved in chloroform and used for nuclear magnetic resonance (NMR).

Structural Analysis of Glycolipids by NMR

Acetylated lipids were dissolved in CDCl_3 . These structures were analyzed by $^1\text{H-NMR}$ at 600 MHz (Bruker AV-600), 400 MHz (Varian 400-MR) or 270 MHz (JEOL JNM-EX-270) for protons. Internal tetramethylsilane (σ 0 ppm) in CDCl_3 was used as the standard.

Chemical shifts were expressed in parts per million (ppm) with reference to the standard. The multiplicity of signals was abbreviated as follows: s = singlet, d = doublet, dd = doublet of doublets, t = triplet, and m = multiplet. The protons of the sugar head groups were denoted as H-1, H-1', H-2, H-2', H-3, H-3', H-4, H-4', H-5, H-5', H-6a, H-6'a, H-6b and H-6'b. The protons of the glycerol backbone were denoted as H-1''a, H-1''b, H-2'', H-3''a, and H-3''b. In MGDG (Fig. II-3A), $^1\text{H-NMR}$ (600 MHz, CDCl_3) δ 5.39–5.38 (d, 1H, $J_{3',4'} = 3.3$ Hz, H-4), 5.36–5.34 (m, 1.7H, fatty acid), 5.20–5.17 (m, 2H, H-2 and H-2''), 5.01 (dd, 1H, $J_{2',3'} = 10.3$ Hz, $J_{3',4'} = 3.3$ Hz, H-3), 4.48 (d, 1H, $J_{1',2'} = 7.9$ Hz, H-1), 4.31 (dd, 1H, $J_{1a,1b} = 12.0$ Hz, $J_{1a,2} = 3.4$ Hz, H-1''a), 4.18–4.08 (m, 3.5H, H-6a,6b, and H-1''b), 3.96 (dd, 1H, $J_{3a,3b} = 11.0$ Hz, $J_{2,3a} =$

= 5.0 Hz, H-3''a), 3.90 (t, 1H, $J_{5',6'a} = J_{5',6'b} = 6.7$ Hz, H-5), 3.77–3.66 (m, 1.7H, $J_{3a,3b} = 11.0$ Hz, $J_{2,3b} = 5.7$ Hz, H-3''b). In MGlcDG (Fig. II-3B), $^1\text{H-NMR}$ (600 MHz, CDCl_3) δ 5.35–5.34 (m, 1H, fatty acid), 5.20 (t, 1H, $J_{2',3'} = J_{3',4'} = 9.5$ Hz, H-3), 5.21–5.18 (m, 1H, H-2''), 5.08 (t, 1H, $J_{3',4'} = J_{4',5'} = 9.5$ Hz, H-5), 4.97 (dd, 1H, $J_{1',2'} = 7.9$ Hz, $J_{2',3'} = 9.5$ Hz, H-2), 4.52 (d, 1H, $J_{1',2'} = 7.9$ Hz, H-1), 4.30 (dd, 1H, $J_{6'a,6'b} = 12.0$ Hz, $J_{5',6'} = 3.4$ Hz, H-6a), 4.26 (dd, 1H, $J_{1a,1b} = 12.4$ Hz, $J_{1a,2} = 4.7$ Hz, H-1''a), 4.14–4.11 (m, 2H, H-6b and H-1''b), 3.95 (dd, 1H, $J_{3a,3b} = 10.9$ Hz, $J_{2,3a} = 4.9$ Hz, H-3''a), 3.69–3.66 (m, 3H, H-5, H-3''b, and fatty acid). In diglucosyldiacylglycerol (DGlcDG, Fig. II-4B), $^1\text{H-NMR}$ (400 MHz, CDCl_3) δ 5.36–5.33 (m, 4H, fatty acid), 5.21–5.16 (m, 3H, H-2'', H-4, and H-4'), 5.07 (t, 1H, $J_{2'',3''} = J_{3'',4''} = 10.0$ Hz, H-3'), 4.98 (dd, 1H, $J_{1',2'} = 7.9$ Hz, $J_{2',3'} = 9.5$ Hz, H-2), 4.92 (dd, 1H, $J_{1'',2''} = 9.7$ Hz, $J_{2'',3''} = 7.9$ Hz, H-2'), 4.89 (t, 1H, $J_{2',3'} = J_{3',4'} = 9.5$ Hz, H-3), 4.57 (d, 1H, $J_{1',2'} = 7.9$ Hz, H-1), 4.47 (d, 1H, $J_{1'',2''} = 7.9$ Hz, H-1'), 4.31–4.26 (m, 2H, H-1''a and H-6'a), 4.14–4.09 (m, 2H, H-1''b and H-6'b), 3.97 (dd, 1H, $J_{6'a,6'b} = 10.8$ Hz, $J_{5',6'} = 5.1$ Hz, H-6a), 3.87 (dd, 1H, $J_{3a,3b} = 10.8$ Hz, $J_{2,3a} = 2.0$ Hz, H-3''a), and 3.73–3.65 (m, 4H, H-5, H-5', H-3''b, and H-6b). In MGDG (Fig. II-5B), $^1\text{H-NMR}$ (270 MHz, CDCl_3) δ 5.38 (d, 1H, $J_{3',4'} = 3.3$ Hz, H-4), 5.20 (dd, 1H, $J_{1',2'} = 7.9$ Hz, $J_{2',3'} = 10.3$ Hz, H-2), 5.01 (dd, 1H, $J_{2',3'} = 10.5$ Hz, $J_{3',4'} = 3.3$ Hz, H-3), 5.00–4.93 (m, 1H, H-2''), 4.47 (d, 1H, $J_{1',2'} = 7.9$ Hz, H-1), 4.20–4.05 (m, 2H, H-6a, 6b), 3.88 (dd, 2H, $J = 11.9, 6.0$ Hz, H-5, H-1''a), 3.60 (dd, 1H, $J_{1a,1b} = 11.1$ Hz, $J_{1b,2} = 4.1$ Hz, H-1''b), 3.15–3.10 (m, 1.7H, H-3''a, 3''b).

References

Awai, K., Kakimoto, T., Awai, C., Kaneko, T., Nakamura, Y., Takamiya, K., Wada, H., and

Ohta, H. 2006, Comparative genomic analysis revealed a gene for

monoglucosyldiacylglycerol synthase, an enzyme for photosynthetic membrane lipid

synthesis in cyanobacteria, *Plant Physiol.*, 141, 1120–1127.

Blankenship, R.E. 2010, Early evolution of photosynthesis, *Plant Physiol.*, 154, 434–438.

Bligh, E.G., and Dyer, W.J. 1959, A rapid method of total lipid extraction and purification,

Can. J. Biochem. Physiol., 37, 911–917.

Botté, C.Y., Yamaryo-Botté, Y., Janouskovec, J., Rupasinghe, T., Keeling, P.J., Crellin, P.,

Coppel, R.L., Maréchal, E., McConville, M.J., and McFadden, G.I. 2011, Identification of

Plant-like Galactolipids in *Chromera velia*, a Photosynthetic Relative of Malaria Parasites, *J.*

Biol. Chem., 286, 29893-29903

Edgar, R.C. 2004, MUSCLE: multiple sequence alignment with high accuracy and high

throughput, *Nucleic Acids Res.*, 32, 1792–1797.

Hanada, S., Hiraishi, A., Shimada, K., and Matsuura, K. 1995, *Chloroflexus aggregans* sp.

nov., a filamentous phototrophic bacterium which forms dense cell aggregates by active

gliding movement, *Int. J. Syst. Bacteriol.*, 45, 676–681.

Harper, J.T., and Keeling, P.J. 2003, Nucleus-encoded, plastid-targeted glyceraldehyde-3-phosphate dehydrogenase (GAPDH) indicates a single origin for chromalveolate plastids, *Mol. Biol. Evol.*, 20, 1730–1735.

Hözl, G., and Dörmann, P. 2007, Structure and function of glycoacyl lipids in plants and bacteria, *Prog. Lipid. Res.*, 46, 225–243.

Hözl, G., Zähringer, U., Warnecke, D., and Heinz, E. 2005, Glycoengineering of cyanobacterial thylakoid membranes for future studies on the role of glycolipids in photosynthesis, *Plant Cell Physiol.*, 46, 1766–1778.

Jobb, G., von Haeseler, A., and Strimmer, K. 2004, TREEFINDER: a powerful graphical analysis environment for molecular phylogenetics, *BMC Evol. Biol.*, 4, 18.

Knudsen, E., Jantzen, E., Bryn, K., Ormerod, J., and Sirevåg, R. 1982, Quantitative and structural characterization of lipids in *Chlorobium* and *Chloroflexus*, *Arch. Microbiol.*, 132, 149-154.

Masuda, S., Harada, J., Yokono, M., Yuzawa, Y., Shimojima, M., Murofushi, K., Tanaka, H., Masuda, H., Murakawa, M., Haraguchi, T., Kondo, M., Nishimura, M., Yuasa, H., Noguchi, M., Oh-Oka, H., Tanaka, A., Tamiaki, H., and Ohta, H. 2011, A

Monogalactosyldiacylglycerol Synthase Found in the Green Sulfur Bacterium

Chlorobaculum tepidum Reveals Important Roles for Galactolipids in Photosynthesis, *Plant Cell*, 23, 2644-2658

Nelissen, B., Van de Peer, Y., Wilmotte, A., and De Wachter, R. 1995, An early origin of plastids within the cyanobacterial divergence is suggested by evolutionary trees based on complete 16S rRNA sequences, *Mol. Biol. Evol.*, 12, 1166–1173.

Ronquist, F., and Huelsenbeck, J.P. 2003, MrBayes 3: Bayesian phylogenetic inference under mixed models, *Bioinformatics*, 19, 1572–1574.

Yoon, H.S., Hackett, J.D., Pinto, G., and Bhattacharya, D. 2002, The single, ancient origin of chromist plastids, *Proc. Natl. Acad. Sci. U. S. A.*, 99, 15507–15512.

Sato, N., and Murata, N. 1982, Lipid biosynthesis in the blue-green alga, *Anabaena variabilis*

I. Lipid classes, *Biochim. Biophys. Acta.*, 710, 271–278.

Stamatakis, A. 2006, RAxML-VI-HPC: maximum likelihood-based phylogenetic analyses with thousands of taxa and mixed models, *Bioinformatics*, 22, 2688–2690.

Suzuki, K., and Miyagishima, S.Y. 2010, Eukaryotic and eubacterial contributions to the establishment of plastid proteome estimated by large-scale phylogenetic analyses, *Mol. Biol. Evol.*, 27, 581-590.

Thompson, J.D., Muller, A., Waterhouse, A., Procter, J., Barton, G.J., Plewniak, F., and Poch, O. 2006, MACSIMS: multiple alignment of complete sequences information management system, *BMC Bioinformatics*, 7, 318.

Turner, S., Pryer, K.M., Miao, V.P., and Palmer, J.D. 1999, Investigating deep phylogenetic relationships among cyanobacteria and plastids by small subunit rRNA sequence analysis, *J. Eukaryot. Microbiol.*, 46, 327–338.

Yamada, M., Zhang, H., Hanada, S., Nagashima, K.V., Shimada, K., and Matsuura, K. 2005, Structural and spectroscopic properties of a reaction center complex from the

chlorosome-lacking filamentous anoxygenic phototrophic bacterium *Roseiflexus castenholzii*,

J. Bacteriol., 187, 1702-1709.

II-2 The estimation of divergence point type A and B MGDG synthases

Results and Discussion

The Divergence Point of Type A and Type B MGDs

Determining the time at which the 2 types of MGDs (type A and type B) diverged is important to understand the evolution of photosynthetic membranes in land plants (Kobayashi et al., 2009). Using both Bayesian inference and ML methods, I performed phylogenetic analyses on MGD gene sequences of land plants, excluding 3rd codon positions (fig. II-8 and 9). Results from these analyses generally agreed with accepted phylogenetic relationships of land plants. For example, *Angiospermae* were clearly divided into *Monocotyledoneae* (monocots) and *Dicotyledoneae* (dicots) in both types of MGDs. The groupings received strong support by both Bayesian inference and ML methods (fig. II-8 and 9). These results indicate that MGDs have been conserved throughout the course of land plant evolution. Importantly, one full-length MGD gene sequence of *Picea glauca* was available among *Gymnospermae*, and both Bayesian and ML analyses placed the *Picea* sequence close to the type B MGD clade. Although a *Gymnospermae* type A MGD has not yet been identified, this result suggests that the type A/B divergence may have preceded that of *Angiospermae* and *Gymnospermae*.

Based on the phylogenetic tree, I estimated a MGD type A/B divergence time using

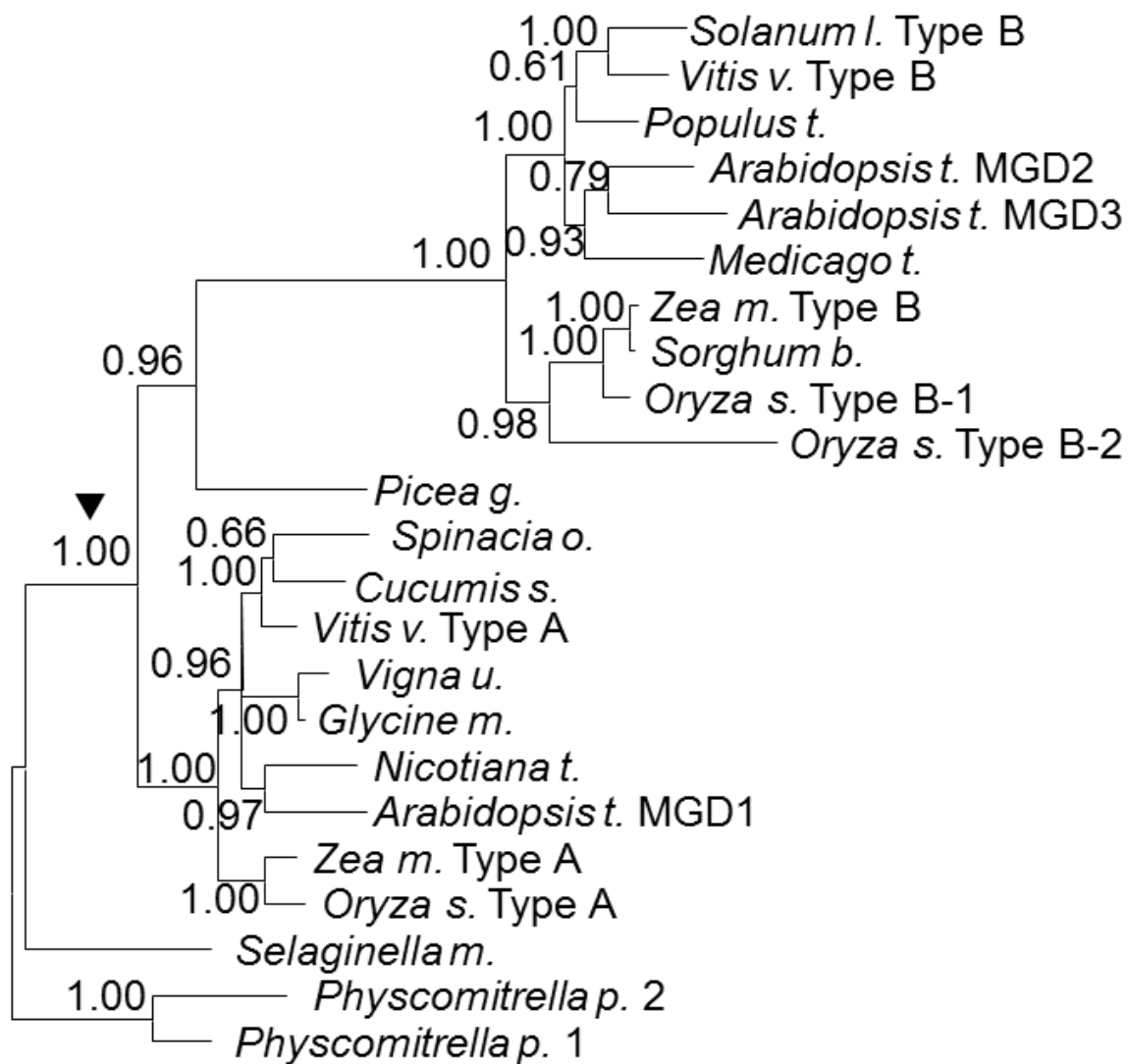


FIG. II-8. A phylogenetic tree of land plant MGDs based on Bayesian inference under the GTR + G₄ model. The nucleotide dataset of the 1st and 2nd codon positions was used for the analysis. Numbers associated with individual branches represent the posterior probability. Arrowhead indicates the divergence of type A and type B MGDs.

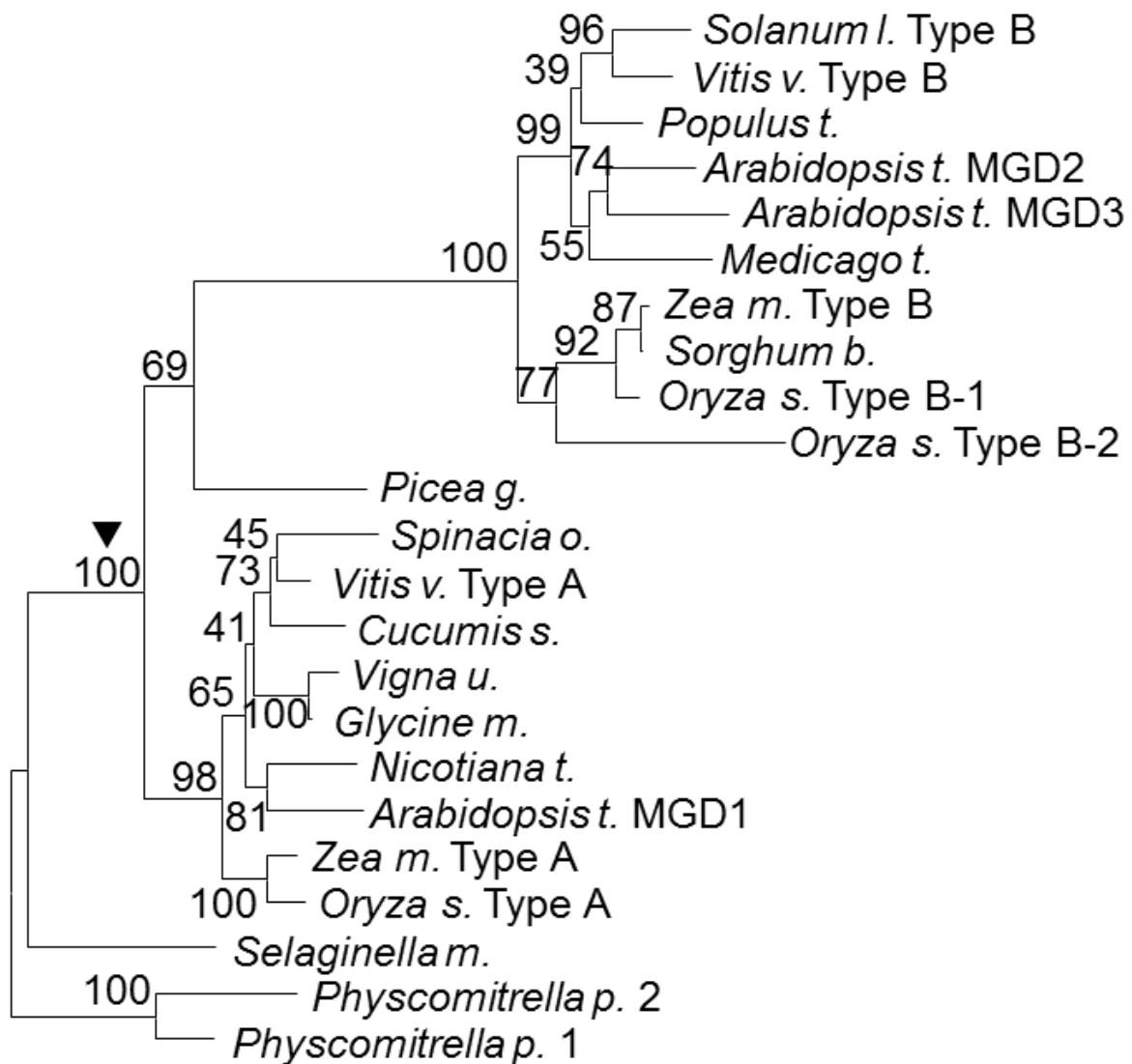


FIG. II-9. An ML tree of land plant MGDs analyzed with RAxML under the GTR + G_8 model. The nucleotide dataset of the 1st and 2nd codon positions was used for the analysis. Numbers associated with individual branches represent bootstrap probabilities based on 1,000 bootstrap replications. Arrowhead indicates the divergence of type A and type B MGDs.

4 calibration points (similar to Yoon et al.; Yoon et al., 2004). My analysis indicated that MGDs likely diverged ~323 million years ago (MYA), with 298–357 MYA representing the 95% confidence interval (Fig. II-10). This divergence time corresponds to the Carboniferous period, which came after *Spermatophyta* appeared (355–370 MYA). I propose, therefore, that the acquisition of 2 types of MGDs occurred in the common ancestor of *Spermatophyta*.

My data indicate that MGD gene duplication and subsequent functional differentiation occurred in *Spermatophyta* (Fig. II-11). Jiao et al. showed that a whole-genome duplication (WGD) event occurred in the common ancestor of all seed plants (Jiao et al., 2011). This WGD allowed for major adaptive changes in these organisms and contributed to the dominance of seed plants. Interestingly, type B *MGD* expression is elevated during the reproduction stage of seed plants (Kobayashi et al., 2004). The expression is detected in non-photosynthetic tissues such as flowers and roots. In floral organ, especially, the strong expression is observed in pollen grains and tubes. Indeed, the accumulations of MGD and DGDG during pollen tube growth were reported (Nakamura et al., 2009).

Additionally, it was revealed that DGDG localizes in the plasma membrane of the pollen tube and MGDG and DGDG contributes membrane expansion (Botte et al., 2011). During the Carboniferous period, spore-producing plants were dominant (DiMichele et al., 2001), whereas this dominance shifted to seed plants shortly thereafter. The Carboniferous and Permian periods were also characterized by dramatic changes to the global climate, primarily

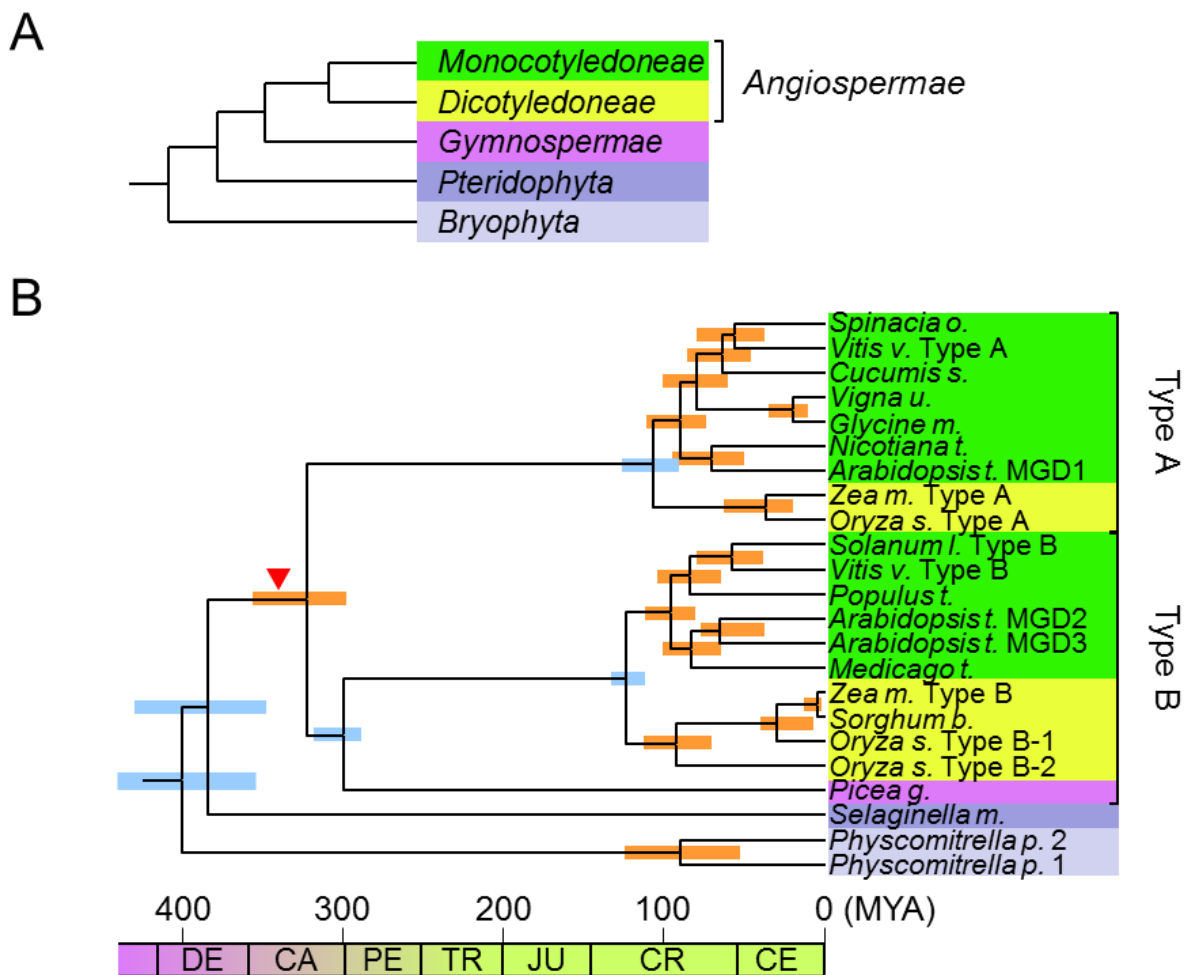


FIG. II-10. The divergence time of type A and type B MGDs.

(A) A generally accepted evolution model of land (Pryer et al., 2001, Palmer et al., 2004). (B) Divergence time estimation among MGDs of land plants based on the nucleotide dataset of the 1st and 2nd codon positions. Horizontal bars (blue and orange) indicate 95% credible intervals of the divergence time estimates. The 5 nodes used as time constraints are indicated with blue bars. The original ML and Bayesian trees used for the divergence time estimation are shown in figure II-8 and 9. Arrowhead indicates the divergence of type A and type B MGDs. DE, Devonian; CA, Carboniferous; PE, Permian; TR, Triassic; JU, Jurassic; CR, Cretaceous; CE, Cenozoic.

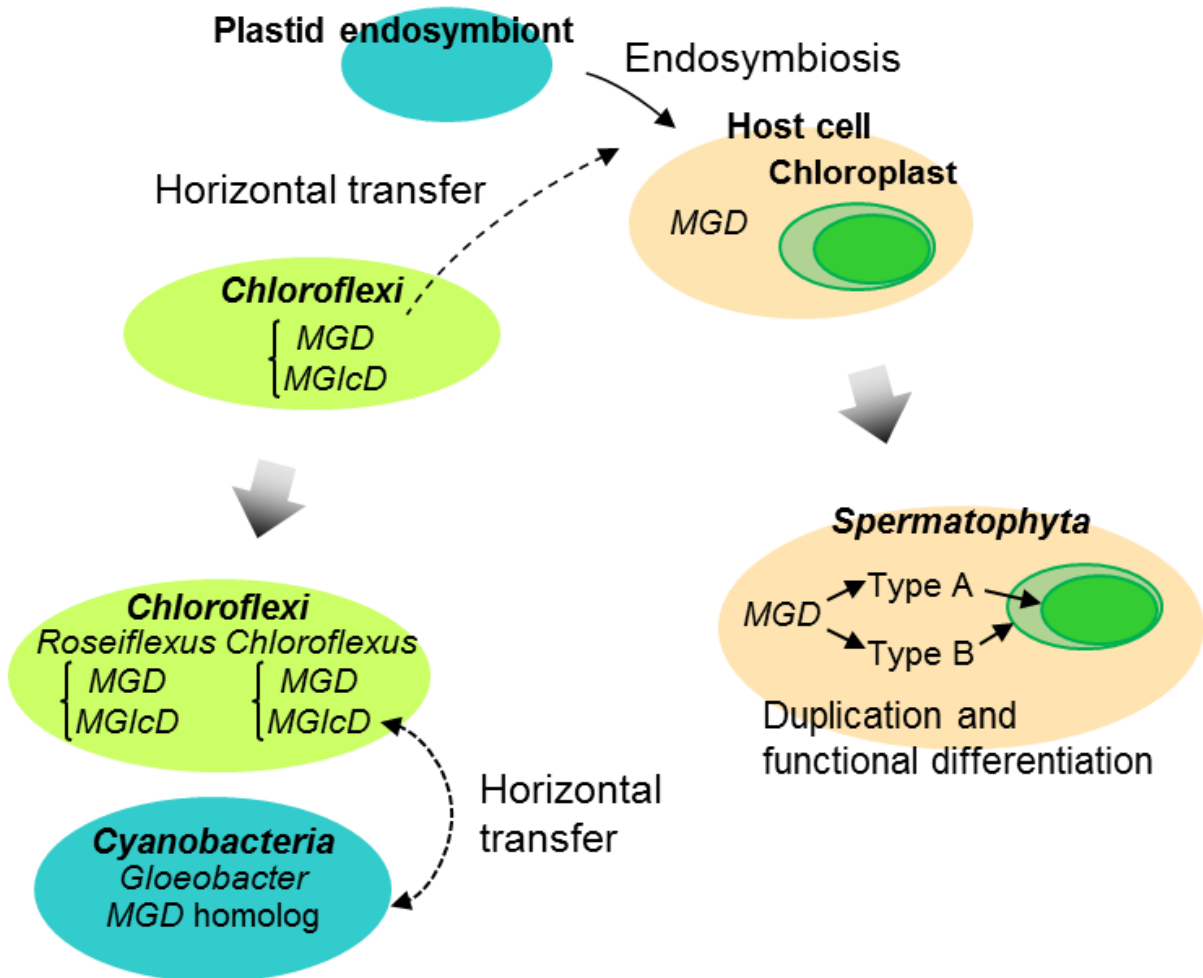


FIG. II-11. Proposed model for MGD evolution.

The requirement of MGDG in photosynthetic processes was established in ancient times. For MGDs, duplication and functional divergence occurred in *Spermatophyta*. Black dashed arrows indicate horizontal gene transfer. Large, shaded black arrows indicate evolutionary progression.

drying. Expression of type B MGDs is elevated during phosphate deprivation, a response that is regulated by both auxin and cytokinin (Kobayashi et al., 2006). These regulatory mechanisms may have worked for response to these climate changes. More extensive research concerning the MGDs of *Gymnospermae* is required for a thorough understanding of MGD gene evolution. It is important to determine whether there is a species of *Gymnospermae* that has 2 types of MGDs. The evolution of *Gymnospermae*, however, has not been adequately mapped, in part because a complete genome sequence is not available. Determining the divergence time of type A and B MGDs in *Gymnospermae* may prove critical if we are to understand the divergence of land plants.

Table II-S1. MGD Gene Sequences Used for Analysis

Classification	Species	Indication in Phylogenetic tree	Types of MGDG Synthases	Accession Number	Database
Angiosperm	<i>Arabidopsis thaliana</i>	<i>Arabidopsis t.</i> MGD1	Type A (MGD1)	NM_119327	NCBI
Angiosperm	<i>Arabidopsis thaliana</i>	<i>Arabidopsis t.</i> MGD2	Type B (MGD2)	NM_122048	NCBI
Angiosperm	<i>Arabidopsis thaliana</i>	<i>Arabidopsis t.</i> MGD3	Type B (MGD3)	NM_126865	NCBI
Angiosperm	<i>Cucumis sativus</i>	<i>Cucumis s.</i>	Type A	U62622	GenBank
Angiosperm	<i>Glycine max</i>	<i>Glycine m.</i>	Type A	AB047475	GenBank
Angiosperm	<i>Medicago truncatula</i>	<i>Medicago t.</i>	Type A	BT053131	GenBank
Angiosperm	<i>Nicotiana tabacum</i>	<i>Nicotiana t.</i>	Type A	AB047476	GenBank
Angiosperm	<i>Oryza sativa</i>	<i>Oryza s.</i> Type A	Type A	AK243359	GenBank
Angiosperm	<i>Oryza sativa</i>	<i>Oryza s.</i> Type B-1	Type B	AB112060	GenBank
Angiosperm	<i>Oryza sativa</i>	<i>Oryza s.</i> Type B-2	Type B	NM_001068022	NCBI
Angiosperm	<i>Populus trichocarpa</i>	<i>Populus t.</i>	Type B	XM_002324578	NCBI
Angiosperm	<i>Solanum lycopersicum</i>	<i>Solanum l.</i>	Type B	AK247697	GenBank
Angiosperm	<i>Sorghum bicolor</i>	<i>Sorghum b.</i>	Type B	XM_002452947	NCBI
Angiosperm	<i>Spinacia oleracea</i>	<i>Spinacia o.</i>	Type A	AJ249607	GenBank
Angiosperm	<i>Vigna unguiculata</i>	<i>Vigna u.</i>	Type A	DQ205521	GenBank
Angiosperm	<i>Vitis vinifera</i>	<i>Vitis v.</i> Type A	Type A	AM488307	GenBank
Angiosperm	<i>Vitis vinifera</i>	<i>Vitis v.</i> Type B	Type B	CU459387	GenBank
Angiosperm	<i>Zea mays</i>	<i>Zea m.</i> Type A	Type A	EU954700	GenBank
Angiosperm	<i>Zea mays</i>	<i>Zea m.</i> Type B	Type B	EU956572	GenBank
Gymnosperm	<i>Picea glauca</i>	<i>Picea g.</i>	Type B	EX354732, DR562549	GenBank
Pteridophyta	<i>Selaginella moellendorffii</i>	<i>Selaginella m.</i>		XM_002973090	NCBI
Bryophyta	<i>Physcomitrella patens</i>	<i>Physcomitrella p.</i> 1		XM_001758638	NCBI
Bryophyta	<i>Physcomitrella patens</i>	<i>Physcomitrella p.</i> 2		XM_001755818	NCBI

Materials and Methods

Phylogenetic Analyses

To calculate the divergence time of type A and type B MGDs, the nucleotide sequences of land plant MGDs (the 1st and 2nd codon positions) were subjected to Bayesian and ML phylogenetic analyses. Sequence data are listed in Table II-S1. MrBayes ver 3.1.2 was used for Bayesian tree inference with 1,000,000 generations under the GTR + Γ_8 model. Trees were sampled every 100 generations, and the first 2,500 trees (250,000 generations) were discarded as burn-in. The ML tree was estimated using RAxML ver. 7.0.4 under the GTR + Γ_4 model with 1,000 bootstrap replications. In both phylogenetic analyses, different model parameters were estimated between the 1st and 2nd codon position data. Divergence times were estimated based on the 1st and 2nd codon sequences under a relaxed clock model using the MCMCTREE program in the PAML4 package (Yang et al., 2007). The model parameters were separately estimated between the 1st and 2nd codon sequences under the HKY + Γ_5 model. The number of MCMC samples and burn-in were set to 10,000 and 2,500, respectively. The following constraints were used for time calibrations (similar to Yoon et al.²): 1) divergence of vascular plants from other land plants < 432 million years ago (MYA) (Kenrick and Crane (Kenrick and Crane, 1997) provided the origin of land plants), 2) divergence of seed plants from other vascular plants > 355 MYA (Gillespie et al. (Gillespie et al., 1981) provided the oldest known seeds), 3) 290–320 MYA for the *Angiospermae*–

Gymnospermae split, and 4) 90–130 MYA for the *Monocotyledoneae–Dicotyledoneae* split

(Crane et al., 1995).

References

- Botté, C.Y., Deligny, M., Roccia, A., et al. 2011, Chemical inhibitors of monogalactosyldiacylglycerol synthases in *Arabidopsis thaliana*, *Nat. Chem. Biol.*, 7, 834-842.
- Crane, P.R., Friis, E.M., and Pedersen, K.R. 1995, The origin and early diversification of angiosperms, *Nature*, 374, 27–33.
- DiMichele, W.A., Pfefferkorn, H.W., and Gastaldom, R.A. 2001, Response of late carboniferous and early Permian plant communities to climate change, *Annu. Rev. Earth. Planet Sci.*, 29, 461–487.
- Gillespie, W.H., Rothwell, G.W., and Scheckler, S.E. 1981, The earliest seeds, *Nature*, 293, 462–464.
- Jiao, Y., Wickett, N.J., Ayyampalayam, S., et al. 2011, Ancestral polyploidy in seed plants and angiosperms, *Nature*, 473, 97–100.
- Kenrick, P., and Crane, P.R. 1997, The origin and early evolution of plants on land, *Nature*,

389, 33–39.

Kobayashi, K., Awai, K., Takamiya, K., and Ohta, H. 2004, Arabidopsis type B monogalactosyldiacylglycerol synthase genes are expressed during pollen tube growth and induced by phosphate starvation, *Plant Physiol.*, 134, 640–648.

Kobayashi, K., Masuda, T., Takamiya, K., and Ohta, H. 2006, Membrane lipid alteration during phosphate starvation is regulated by phosphate signaling and auxin/cytokinin cross-talk, *Plant J.*, 47, 238–248.

Kobayashi, K., Nakamura, Y., and Ohta, H. 2009, Type A and type B monogalactosyldiacylglycerol synthases are spatially and functionally separated in the plastids of higher plants, *Plant Physiol. Biochem.*, 47, 518-525.

Nakamura, Y., Kobayashi, K., and Ohta, H. 2009, Activation of galactolipid biosynthesis in development of pistils and pollen tubes, *Plant Physiol. Biochem.*, 47, 535-539.

Palmer, J.D., Soltis, D.E., and Chase, M.W. 2004, The plant tree of life: an overview and some points of view, *Am. J. Bot.*, 91, 1437–1445.

Pryer, K.M., Schneider, H., Smith, A.R., et al. 2001, Horsetails and ferns are a monophyletic group and the closest living relatives to seed plants, *Nature*, 409, 618–622.

Yang, Z. 2007, PAML 4: phylogenetic analysis by maximum likelihood, *Mol. Biol. Evol.*, 24, 1586–1591.

Yoon, H.S., Hackett, J.D., Ciniglia, C., Pinto, G., and Bhattacharya, D. 2004, A molecular timeline for the origin of photosynthetic eukaryotes, *Mol. Biol. Evol.*, 21, 809–818.

Chapter III

The analyses for the cyanobacterial pathway for MGDG synthesis

Introduction

As described in Chapter II, the pathways for MGDG synthesis in cyanobacteria and higher plants are different. Plant-type MGDG synthase (MGD) is generally absent in cyanobacterial genomes. Instead, genes for MGlcDG synthase (MGlcD) are widely found in cyanobacteria (Chapter I, Fig. I-1). In cyanobacteria, MGlcDG is synthesized as the intermediate for MGDG synthesis (Sato and Murata, 1982a). Under normal growth conditions, the amount of MGlcDG in cyanobacteria is less than 1% of the total membrane lipids. However, it has been reported that MGlcDG was accumulated upon heat stress in *Synechocystis* sp. PCC 6803 (Balogi et al., 2005, Shimojima et al., 2009). MGlcDG contained highly saturated fatty acids and the ratio of saturated fatty acids in MGlcDG was increased by heat-shock treatment. It was indicated that the ratio of saturated fatty acids to unsaturated fatty acid and the perturbation of membrane lipoprotein complexes are involved in the perception of rapid temperature changes in yeast (Carratù et al., 1996). Additionally, it was also reported that MGlcDG was strongly interacted with heat-shock protein HSP17. In *Synechocystis*, heat shock proteins such as HSP17 and chaperonins (GroEL etc) have been reported to regulate

thylakoid membrane fluidity (Horváth et al., 1998, Vigh et al., 1998). These reports suggested that MGlcDG was involved in heat-stress response to stabilize thylakoid membranes by interacting with HSP17. However, physiological function of MGlcDG has not been well established. One of the reasons is that lack of MGlcD gene (*mgld*) may cause lethality in cyanobacteria because it consequently leads to deficiency in the most abundant lipid MGDG that is critical for phototrophs (Kobayashi et al., 2007, Masuda et al., 2011). In this study, to clarify the physiological function of MGlcDG, I performed complementation of the cyanobacterial MGDG synthesis pathway by higher plant MGD. The complementation strain showed a significant reduction of MGlcDG synthesis activity and no accumulation of MGlcDG. In this chapter, I discuss the influence of MGlcDG deficiency in *Synechocystis*.

Results

Complementation of the cyanobacterial MGDG synthesis pathway by higher plant and bacterial MGDG synthases

In order to clarify the physiological function of MGlcDG, construction of MGlcDG deficient mutant is necessary. Figure III-1A shows that a schematic description for the kanamycin cassette insertion into the coding region of MGlcDG synthase (MGlcD, encoded by sll1377) gene (*mglcd*) in *Synechocystis* sp. PCC 6803. However, as *mglcd* is present as a single-copy gene in a chromosomal DNA of *Synechocystis*, complete knockout of *mglcd* would result in MGDG deficiency which is critical in the cyanobacterium. In fact, although $\Delta mglcd$ heterozygous mutant (Het) was continuously cultivated in BG-11 plate with kanamycin, the homozygous mutant was not screened. Moreover, Het was grown under heterotrophic condition (BG-11 plate with 5 mM glucose) because the reduction of MGDG would affect to the photosynthesis activity. However, I could not isolate the homozygous mutant. To obtain $\Delta mglcd$, I expressed *Arabidopsis thaliana* MGD1 (AtMGD1) or *Chlorobaculum tepidum* MGDG synthase A (CtMgdA) (Masuda et al., 2011) in Het, and then $\Delta mglcd$ mutant was screened. Additionally, plasmid-derived *mglcd* complemented line was also constructed in homozygous $\Delta mglcd$ background as a control. Table III-1 showed abbreviations of each strain. Since a *Synechocystis* cell has around ten copies of the chromosomal DNA (Herdman et al., 1979), I checked the disruption of *mglcd* by PCR. In the

Table III-1. Abbreviation of each strain

Abbreviations	
WT	Wild type
Het	Heterozygous line of $\Delta mglcd$
MGlCD-CP	pSL1211:: <i>mglcd</i> / $\Delta mglcd$
MGD1-CP	pSL1211:: <i>AtMGD1</i> / $\Delta mglcd$
MgdA-CP	pSL1211:: <i>ctmgdA</i> / $\Delta mglcd$

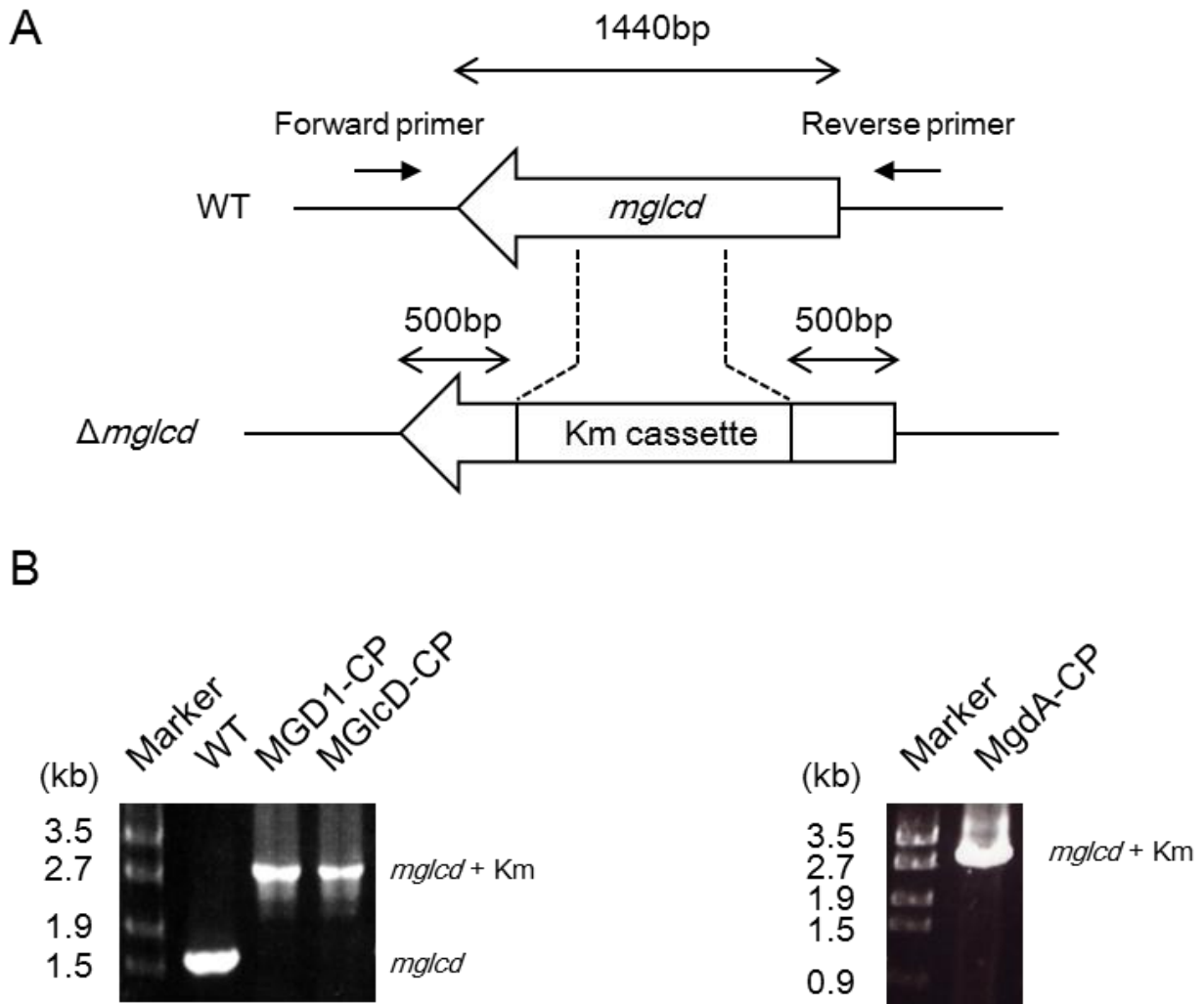


FIG. III-1. Construction of each strain of *Synechocystis* sp. PCC 6803.

(A) Schematic description of gene manipulation for MGlcdG synthase mutant ($\Delta mglcd$). Forward primer and reverse used for genome PCR analysis are shown. WT, wild type; Km, kanamycin.

(B) PCR analysis for checking the genotypes of *mglcd* locus in each strain. MGD1-CP, complemented strain by *AtMGD1*; MGlcd-CP, complemented strain by plasmid-derived *mglcd*; MgdA-CP, complemented strain by *ctmgdA*; Km, kanamycin cassette.

case of the wild type, using a primer set for *mglcd* (Fig. III-1A), it is expected that ~1.5 kb DNA fragment is amplified. On the other hand, in $\Delta mglcd$, ~2.8 kb DNA fragment was amplified, whereas the native fragment was not amplified. This PCR analysis showed that all copies of *mglcd* were disrupted by the kanamycin cassettes (Fig. III-1B). Then, I measured MGlcDG synthesis activity using membrane fractions of each strain with radiolabeled UDP-Glc as a substrate. MGlcD has transmembrane domains and the MGlcDG synthase activity is found in a membrane fraction in *Synechocystis* (Awai et al., 2006, Shimojima et al., 2009). Figure III-2 showed that MGlcDG synthesis activity was dramatically decreased in both MGD1-CP and MgdA-CP. It demonstrated that their cyanobacterial MGDG synthesis pathways were disrupted.

To confirm whether each MGD is functional, MGDG synthesis activity was measured using soluble fractions of each strain with UDP-Gal as a substrate (Fig. III-3). The products of these reactions were developed by thin layer chromatography. In this experiment, cucumber (*Cucumis sativus*) MGD (CsMGD) and *Synechocystis* wild type extract were used as positive and negative controls for MGDG synthesis, respectively. In MGD1-CP and MgdA-CP, MGDG was synthesized by each enzyme. Obviously, it was revealed that plant-type pathway for MGDG synthesis is functional in *Synechocystis* and the cyanobacterial MGDG synthesis pathway is able to be replaced by the plant-type pathway *in vivo*.

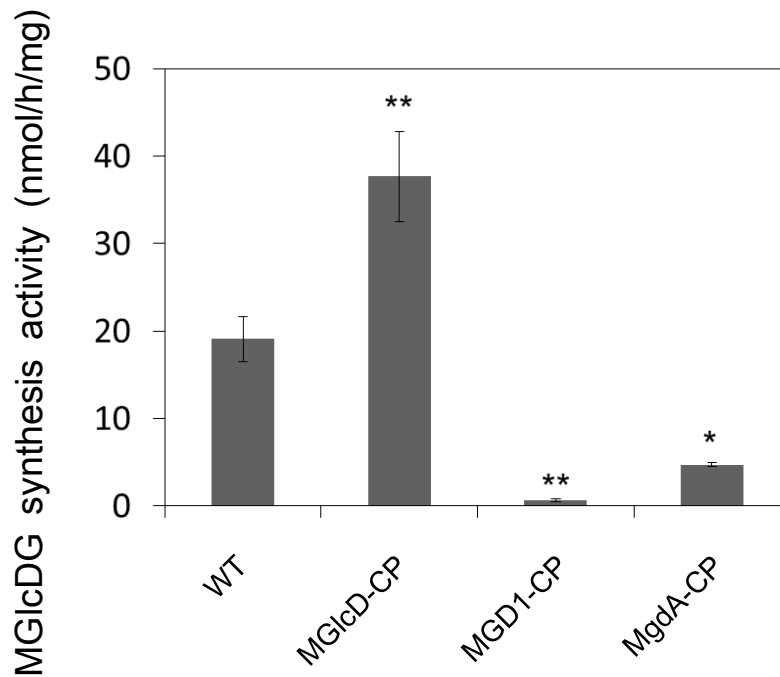


FIG. III-2. MGlcDG synthesis activity.

MGlcDG synthesis activity was measured with membrane fraction of each strain. The values are the means \pm SD of three biological replications. *P < 0.025, **P < 0.01, t test (compared with the wild type).

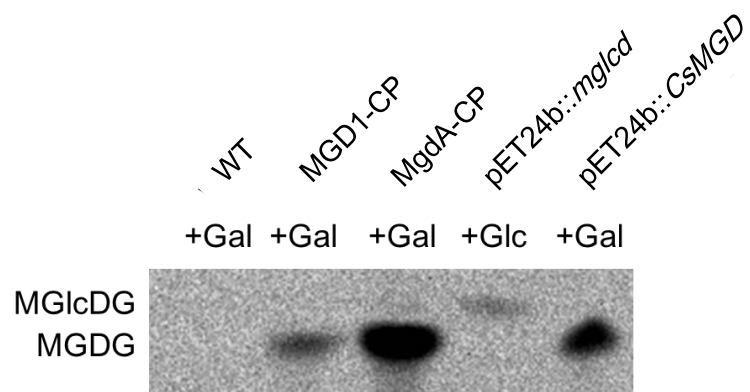


FIG. III-3. MGDG synthesis activity.

Radiolabeled UDP-Gal (+Gal) or UDP-Glc (+Glc) was used as substrates. The resulting lipids were separated by TLC (chloroform-hexane-tetrahydrofuran-isopropanol-water, 50:100:1:80:2 by volume) and visualized by autoradiography. *CsMGD* (pET24b) and *mgld* (pET24b) were used as controls for MGDG and MGlcDG, respectively.

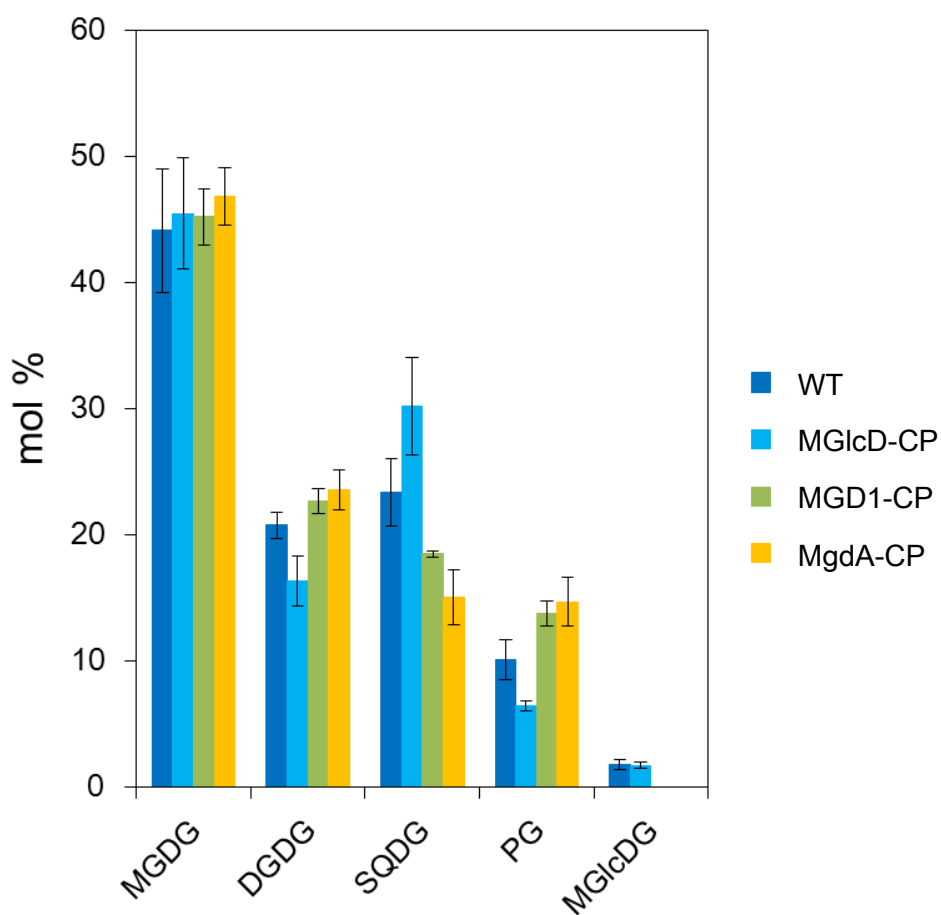


FIG. III-4. Lipid composition of each strain of *Synechocystis*.

Cells were grown at 30°C in BG-11 medium under photoautotrophic condition. The values are the means \pm SD of three biological replications.

Lipid composition of MGlcDG deficient mutants

To check the content of MGlcDG in each strain, lipids were extracted from *Synechocystis* whole cells and analyzed by gas chromatography (GC). In Figure III-4, changes in the contents of MGlcDG were shown in the wild type and complemented lines. Although cells of the wild type and MGlcD-CP contain MGlcDG, MGlcDG was not detected in MGD1-CP and MgdA-CP. Since the amount of MGlcDG is ~1% of total lipid, detection of much smaller amount of MGlcDG is difficult. It was reported that the amount of MGlcDG in *Synechocystis* grown in BG-11 with 5 mM glucose was much increased (Sato, 1994). To clarify whether a small amount of MGlcDG is synthesized in the complemented strains, lipids from *Synechocystis* grown under this accumulation condition were analyzed. Figure III-5 showed the MGlcDG contents in the wild type and MGD1-CP grown in BG-11 medium with 5 mM glucose. In case of the wild type, MGlcDG was accumulated ~7% of total lipids under glucose-containing conditions. However, in MGD1-CP, MGlcDG is not accumulated even under glucose-containing conditions. These results demonstrated that MGlcDG is completely lacking or otherwise, the amount is very slight in MGlcDG-deficient mutants.

Influence of MGlcDG deficiency on photosynthesis

To examine the effect of MGlcDG deficiency on photosynthesis, I monitored the growth rate in each strain (Fig. III-6). Under photoautotrophic conditions, despite the lack of MGlcDG,

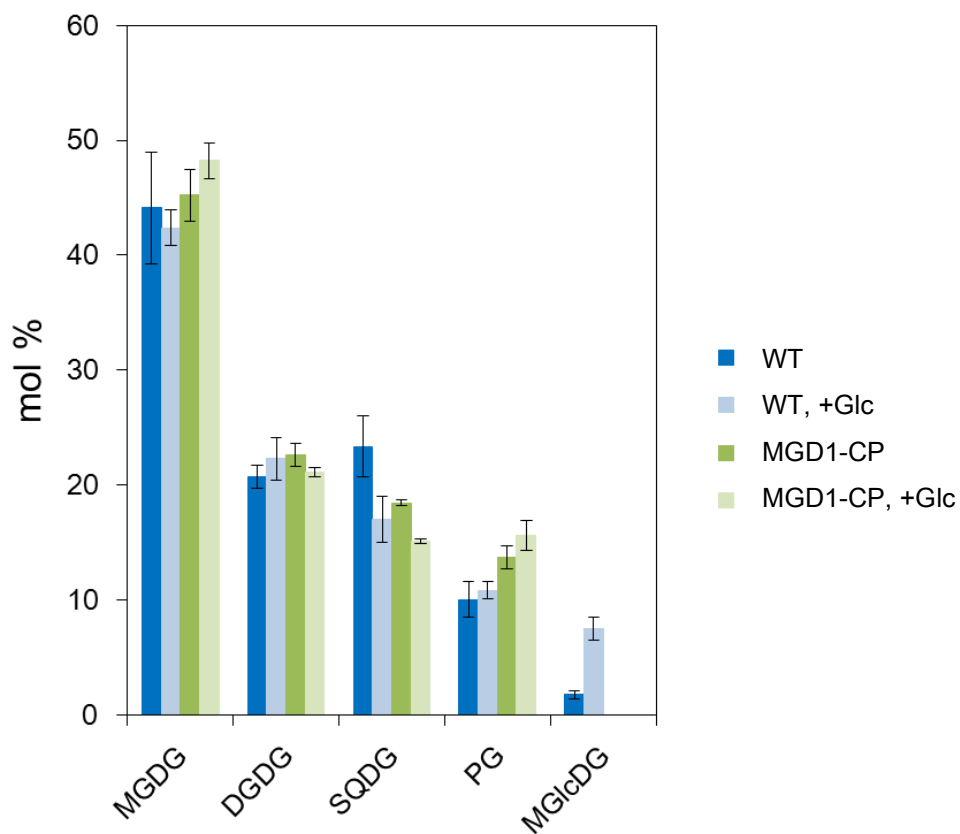


FIG. III-5. Lipid compositions of the wild type and MGD1-CP. +Glc, cells were grown at 30°C in BG-11 medium with 5 mM glucose. The values are the means \pm SD of three biological replications.

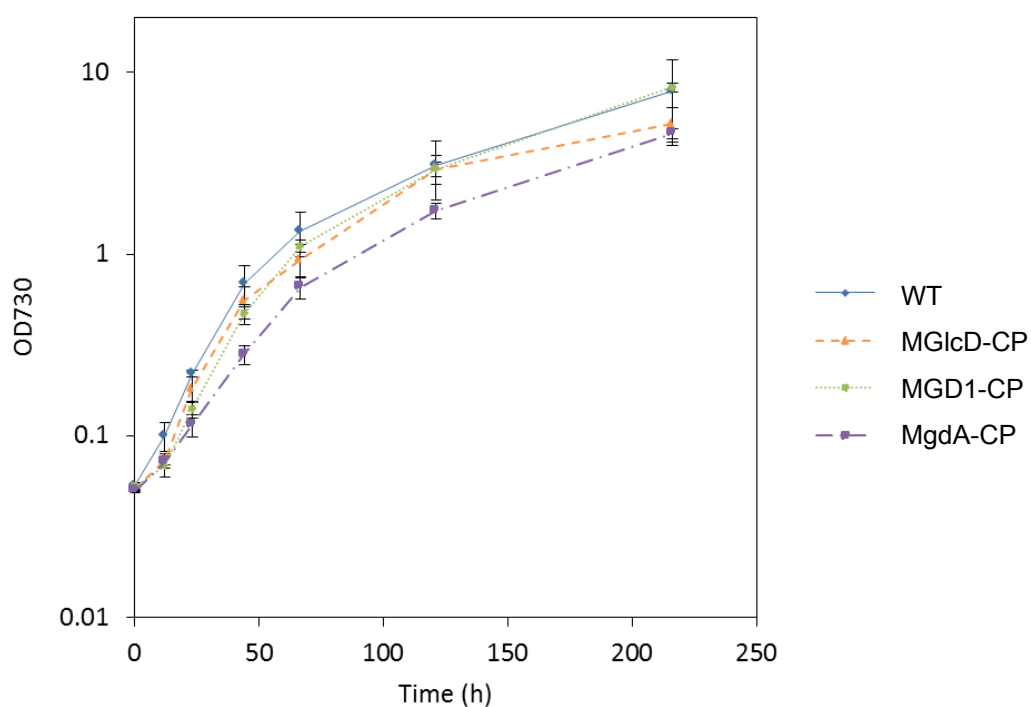


FIG. III-6. Monitoring of growth rate.

The growth rate was measured using the cells grown without antibiotic. The values are the means \pm SD of three biological replications.

Table III-2. Chlorophyll fluorescence parameters in *Synechocystis* strains

	WT	MGD1-CP	MgdA-CP
F_v/F_m	0.504 ± 0.018	0.484 ± 0.036	0.556 ± 0.008
qP	0.692 ± 0.077	0.821 ± 0.018	0.800 ± 0.047
NPQ	0.185 ± 0.057	0.201 ± 0.073	0.467 ± 0.041
φ II	0.321 ± 0.048	0.370 ± 0.007	0.339 ± 0.023

Chlorophyll fluorescence parameters are the means \pm SD of 3 biological replications.

the growth of each strain was not significantly changed compared with that of the wild type, although MgdA-CP grew slightly slower. Table III-2 showed the chlorophyll fluorescence parameters of the wild type and MGlcDG deficient mutants. I measured these parameters at room temperature. In the level of F_v/F_m which reflects the photochemical efficiency of photosystem II (PSII) and the quantum yield of electron transfer through PSII (ϕ_{II}), there was no significant difference among these strains, suggesting that MGlcDG deficiency does not affect PSII complexes. This result also demonstrated that MGlcDG is not essential for the growth and photosynthesis in *Synechocystis* under normal conditions. On the other hand, levels of photochemical quenching (qP) in both mutants, which indicate the redox state of PSII, were higher than that of the wild type, suggesting that the redox state of PSII is more oxidized than the wild type. Moreover, MgdA-CP showed much higher value of non-photochemical quenching (NPQ) in *Synechocystis*, compared with the wild type. This high value of NPQ might be associated with the low growth rate in MgdA-CP and *ctmgdA* gene could not well complement MGlcDG deficiency. Therefore, in order to focus the influences of MGlcDG deficiency, I used the wild type and MGD1-CP in the subsequent experiments

Changes in photosynthetic activities under heat-stress conditions

In a previous study, it was reported that MGlcDG was induced under heat-stress conditions in

Synechocystis and contributed thermal stability of thylakoid membranes (Balogi et al., 2005). To investigate the influence of MGlcDG deficiency under heat-shock stress in *Synechocystis*, I analyzed heat susceptibility of the mutant cells and compared to that of the wild type cells. As shown in Figure III-7A, in the wild type and MGD1-CP, the incubation for 30 min did not affect their photosynthetic activities until 44°C. After that, their photosynthetic activities were inhibited at 47°C. Under normal growth conditions, there was no significant difference between the wild type and MGD1-CP. Balogi et al. revealed that exposure to 42°C for 3 h in the light enhanced photosynthetic thermotolerance in *Synechocystis* cells and suggested that MGlcDG might be involved in this thermotolerance. Figure III-7B showed that the wild type cells induced this thermotolerance by heat-shock treatment (42°C, 3 h, in the light). On the other hand, despite the lack of MGlcDG, the cells of MGD1-CP exposed to heat-shock also showed equivalent thermotolerance compared with the wild type cells. This result indicates that MGlcDG is not essential to induce photosynthetic thermotolerance in *Synechocystis*.

Development of photosynthetic membranes

MGDG is essential for thylakoid biogenesis (Kobayashi et al., 2007). In *MGDI* null mutant in *Arabidopsis* (*mgd1-2*), the plant lacks most of MGDG and becomes small and albino phenotype where thylakoid membranes are almost disrupted. Figure III-4 showed that the ratio of galactolipids (MGDG and DGDG) to total lipids was not significantly changed in

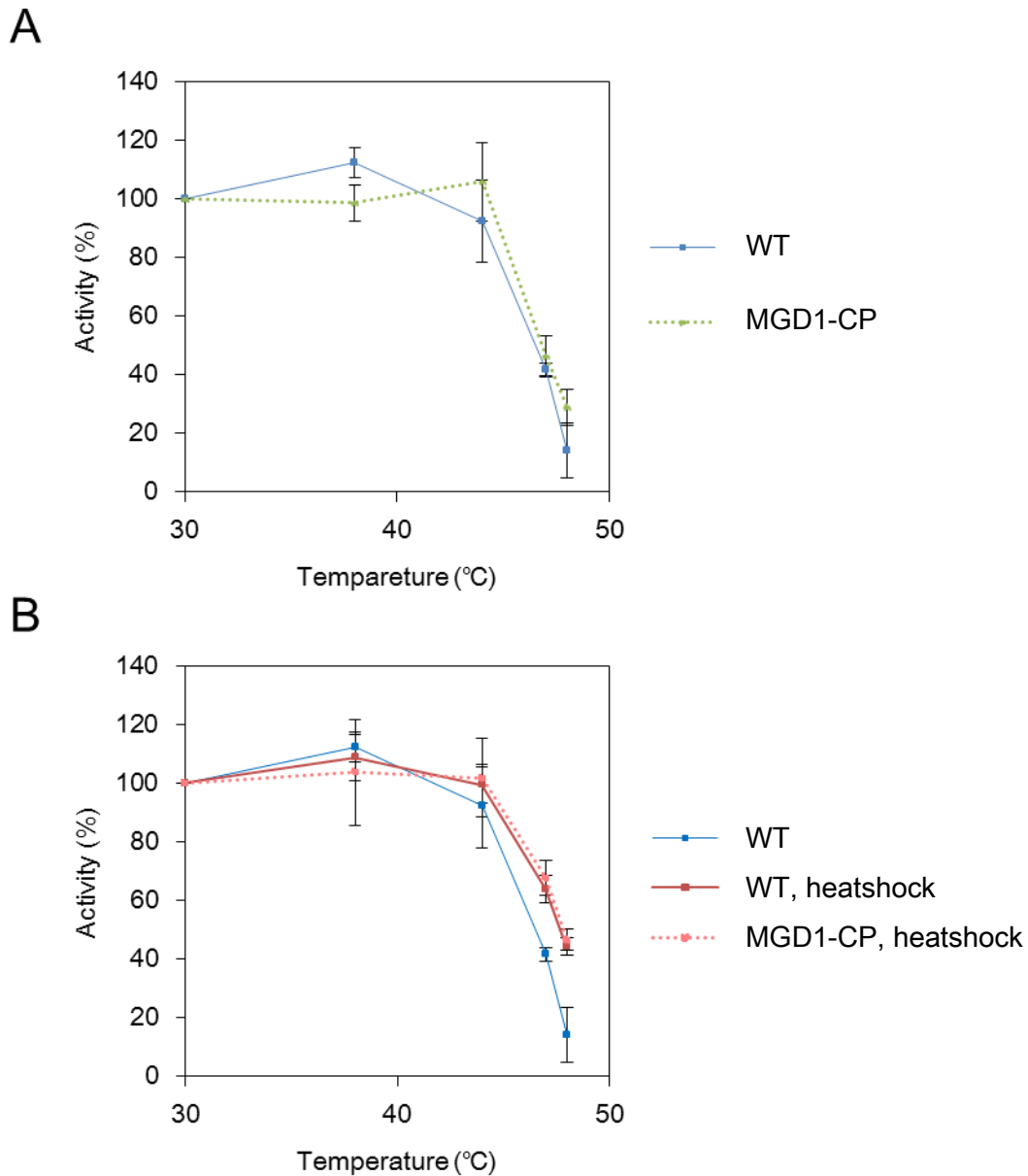


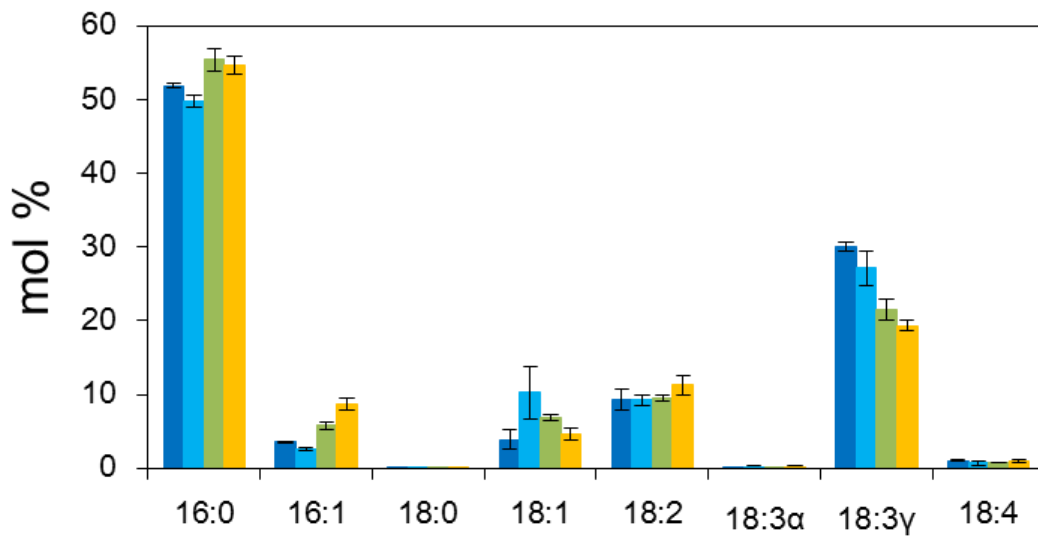
FIG. III-7. Comparison of heat susceptibility of photosynthetic oxygen evolving activity. *In vivo* photosynthetic activity was monitored by a Clark-type oxygen electrode (Oxygraph system) under $1,500 \mu\text{mol photons m}^{-2} \text{s}^{-1}$ (Lunminar Ace, LA-150SX, HAYASHI). Measurements of whole-cell O_2 evolution were conducted at 30°C on vigorously stirred samples containing $5 \mu\text{g chl/ml}$ in BG-11 medium. Cells grown at 30°C and kept at 30°C (A) or exposed to 42°C (B, heat-shock) were incubated for 30 min at designated temperatures ($30, 38, 44, 47$ and 48°C) in the dark. Then photosynthetic oxygen evolving activity was measured. 100% activities were the activities after incubation at 30°C for 30 min in each strain. The values are the means \pm SD of three biological replications.

MGlcDG deficient lines. DGDG, one of the major lipids in cyanobacteria and chloroplasts, is synthesized by galactose transfer from UDP-Gal to MGDG (Kelly and Dörmann 2002, Kelly et al. 2003, Awai et al., 2007, Sakurai et al., 2007). These fatty acid compositions were changed compared with those of the wild type (Fig. III-8). In MGDGs of MGlcDG deficient mutants, 18:3 γ fatty acids were reduced ~30%. In DGDGs, 18:3 γ fatty acids were also reduced ~20%. In $\Delta mglcd$ heterozygous line (Het), the reduction of molar ratio of 18:3 γ fatty acids was observed in MGDG and DGDG (Fig. III-S1B and C). Moreover, the ratio of 18:3 γ fatty acids to total fatty acids in MGD1-CP was also reduced compared with that of the wild type (Fig. III-S2). However, the amounts of chlorophyll *a* and total carotenoids were not significantly different between the wild type and MGD1-CP (Fig. III-9). In TEM observation, their thylakoid membranes were also not largely affected, but the mutant thylakoids were slightly swollen compared with the wild type (Fig. III-10). These results indicated that MGlcDG is not essential for thylakoid development itself, whereas MGDG is crucial for the cyanobacterial growth. On the other hand, it was suggested that MGlcDG is involved in fatty acid desaturation from 18:2 to 18:3 γ .

Growth under low temperature

Changes in fatty acid composition directly affect their membrane fluidity of thylakoids (Tasaka et al., 1996). In the next study, thylakoid membrane fluidity was therefore

A MGDG



B DGDG

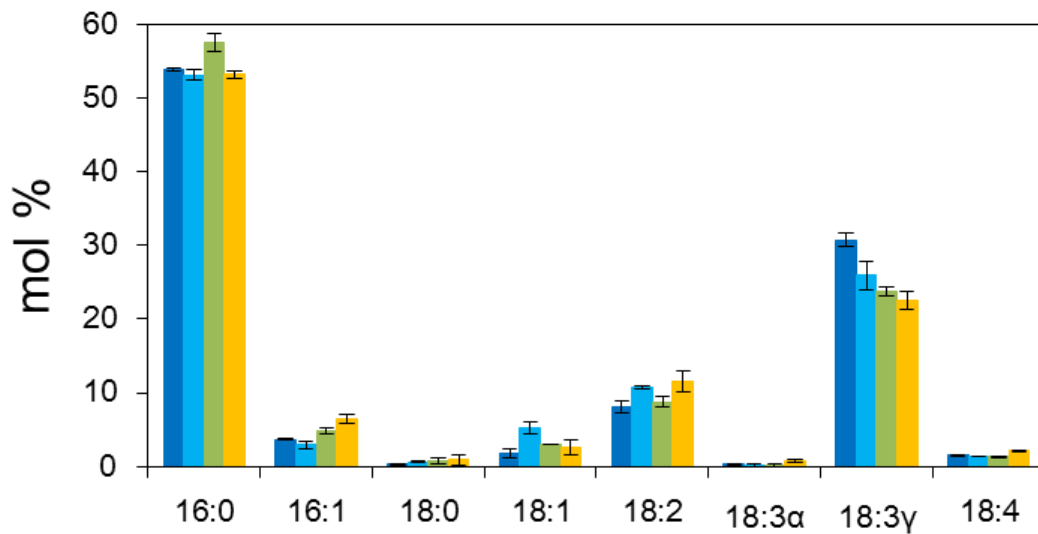


FIG. III-8. Fatty acid compositions of MGDG and DGDG in *Synechocystis* strains. The values are the means \pm SD of three biological replications.

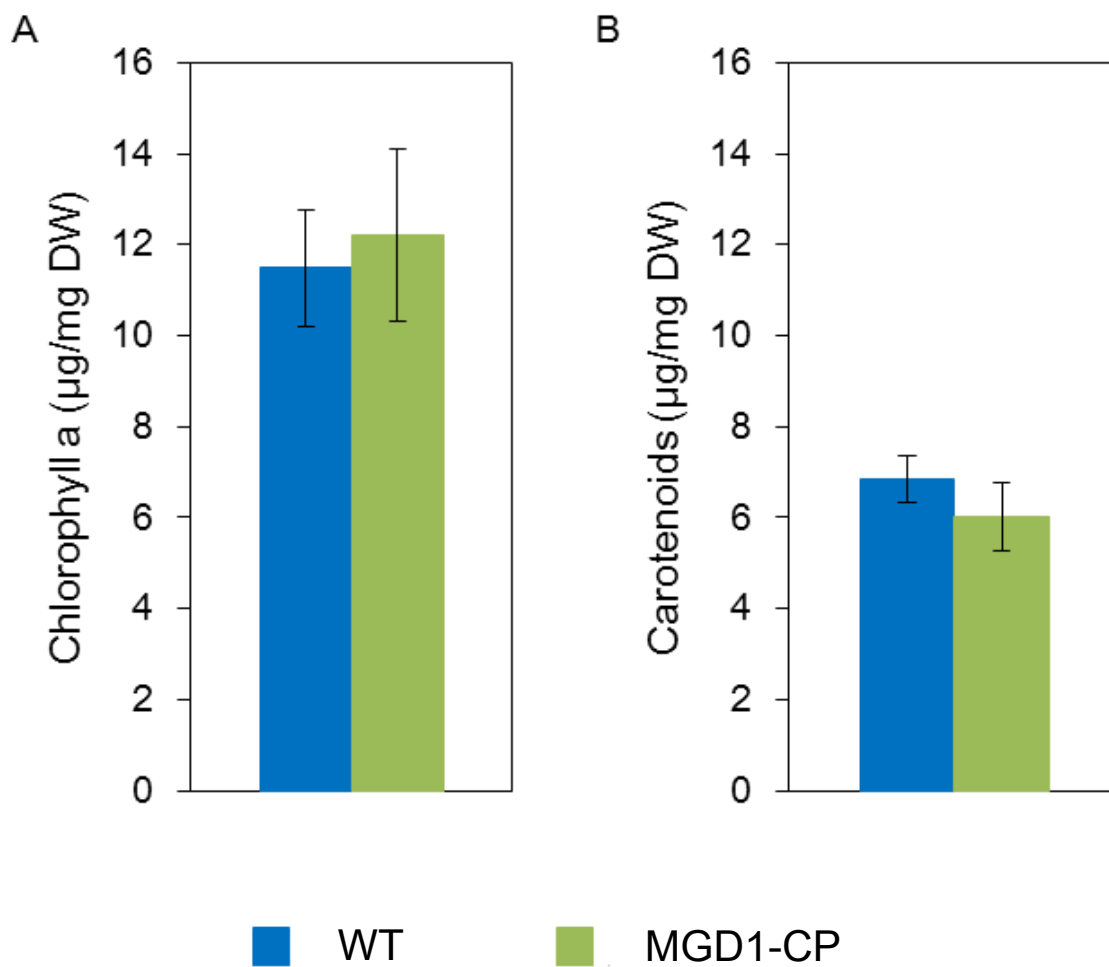


FIG. III-9. The amounts of pigments in *Synechocystis* strains.

(A) chlorophyll *a* and (B) total carotenoids were extracted from *Synechocystis* cells grown under photoautotrophic condition and measured. The values are the means \pm SD of three biological replications.

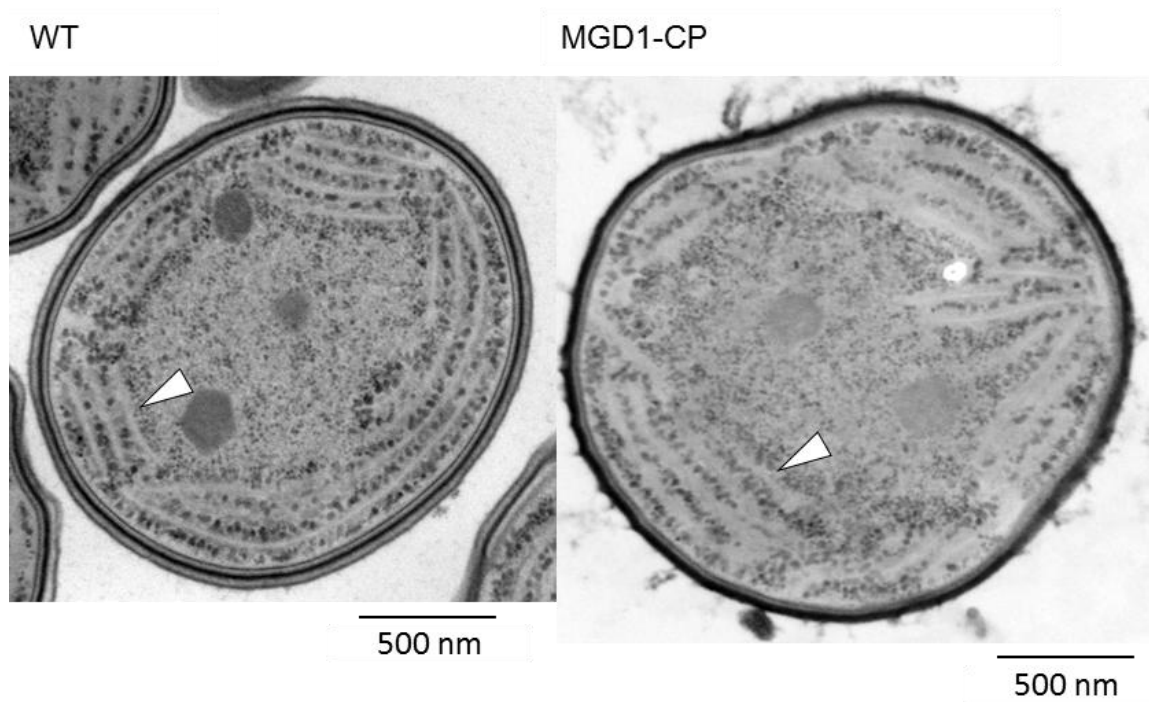


FIG. III-10. TEM images of *Synechocystis* cells.

Electron micrographs of the wild type (left) and MGD1-CP (right) were shown. White arrowheads indicate thylakoid membranes in each strain, respectively.

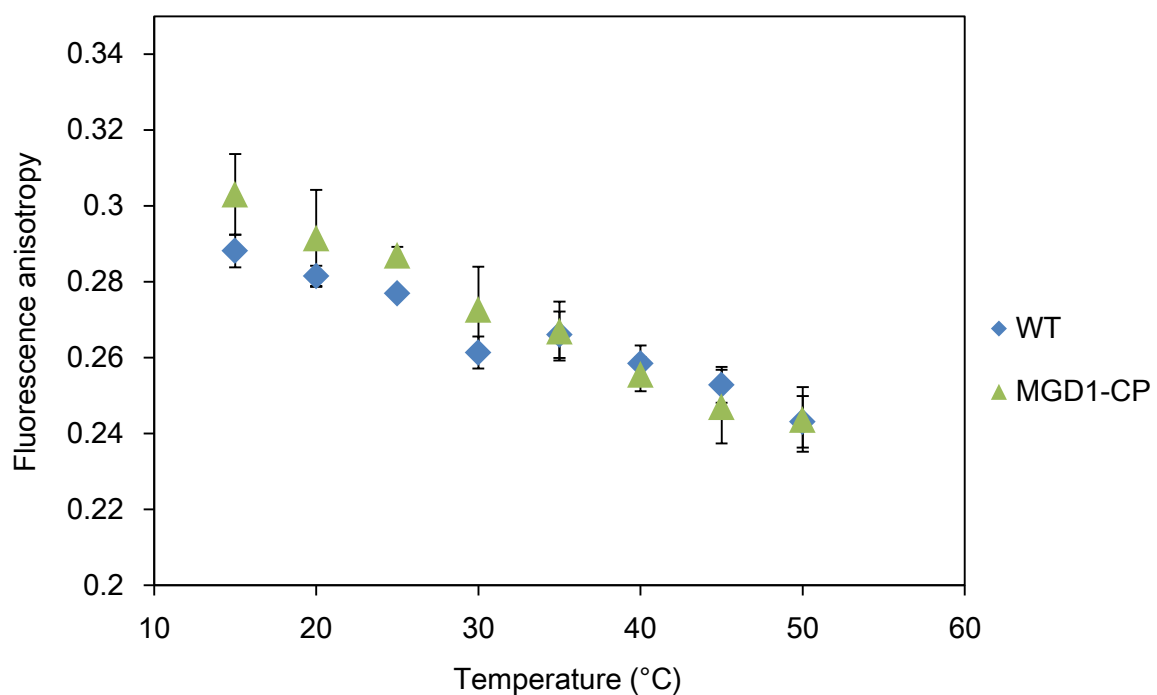


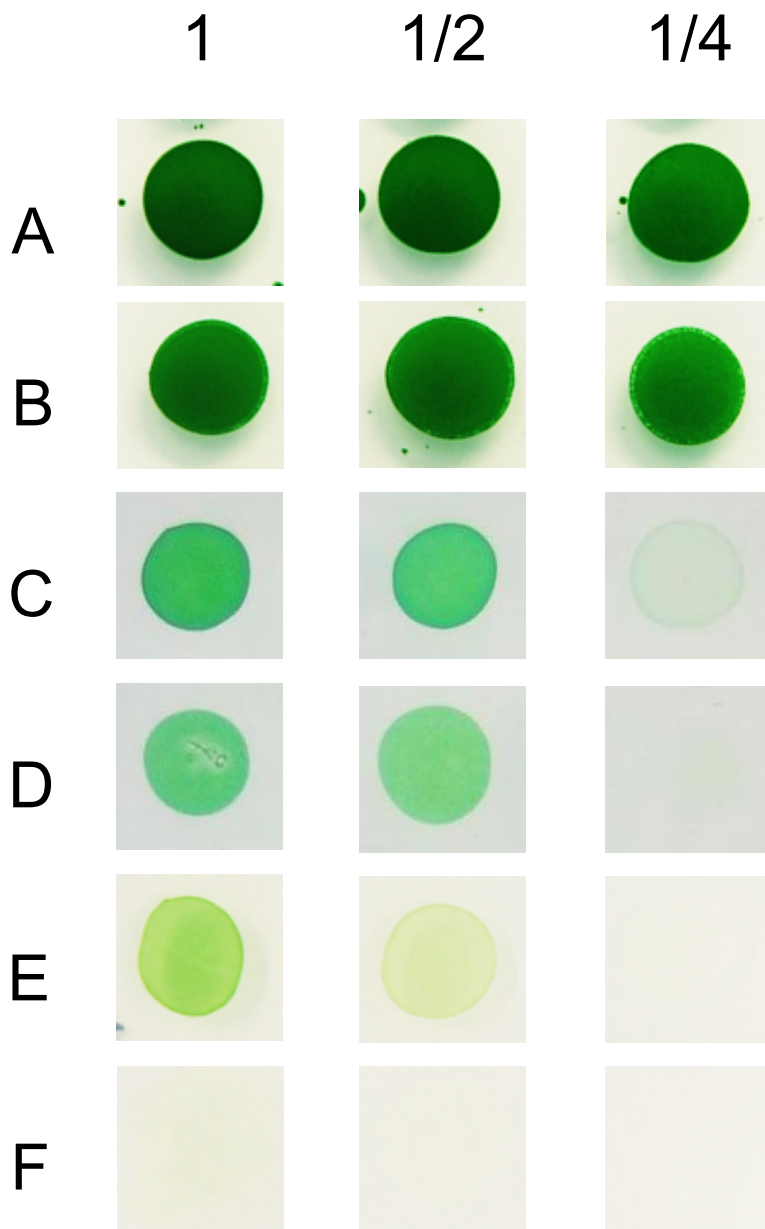
FIG. III-11. Fluorescence anisotropy of DPH in thylakoid membranes isolated from *Synechocystis* strains.

Thylakoid membranes were isolated from *Synechocystis* cells (WT and MGD1-CP) grown at 30°C in BG-11 medium under photoautotrophic condition. The values are the means \pm SD of 3 biological replications.

determined. The anisotropy of thylakoid membranes isolated from cells of the wild type and MGD1-CP grown at 30°C were analyzed (Fig. III-11). Between these strains, the anisotropy at 47°C was not significantly changed. However, under 30°C, the thylakoid membrane fluidity of WT was much higher than that of MGD1-CP. This result suggests that MGLcDG deficiency affected thylakoid membrane fluidity on temperature change (Fig. III-8 and S1). Since it is possible that the influence on membrane fluidity is more serious under low temperature, I analyzed the growth of the MGLcDG-deficient strain at 15°C (Fig. III-12). In liquid culture, MGD1-CP showed similar growth to the wild type. However, on plate, the growth of MGD1-CP was dramatically impaired, suggesting that cold stress affected the growth of MGLcDG-deficient cells particularly in their early growth. The lipid composition of cells exposed to low temperature was different between the wild type and MGD1-CP (Fig. III-13). In MGDG and DGDG of MGD1-CP, molar ratio of 18:3 γ was reduced compared with that of the wild type. On the other hand, molar ratio of 18:3 α in SQDG and PG was the same level compared with that of the wild type. These results indicated that the low temperature sensitivity of MGD1-CP is probably caused by the difference in the extent of desaturation in MGDG and DGDG at ambient temperature.

A

Dilution rate



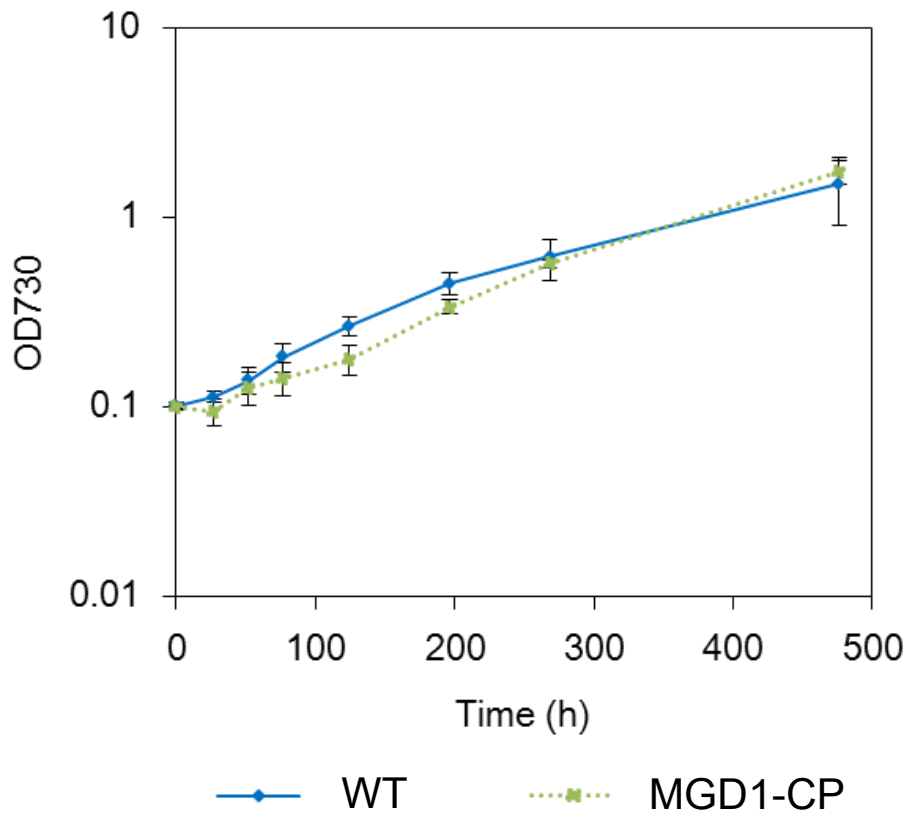
B

FIG. III-12. Growth of *Synechocystis* strains under low temperature.

(A) WT (A, C, and E) and MGD1-CP (B, D, and F) were inoculated at each dilution rate, one, one-two, and one-fourth, on BG-11 plate. These cells were grown at 30°C (for 3 days, A and B), 22°C (for 5 days, C and D), or 15°C (for 9 days, E and F).

(B) The growth of *Synechocystis* cells were monitored at 15°C in BG-11 medium. Cells adjusted their concentrations to $OD_{730} = 0.1$ were grown under photoautotrophic condition. The values are the means \pm SD of three biological replications.

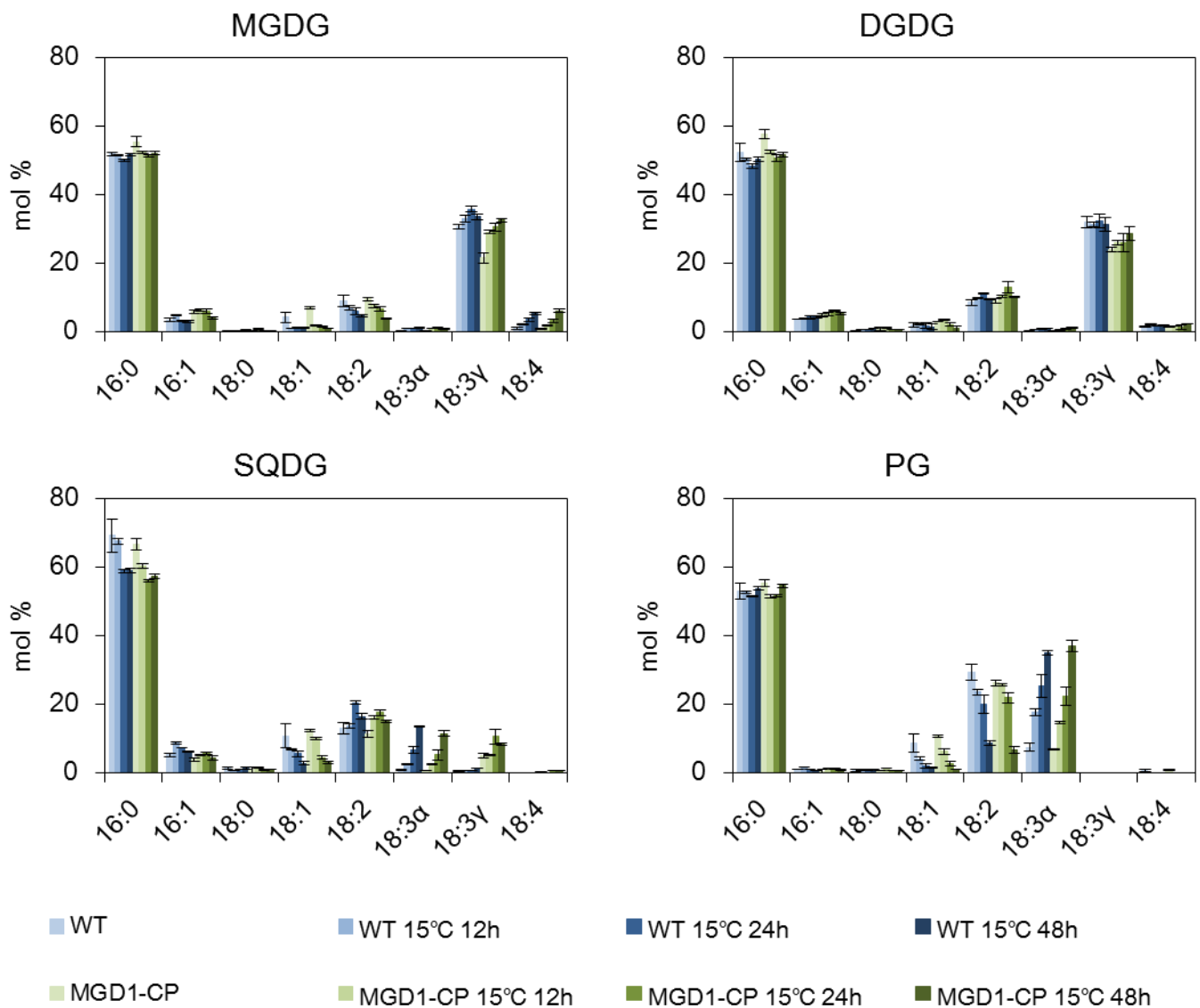


FIG. III-13. Effect of low temperature stress on fatty acid composition of membrane lipids in each strain of *Synechocystis* sp. PCC 6803.

Synechocystis cells were grown at 30°C in BG-11 medium under photoautotrophic condition. Then cells were kept at 30°C (WT and MGD1-CP) or exposed to 15°C for 12h, 24h or 48h. The values are the means \pm SD of 3 biological replications.

Discussion

In this study, to clarify physiological roles of MGlcDG in cyanobacteria, I created MGlcDG deficient mutants by complementation with plant and bacterial MGDG synthases in *Synechocystis* sp. PCC 6803. MGlcDG synthase gene is commonly found in many cyanobacterial genomes, although functional counterpart for plant-type MGDG synthase has never been identified in cyanobacteria (see Chapter II). Lines of evidence suggest that MGlcDG-dependent MGDG synthesis is a common feature in cyanobacterial species. However, it is not known why the presence of this minor lipid MGlcDG is so highly conserved in cyanobacteria. Here I presented new insight into the function of MGlcDG.

At first, growth of the MGlcDG-deficient cells was almost the same as that of the wild type cells under normal conditions, indicating that *Synechocystis* does not require MGlcDG for its normal growth if MGDG is fully supplied by different pathway (Fig. III-6). However, in wild type cyanobacteria, MGlcDG is crucial for MGDG biosynthesis, because I could not identify any $\Delta mglcd$ mutants without complementation by plant or bacterial MGDG synthases. This result is consistent with the finding that MGDG-deficient mutant of *Arabidopsis* is lethal (Kobayashi et al., 2007). MGlcDG-deficient mutants showed normal photosynthetic activity compared with the wild type, suggesting that photosynthetic activity is also not affected by MGlcDG deficiency (Table III-2). As shown in Figure III-10, thylakoid membranes were well developed in the mutant, although the membranes are slightly swollen.

Moreover, the contents of chlorophyll and carotenoids were not changed (Fig. III-9), suggesting that MGlcDG is not essential for development of photosynthetic membranes. However, these mutants showed higher values of qP than the wild type. Higher qP (more oxidized plastoquinone pool) is known to be observed in the mutants with higher PSI content (Sonoike et al., 2001). Decrease in SQDG was observed in the MGlcDG-deficient mutants, which may be attributed to the imbalance of the DAG supply between for MGDG and SQDG syntheses. The importance of SQDG for PSII complex has already been demonstrated in *Synechocystis* (Aoki et al., 2004). SQDG deficient mutant was reported to have severe damage in PSII. Moreover, in case of MgdA-CP, NPQ was much higher than that of the wild type. It should be noted that CtMgdA has much stronger activity than AtMGD1 (Fig. III-3; Masuda et al., 2011), suggesting that UDP-Gal and DAG supply are disturbed. As both SQDG and galactolipids require DAG for their biosyntheses (Fig. III-14), the strong activity of CtMgdA may cause a decrease in the contents of SQDG. *sqdB* (UDP-sulfoquinovose synthase) mutant has shown loss of SQDG and increase in DGDG and PG (Güler et al., 1996). PG and SQDG are anionic lipids and compensate each other. Indeed, complemented strains showed increase in PG by reducing relative amount of SQDG (Fig. III-4). DGDG was also significantly increased in both mutants. The imbalance of lipid composition in MgdA-CP was more severe than that in MGD1-CP. Further analyses of the cytochrome *b₆f* complex and PSI may be required for clarifying this influence.

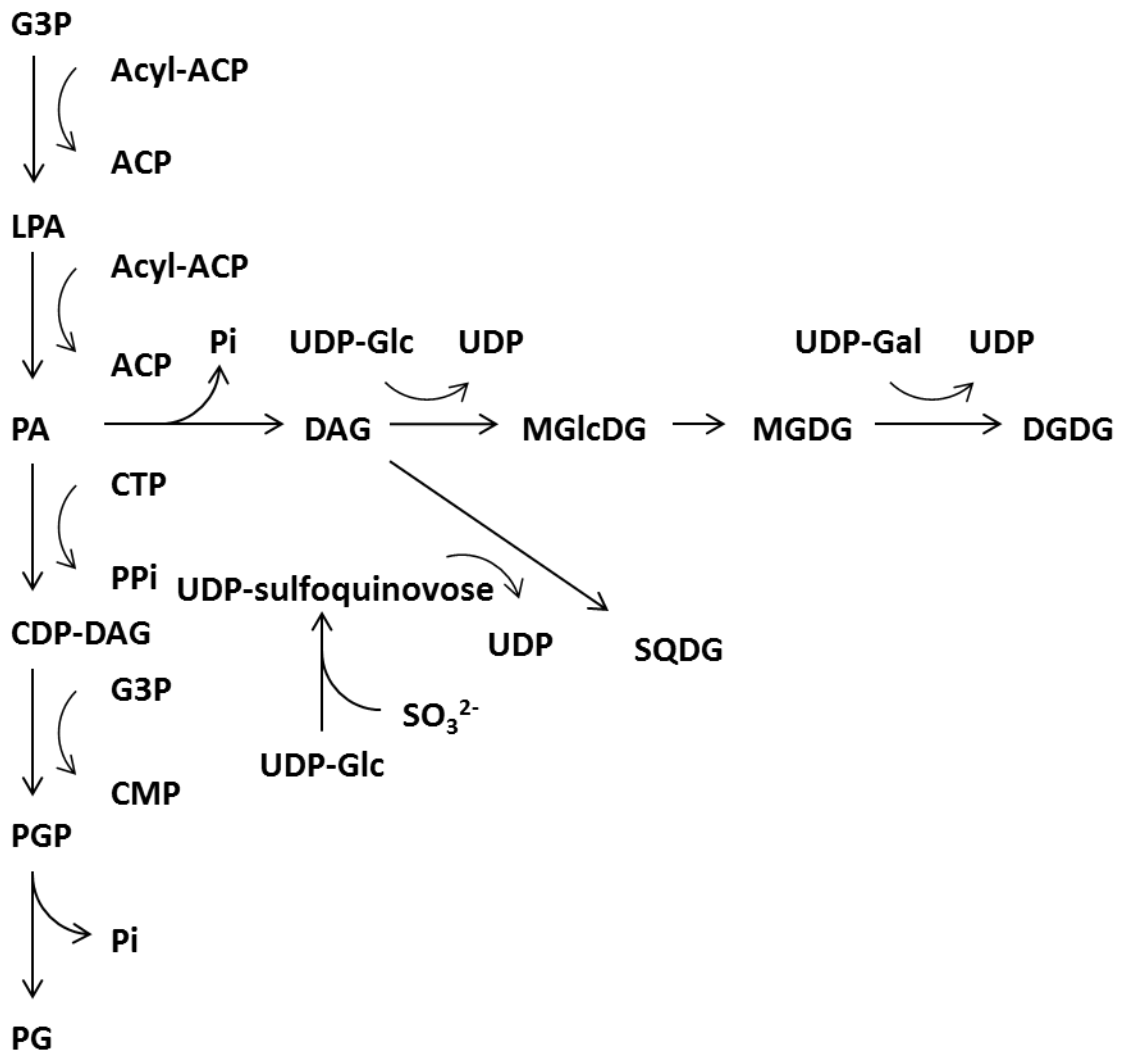


FIG. III-14. Membrane lipid synthesis pathway in *Synechocystis* (Sato and Wada, 2009). G3P, glycerol 3-phosphate; ACP, acyl-carrier protein; PA, phosphatidic acid; LPA, lyso-PA; Pi, inorganic phosphate; PPi, pyrophosphate.

In both MGDG and DGDG, 18:3 γ fatty acids of the mutants were 20-30% less than those of the wild type (Fig. III-8). In parallel, 16:0 and 16:1 were increased. In cyanobacteria, most of galactolipids are 18:X/16:X molecular species in *sn*-1/*sn*-2 positions (Fig. III-15A). MGDG and DGDG in the mutants contain more than 50% of 16 carbon fatty acids. This may be due to that AtMGD1 and CtMgdA utilize much more DAG species containing 16:0 at *sn*-1 position than MGlcD, and therefore, 18 carbon unsaturated fatty acids were dramatically decreased (Fig. III-15B), suggesting that this may be due to difference in substrate preference between MGlcDG and MGDG synthases. This difference in substrate specificity also influenced SQDG synthesis because SQDG mainly utilizes 16:0/16:0 molecular species which is also utilized by AtMGD1 and CtMgdA. This may reduce DAG pool size which is available for SQDG biosynthesis.

Despite the lack of MGlcDG, MGD1-CP mutant acquired thermal stability of the photosynthetic activity by heat-shock treatment (Fig. III-7B). This result revealed that MGlcDG is not essential in this mechanism. On the other hand, this mutant showed dramatically slow growth at 15°C on BG-11 plate (Fig. III-12). In cyanobacteria, it was reported that desaturation of fatty acids was induced for increasing membrane fluidity under low temperature conditions (Sato et al., 1979). The membrane fluidity depends on the extent of unsaturation of fatty acids (Tasaka et al., 1996) and membranes constructed from

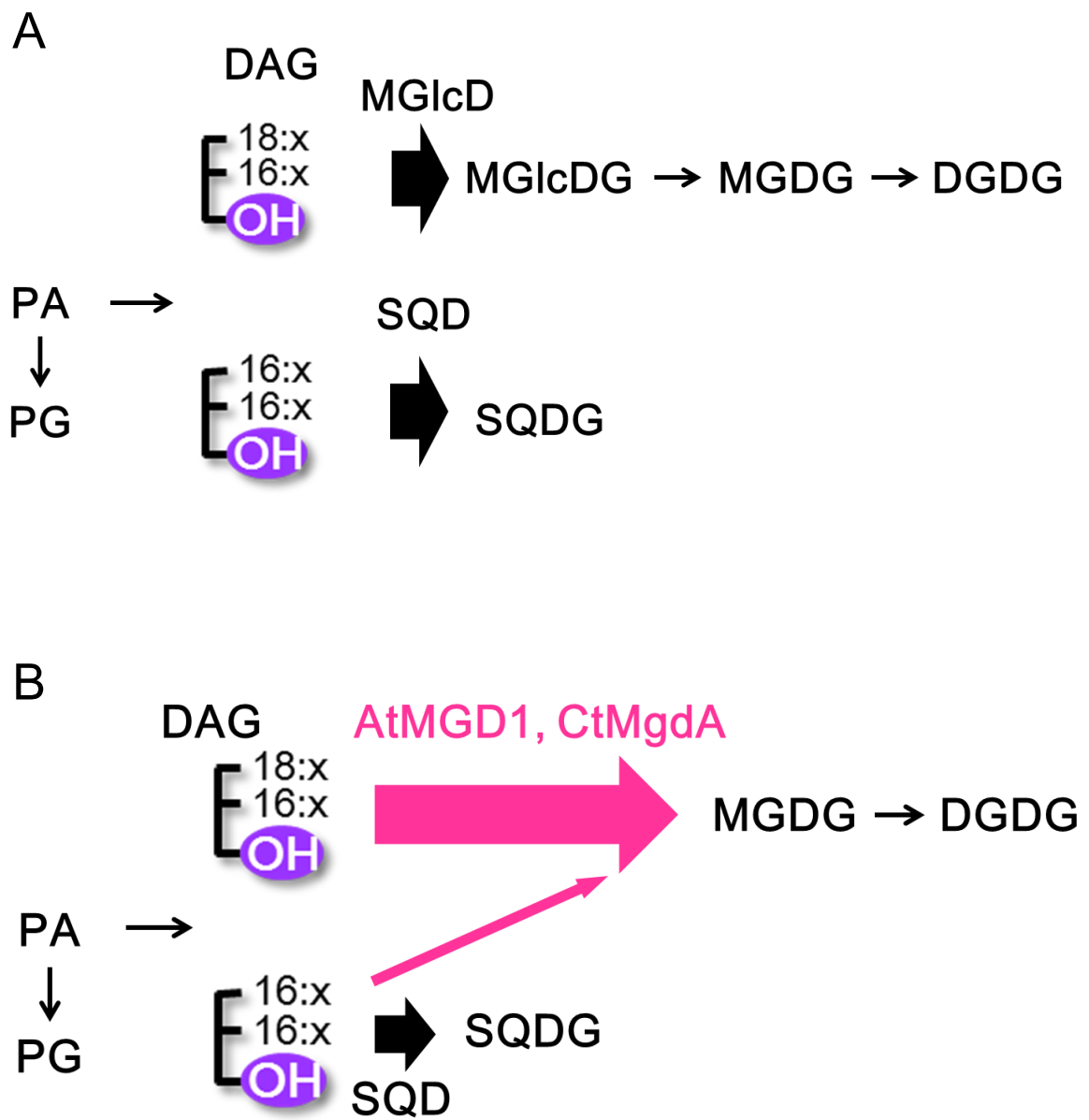


FIG. III-15. Schematic model of glycolipid synthesis in (A) wild type and (B) MGDG deficient mutant.

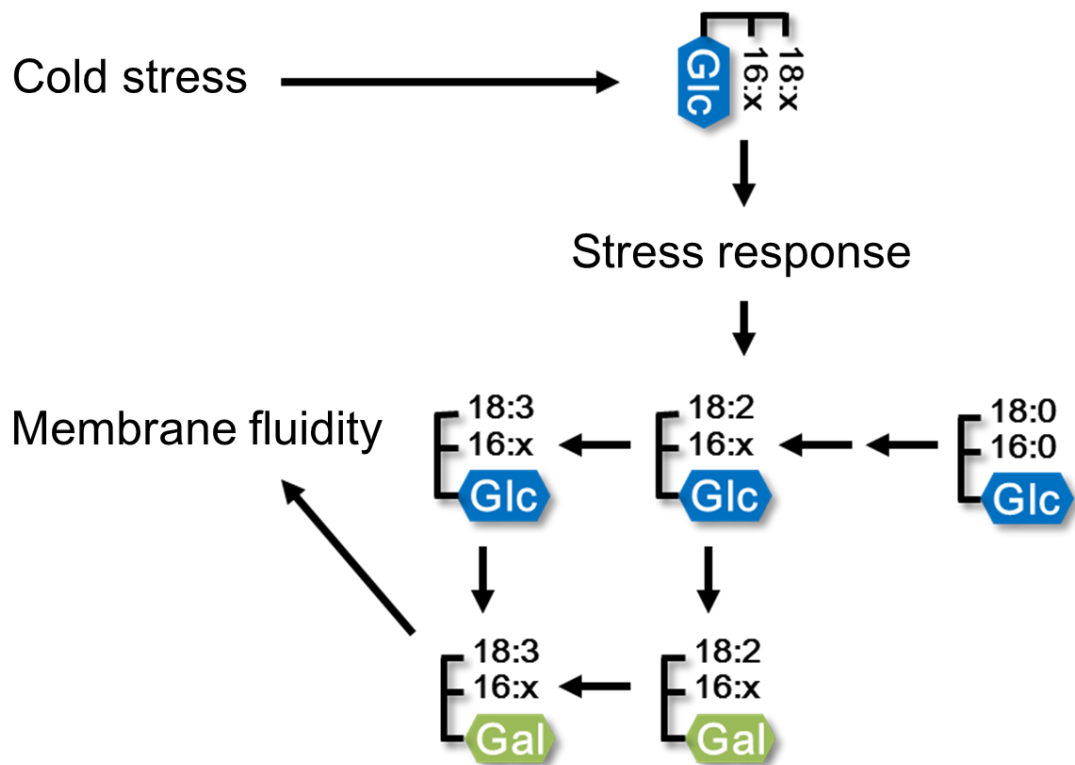
unsaturated fatty acids are more fluid than saturated membranes. Indeed, in *Synechocystis*, during temperature shifting from 30 to 18°C, 18:3 fatty acids were much increased (Wada et al., 1990, Sheng et al., 2011). In particular, the degree of these unsaturated fatty acids was more increased in MGDG (18:3 γ) and PG (18:3 α). In wild type of *Synechocystis*, most of MGlcDGs are occupied by saturated fatty acids (Fig. III-S3). This means that MGlcDG containing unsaturated fatty acids were immediately converted to MGDG (Fig. III-15). Sato and Murata (1982b) reported their study by pulse-chase experiments with ¹⁴C labeled compound in *Anabaena* and concluded that fatty acid unsaturation primarily occurs in MGlcDG but not in MGDG. It is possible that MGlcDG deficiency may cause the decrease in 18:3 γ molecular species of galactolipids by loss of the early desaturation of MGlcDG, and therefore, the mutant is sensitive to cold stress. Figure III-13 supported this speculation. In MGD1-CP, desaturation from 18:2 to 18:3 γ in MGDG and DGDG was delayed compared with the wild type. Moreover, a previous study reported that MGlcDG has lower phase transition temperature than that of MGDG because of lower affinity of the glucose head group for intermolecular hydrogen bonding (Rog et al., 2007). Under cold temperature conditions, the lower phase transition temperature of MGlcDG may also contribute to maintain membrane fluidity.

A histidine kinase, Hik33, is known to sense decreases in temperature and to regulate gene expression in *Synechocystis*. However, DNA micro array analysis revealed that low

temperature-inducible regulation of some genes was unaffected by the mutation of *hik33* gene (Suzuki et al., 2001). It suggested that there are other pathways sensing cold stress in *Synechocystis*. In MGlcDG deficient mutant, the growth of mutant cells was delayed during early logarithmic growth phase under cold stress (Fig. III-12B). However, this delay disappeared in later logarithmic growth phase. I notably observed this delayed growth in cells grown on plate (Fig. III-12A), suggesting that MGlcDG may contribute to this primary adaptation of cold stress.

In conclusion, I achieved complementation of cyanobacterial MGDG synthesis pathway by plant-type MGDG synthesis pathway. These complementation strains demonstrated that plant-type MGDG synthase can compensate a role for MGDG biosynthesis under normal growth conditions, which is essential for life of *Synechocystis*. However, the cyanobacterial pathway may be crucial for environmental adaptation, particularly upon low temperature, which brought about prosperity of cyanobacterial species in ancient Earth (Fig. III-16).

A



B

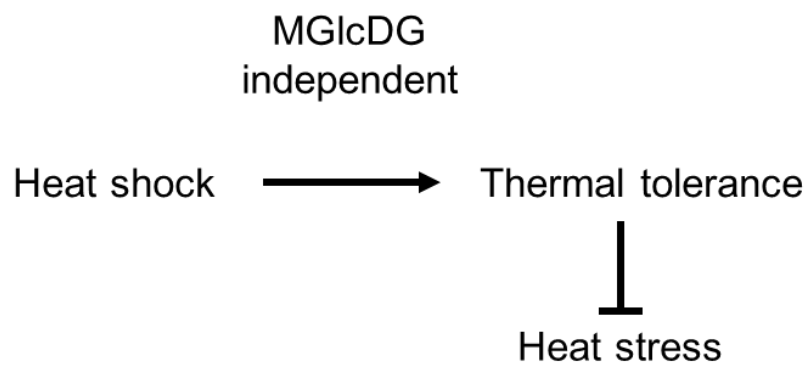
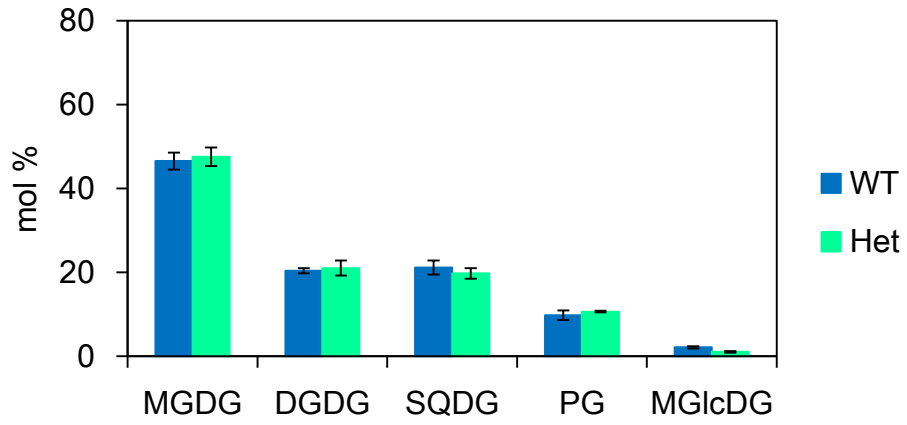
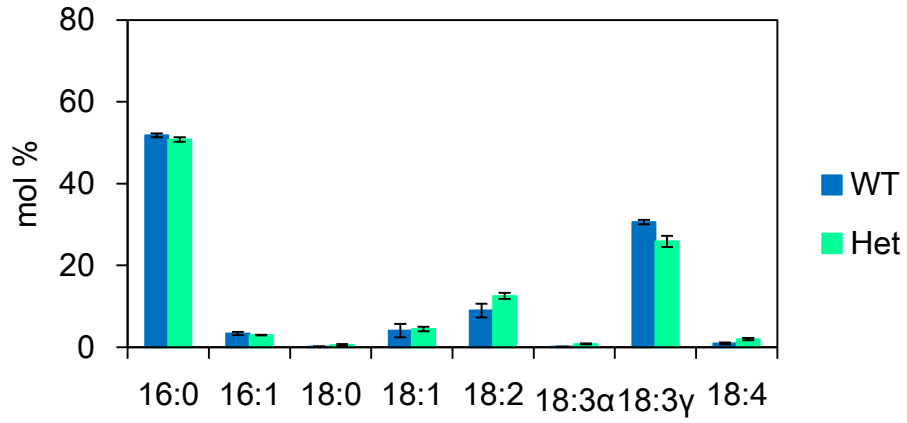
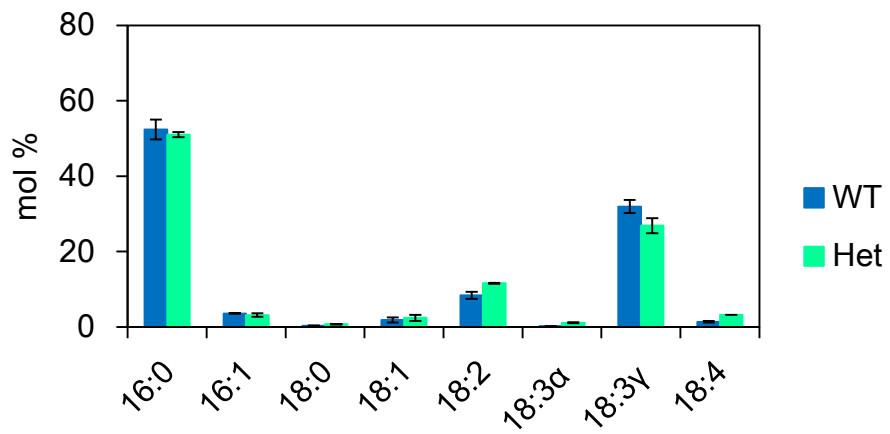


FIG. III-16. Proposed model of contribution of MGlcDG for (A) cold and (B) heat stress.

A**Membrane lipids****B****MGDG****C****DGDG**

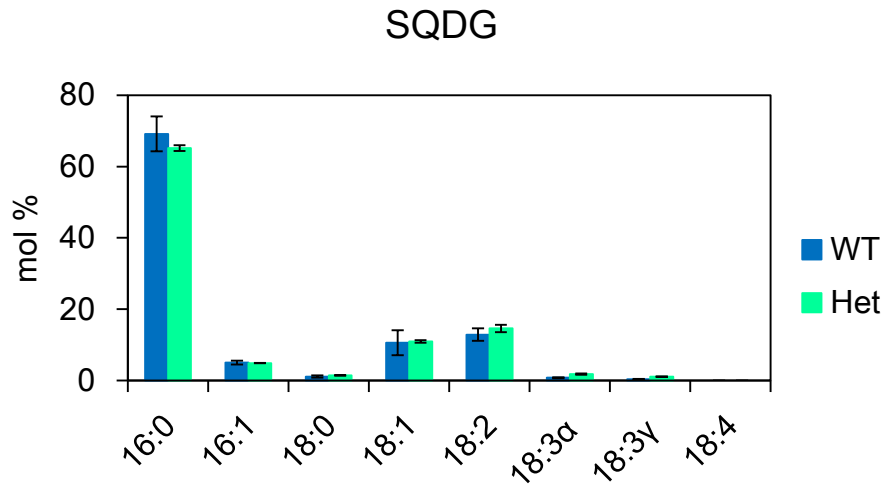
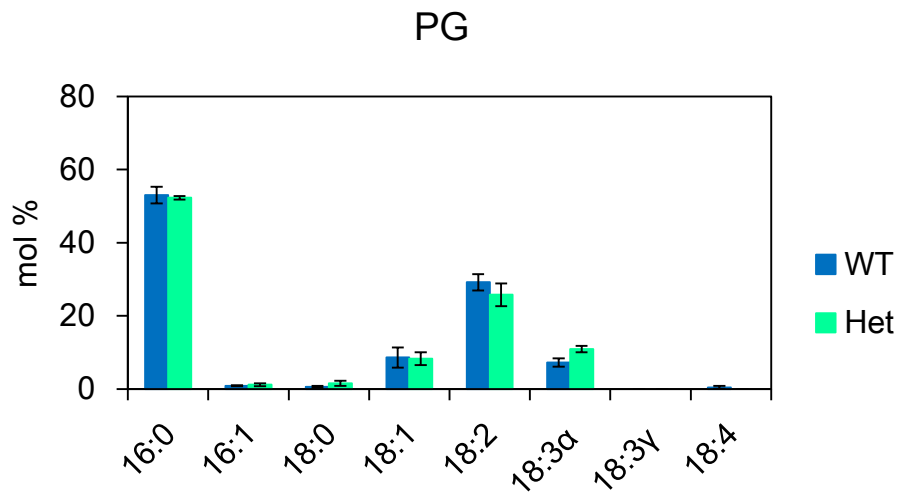
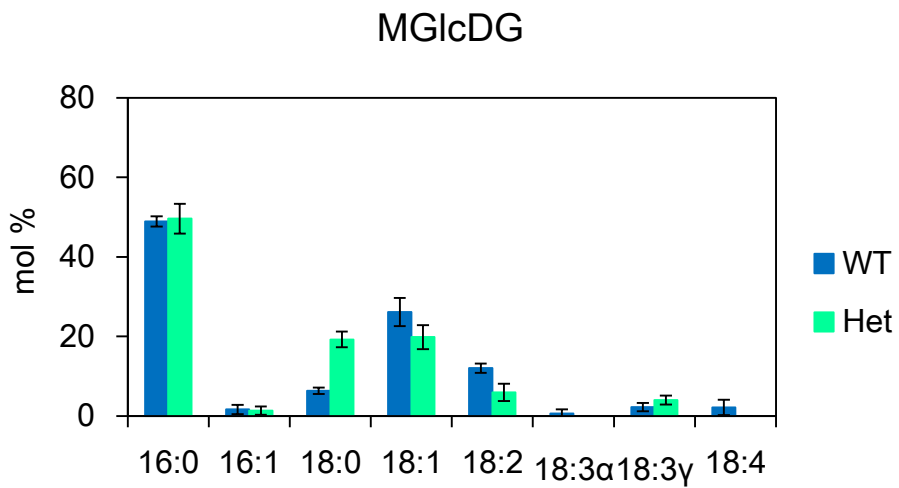
D**E****F**

FIG. III-S1. Membrane lipid and fatty acid composition in WT and Het. The values are the means \pm SD of three biological replications.

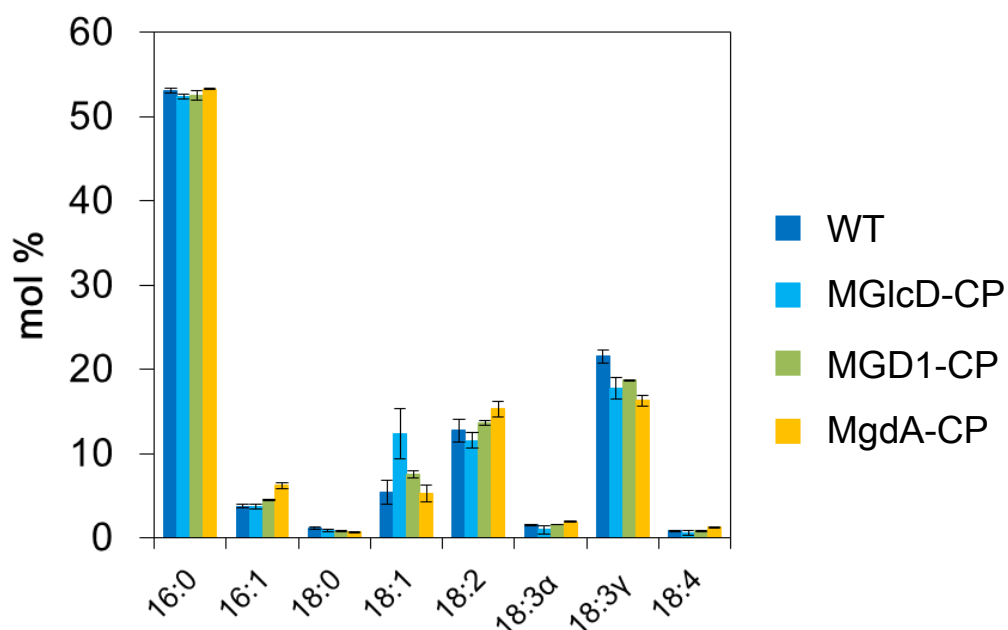


FIG. III-S2. Total fatty acid compositions in *Synechocystis* strains. The values are the means \pm SD of three biological replications.

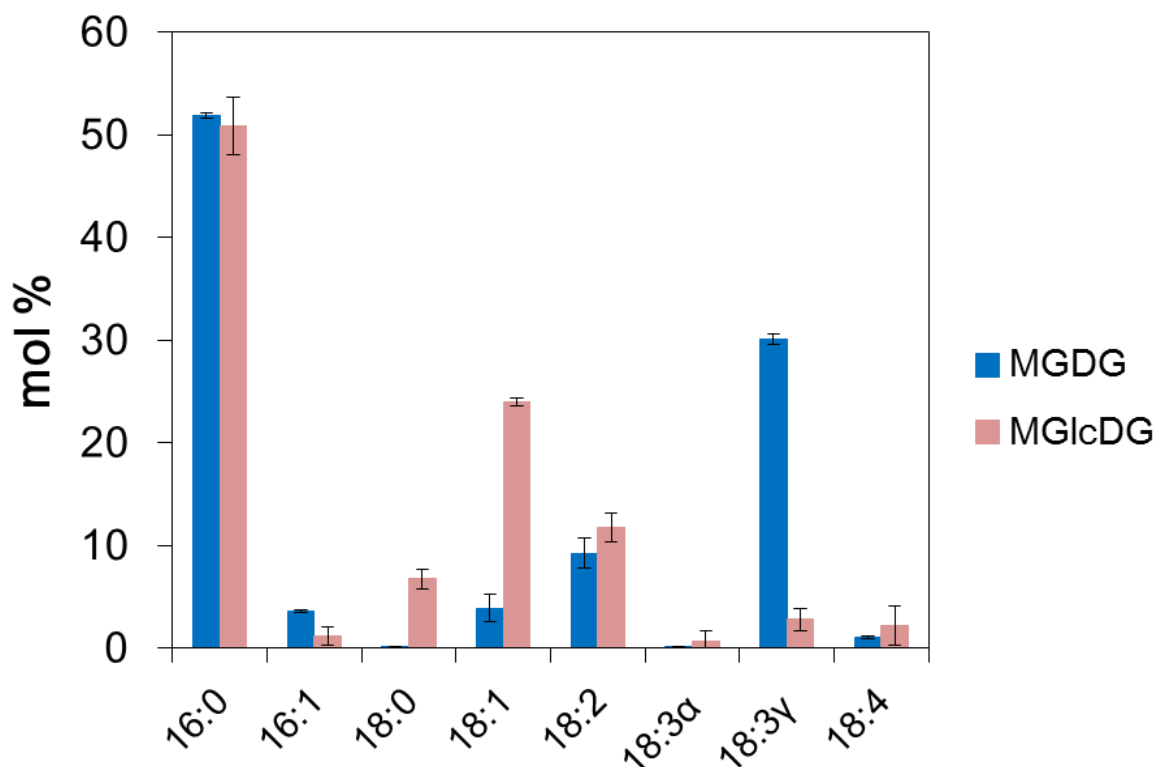


FIG. III-S3. Fatty acid compositions of MGDG and MGlcDG in *Synechocystis* strains. The values are the means \pm SD of three biological replications.

Table III-S1. Chlorophyll fluorescence parameters in *Synechocystis* strains

	WT	MGlcD-CP
<i>Fv/Fm</i>	0.495 ± 0.002	0.452 ± 0.035
qP	0.734 ± 0.012	0.671 ± 0.025
NPQ	0.324 ± 0.003	0.332 ± 0.032
ϕ II	0.318 ± 0.010	0.255 ± 0.021

Chlorophyll fluorescence parameters are the means ± SD of 3 biological replications.

Materials and Methods

Growth conditions of bacterial strains

E. coli was grown at 37°C in LB medium. A glucose tolerant wild type strain of *Synechocystis* sp. PCC 6803 (Williams, 1988, Tajima et al., 2011) was used to generate the mutant and the transformants. All strains were grown at 30°C in BG-11 medium under continuous fluorescent white light at an intensity of $\sim 30 \mu\text{mol photons m}^{-2} \text{s}^{-1}$ with or without appropriate antibiotic(s). A disruption mutant of the MGlcDG synthase gene (*mglcd*) of *Synechocystis* sp. PCC 6803 is referred to as $\Delta mglcd$. In the case of the MGlcD mutant, 15 $\mu\text{g/ml}$ kanamycin was added to the growth medium. Additionally, all transformants were grown in medium with 5 $\mu\text{g/ml}$ gentamycin.

Construction of expression plasmids and their mobilizations into Synechocystis sp. PCC6803

The N-terminal and C-terminal regions of *mglcd* were amplified by PCR using pPICT2::*mglcd* (Awai et al., 2006). Then these fragments were cloned into the pBSSK vector (Stratagene) with kanamycin cassette digested from pUC4-KIXX (Amersham Pharmacia Biotech). This recombinant plasmid was transformed into *Synechocystis* sp. PCC 6803.

DNA fragments of *mglcd*, *AtMGD1* and *ctmgdA* genes were amplified by PCR using genome DNA derived from *Synechocystis* sp. PCC 6803, *Arabidopsis thaliana* and *Chlorobaculum tepidum*, respectively. The *AtMGD1* DNA fragment was omitted its transit

peptide (Yamaryo et al., 2003). In the case of *ctmgdA* gene, the DNA fragment was amplified by PCR using pET28(a)::*ctmgdA* (Masuda et al., 2011). Then these fragments were cloned into the pZErO-2 vector (Invitrogen), and excised out as EcoRI-XhoI DNA fragments. The DNAs were subsequently cloned into the EcoRI-XhoI of a broad-host-range plasmid pSL1211 (Gm^r) (Ng et al., 2000) to generate pSL1211::*mglcd*, pSL1211::*AtMGDI* and pSL1211::*ctmgdA*, respectively. Their expressions are under the control of the IPTG-inducible *trc* promoter (Ptrc). The plasmids were mobilized from *E. coli* S17-1 into *Synechocystis* sp. PCC6803 through conjugation (Kim et al., 2009).

Monitoring of growth rate and Analyses of photosynthetic parameters

The growth rate and photosynthetic parameters were measured using the cells grown without antibiotic. The photosynthetic parameters were measured with MINI PAM (Heinz Walz) after incubation in dark for 5 min. The intensity of actinic light was adjusted at 200 $\mu\text{mol photons m}^{-2} \text{ s}^{-1}$.

Measurement of thylakoid thermostability

In vivo photosynthetic activity was monitored by a Clark-type oxygen electrode (Oxygraph system) under 1,500 $\mu\text{mol photons m}^{-2} \text{ s}^{-1}$ (Lunminar Ace, LA-150SX, HAYASHI). The *Synechocystis* cells grown at 30°C were incubated at designated temperatures for 30 min in

the dark. Measurements of the O₂ evolution were conducted at 30°C on vigorously stirred samples containing 5 µg chl/ml in BG-11 medium.

Measurement of membrane fluidity

Thylakoid membranes were isolated from *Synechocystis* cells. The cells in 1 mM HEPES buffer (10 mM KCl, 0.1 M sorbitol, pH 7.5) (Barber et al., 1984) were broken with 0.1 mm Zirconia/Silica Beads (BioSpec) by a Mini Beadbeater (Wakenyaku). After that, thylakoid membranes were obtained using centrifugation at 20,000 xg for 30 min (Kondo et al., 2007). Thylakoid membranes adjusted 3 µg Chl/ml in PBS (pH 7.4) were labeled with 1, 6-Diphenyl-1, 3, 5-hexatriene (DPH) for 40 min on ice in the dark. 3 µg of 0.2 mM DPH in acetone was added to 3 ml of the membrane fraction (final concentration, 0.2 µM) (Mironov et al., 2011). These membranes rabled by DPH were incubated at designated temperatures for 30 min in the dark. Then fluorescence anisotropy was determined on the labeled membranes with a fluorescence spectrophotometer (F-2700, HITACHI) as described (Schlame et al., 1990). The wavelength of excitation was 360 nm and of emission was 430 nm at 20 nm slits.

Assay for glycolipid synthesis activities

Glycolipids synthetic activities were assayed as described in Chapter II-I (Awai *et al.*, 2006).

These lipids radio-labeled were separated by one-dimensional thin-layer chromatography (TLC) in chloroform-hexane-isopropanol-tetrahydrofuran-water (50:100:80:1:2, by volume) and were detected by image analyzer (STORM860, Molecular Dynamics) or liquid scintillation counter (LS 6500, Beckman).

Lipid analysis

Total lipids were extracted as described in Chapter II-I (Bligh and Dyer, 1959). Lipids were separated by two-dimensional TLC using the following solvent systems: chloroform/methanol/7 M ammonia (15:10:1, v/v/v) for the first dimension and chloroform/methanol/acetic acid/water (170:20:17:3, v/v/v/v) for the second dimension. Fatty acid detection and measurement of membrane lipid content were performed as described (Kobayashi et al., 2006).

Contents of chlorophyll and carotenoids

Pigments were extracted with 100% methanol from freeze-dried *Synechocystis* cells. Contents of chlorophyll and carotenoids were calculated as described (Grimme and Boardman, 1972, Lichtenthaler and Wellburn, 1983).

Microscopy analysis

The cells were collected by centrifugation and dropped on a copper grid. These samples were frozen rapidly in liquid propane using Leica rapid-freezing device (Leica EM CPC system). Then, these samples freeze-substituted in 1% osmium/acetone (3 days at -80°C, 4 h at -20°C, slow thaw to room temperature) were rinsed in acetone and slowly infiltrated with and polymerized in epoxy resin mixture (Quetol 651 mixture, Nissin EM). Embedded samples were cut into serial 75 nm thick sections with Leica Ultracut UCT Ultramicrotome (Leica Microsystems) and collected on formvar-coated copper grids. After staining with aqueous uranyl acetate and lead citrate, these sections were observed with a transmission electron microscopy (TEM) (H-7500, Hitachi) at an accelerating voltage of 80kV.

References

Aoki, M., Sato, N., Meguro, A., and Tsuzuki, M. 2004, Differing involvement of sulfoquinovosyl diacylglycerol in photosystem II in two species of unicellular cyanobacteria, *Eur. J. Biochem.*, 271, 685-693.

Awai, K., Kakimoto, T., Awai, C., Kaneko, T., Nakamura, Y., Takamiya, K., Wada, H., and Ohta, H. 2006, Comparative genomic analysis revealed a gene for monoglucosyldiacylglycerol synthase, an enzyme for photosynthetic membrane lipid synthesis in cyanobacteria, *Plant Physiol.*, 141, 1120–1127.

Awai, K., Watanabe, H., Benning, C., Nishida, I. 2007, Digalactosyldiacylglycerol is required for better photosynthetic growth of *Synechocystis* sp. PCC6803 under phosphate limitation, *Plant Cell Physiol.*, 48, 1517-1523.

Balogi, Z., Török, Z., Balogh, G., Jósvey, K., Shigapova, N., Vierling, E., Vígh, L., and Horváth, I. 2005, Heat shock lipid” in cyanobacteria during heat/light-acclimation, *Arch. Biochem. Biophys.*, 436, 346–354.

Barber, J., Ford, R.C., Mitchell, R.A.C., Millner, P.A. 1984, Chloroplast thylakoid membrane

fluidity and its sensitivity to temperature, *Planta*, 161, 375-380.

Bligh, E.G., and Dyer, W.J. 1959, A rapid method of total lipid extraction and purification, *Can. J. Biochem. Physiol.*, 37, 911–917.

Carratù, L., Franceschelli, S., Pardini, C. L., Kobayashi, G. S., Horvath, I., Vigh, L., and Maresca, B. 1996, Membrane lipid perturbation modifies the set point of the temperature of heat shock response in yeast, *Proc. Natl. Acad. Sci. U. S. A.*, 93, 3870–3875.

Grimme, L.H. and Boardman, N.K. 1972, Photochemical activities of a particle fraction P 1 obtained from the green alga *Chlorella fusca*, *Biochem. Biophys. Res. Commun.*, 49, 1617-1623.

Güler, S., Seeliger, A., Härtel, H., Renger, G., and Benning, C. 1996, A null mutant of *Synechococcus* sp. PCC7942 deficient in the sulfolipid sulfoquinovosyl diacylglycerol, *J. Biol. Chem.*, 271, 7501-7507.

Herdman, M., Janvier, M., Rippka, R., and Stanier, R.Y. 1979, Genome size of cyanobacteria, *J. Gen. Microbiol.*, 111, 73–85.

Horváth, I., Glatz, A., Varvasovszki, V., Török, Z., Páli, T., Balogh, G., Kovács, E., Nádasdi, L., Benkő, S., Joó, F., Vígh, L. 1998, Membrane physical state controls the signaling mechanism of the heat shock response in *Synechocystis* PCC 6803: identification of hsp17 as a "fluidity gene", *Proc. Natl. Acad. Sci.*, 95, 3513–3518.

Kelly, A.A. and Dörmann, P. 2002, DGD2, an *Arabidopsis* gene encoding a UDP-galactose-dependent digalactosyldiacylglycerol synthase is expressed during growth under phosphate-limiting conditions, *J. Biol. Chem.*, 277, 1166-1173.

Kelly, A.A., Froehlich, J.E., and Dörmann, P. 2003, Disruption of the two digalactosyldiacylglycerol synthase genes DGD1 and DGD2 in *Arabidopsis* reveals the existence of an additional enzyme of galactolipid synthesis, *Plant Cell*, 15, 2694-2706.

Kim, E.J., Kim, J.S., Rhee, H.J., and Lee, J.K. 2009, Growth arrest of *Synechocystis* sp. PCC6803 by superoxide generated from heterologously expressed *Rhodobacter sphaeroides* chlorophyllide a reductase, *FEBS Lett.*, 583:219-223.

Kobayashi, K., Kondo, M., Fukuda, H., Nishimura, M., and Ohta, H. 2007, Galactolipid

synthesis in chloroplast inner envelope is essential for proper thylakoid biogenesis, photosynthesis, and embryogenesis, *Proc. Natl. Acad. Sci. U. S. A.*, 104, 17216–17221.

Kobayashi, K., Masuda, T., Takamiya, K., and Ohta, H. 2006, Membrane lipid alteration during phosphate starvation is regulated by phosphate signaling and auxin/cytokinin cross-talk, *Plant J.*, 47, 238–248.

Kondo, K., Ochiai, Y., Katayama, M., Ikeuchi, M. 2007, The membrane-associated CpcG2-phycobilisome in *Synechocystis*: a new photosystem I antenna, *Plant Physiol.*, 144, 1200-1210.

Lichtenthaler, H.K., Wellburn, A.R. 1983, Determinations of total carotenoids and chlorophylls *a* and *b* of leaf extracts in different solvents, *Biochem. Soc. Trans.*, 11, 591-592.

Masuda, S., Harada, J., Yokono, M., Yuzawa, Y., Shimojima, M., Murofushi, K., Tanaka, H.,

Masuda, H., Murakawa, M., Haraguchi, T., Kondo, M., Nishimura, M., Yuasa, H., Noguchi,

M., Oh-Oka, H., Tanaka, A., Tamiaki, H., and Ohta, H. 2011, A

Monogalactosyldiacylglycerol Synthase Found in the Green Sulfur Bacterium

Chlorobaculum tepidum Reveals Important Roles for Galactolipids in Photosynthesis, *Plant*

Cell, 23, 2644-2658.

Mironov, K.S., Sidorov, R.A., Trofimova, M.S., Bedbenov, V.S., Tsydendambaev, V.D., Allakhverdiev, S.I., Los, D.A. 2011, Light-dependent cold-induced fatty acid unsaturation, changes in membrane fluidity, and alterations in gene expression in *Synechocystis*, *Biochim. Biophys. Acta.*, 27, Epub ahead of print.

Ng, W.O., Zentella, R., Wang, Y., Taylor, J.S., Pakrasi, H.B. 2000, *phrA*, the major photoreactivating factor in the cyanobacterium *Synechocystis* sp. strain PCC 6803 codes for a cyclobutane-pyrimidine-dimer-specific DNA photolyase. *Arch. Microbiol.*, 173, 412-417.

Róg, T., Vattulainen, I., Bunker, A., and Karttunen, M. 2007, Glycolipid membranes through atomistic simulations: effect of glucose and galactose head groups on lipid bilayer properties, *J. Phys. Chem. B.*, 111, 10146-10154.

Sakurai, I., Mizusawa, N., Wada, H., and Sato, N. 2007, Digalactosyldiacylglycerol is required for stabilization of the oxygen-evolving complex in photosystem II, *Plant Physiol.*, 145, 1361-1370.

Sato, N. 1994, Effect of exogenous glucose on the accumulation of monoglucosyldiacylglycerol in the cyanobacterium *Synechocystis* PCC 6803, *Plant Physiol. Biochem.*, 32, 121–126.

Sato, N., and Murata, N. 1982a, Lipid biosynthesis in the blue-green alga *Anabaena variabilis* II. Fatty acid and lipid molecular species. *Biochim. Biophys. Acta.*, 710, 271-278.

Sato, N., and Murata, N. 1982b, Lipid biosynthesis in the blue-green alga *Anabaena variabilis* II. Fatty acid and lipid molecular species. *Biochim. Biophys. Acta.*, 710, 279-289.

Sato, N., Murata, N., Miura, Y., and Ueta, N. 1979, Effect of growth temperature on lipid and fatty acid compositions in the blue-green algae, *Anabaena variabilis* and *Anacystis nidulans*. *Biochim. Biophys. Acta.*, 572, 19-28.

Sato, N., and Wada, H. 2009, Lipid Biosynthesis and its Regulation in Cyanobacteria, In *Lipids in Photosynthesis: Essential and Regulatory Functions, Advances in Photosynthesis and Respiration, Vol 30*. Springer, Dordrecht, pp. 157–177.

Schlame, M., Horvath, I., Török, Z., Horvath, L.I., and Vigh, L. 1990, Intramembraneous hydrogenation of mitochondrial lipids reduces the substrate availability, but not the enzyme

activity of endogenous phospholipase A. The role of polyunsaturated phospholipid species, *Biochim. Biophys. Acta.*, 1045, 1-8.

Sheng, J., Kim, H.W., Badalamenti, J.P., Zhou, C., Sridharakrishnan, S., Krajmalnik-Brown, R., Rittmann, B.E., and Vannela, R. 2011, Effects of temperature shifts on growth rate and lipid characteristics of *Synechocystis* sp. PCC6803 in a bench-top photobioreactor, *Bioresour. Technol.*, 102, 11218-11225.

Shimajima, M., Tsuchiya, M., and Ohta, H. 2009, Temperature-dependent hyper-activation of monoglucosyldiacylglycerol synthase is post-translationally regulated in *Synechocystis* sp. PCC 6803, *FEBS Lett.*, 583, 2372-2376.

Sonoike, K., Hihara, Y., and Ikeuchi, M. 2001, Physiological significance of the regulation of photosystem stoichiometry upon high light acclimation of *Synechocystis* sp. PCC 6803, *Plant Cell Physiol.*, 42, 379-384.

Suzuki, I., Kanasaki, Y., Mikami, K., Kanehisa, M., and Murata, N. 2001, Cold-regulated genes under control of the cold sensor Hik33 in *Synechocystis*, *Mol. Microbiol.*, 40, 235-244.

Tajima, N., Sato, S., Maruyama, F., Kaneko, T., Sasaki, N.V., Kurokawa, K., Ohta, H., Kanesaki, Y., Yoshikawa, H., Tabata, S., Ikeuchi, M., Sato, N. 2011, Genomic structure of the cyanobacterium *Synechocystis* sp. PCC 6803 strain GT-S. *DNA Res.*, 18, 393-399.

Tasaka, Y., Gombos, Z., Nishiyama, Y., Mohanty, P., Ohba, T., Ohki, K., and Murata, N. 1996, Targeted mutagenesis of acyl-lipid desaturases in *Synechocystis*: evidence for the important roles of polyunsaturated membrane lipids in growth, respiration and photosynthesis, *EMBO J.*, 15, 6416-6425.

Vigh, L., Maresca, B., and Harwood, J.L. 1998, Does the membrane's physical state control the expression of heat shock and other genes? *Trends. Biol. Sci.*, 23, 369-374.

Wada, H. and Murata, N. 1990, Temperature-Induced Changes in the Fatty Acid Composition of the Cyanobacterium, *Synechocystis* PCC6803, *Plant Physiol.*, 92, 1062-1069.

Williams, J.G.K. 1988, Construction of specific mutations in photosystem II photosynthetic reaction center by genetic engineering methods in *Synechocystis* 6803. *Methods Enzymol.*, 167, 766-78.

Yamaryo, Y., Kanai, D., Awai, K., Shimojima, M., Masuda, T., Shimada, H., Takamiya, K.,

Ohta, H. 2003, Light and cytokinin play a co-operative role in MGDG synthesis in greening

cucumber cotyledons. *Plant Cell Physiol.*, 44, 844-855.

Chapter IV

General Conclusion

In Chapter II, based on phylogenetic and enzymatic analyses, I proposed the evolutionary model of MGD (Fig. II-11). Although no cyanobacteria analyzed possessed the ancestral type of higher plant MGDs, I identified the possible MGD ancestor from *Chloroflexi*. The results suggest that higher plant MGD was originated from this type of *Chloroflexi* MGD.

Eukaryotic MGD may be acquired from ancient *Chloroflexi* via horizontal gene transfer in parallel with the major endosymbiotic event and contributed to the early plastid evolution.

After the acquirement, MGD duplication and functional differentiation of 2 types of MGD, type A and B, occurred along with land plant evolution. This functional differentiation probably had important meanings in further prosperity of seed plants. It is universally accepted that an ancestral cyanobacterium is the origin of the plastid organelle; however, plastid evolution is still heavily debated. These disagreements can be attributed to a very complex process that involved both horizontal and intracellular gene transfer during the course of prokaryotic and eukaryotic evolution (Raymond et al., 2002, Keeling and Palmer, 2008). To generate a more accurate picture of photosynthesis evolution, we believe that focused comprehensive analyses of specific physiological processes are just as important as

more global gene sequence comparisons. In particular, galactolipids are highly enriched in photosynthetic membranes, and deciphering the evolution of galactolipid synthesis pathways provides critical information toward understanding the early evolution of photosynthesis.

In Chapter II-II, I presented the divergence time of type A/B MGDs. Although 2 types of MGDs were only found in *Angiosperm*, type B MGD was found in a gymnosperm. Based on the phylogenetic tree, I estimated a MGD type A/B divergence time is likely diverged ~323 MYA. This divergence time corresponds to the Carboniferous period, which came after *Spermatophyta* appeared (355–370 MYA). I propose, therefore, that the acquisition of 2 types of MGDs occurred in the common ancestor of *Spermatophyta*. In conclusion, based on phylogenetic and enzymatic analyses, I proposed the evolutionary model of MGDs (Fig. II-11) in Chapter II.

In Chapter III, I presented physiological functions of MGlCDG by complementation with plant and bacterial MGDs in *Synechocystis* sp. PCC 6803 (Fig. III-16). MGlCDG deficient mutants demonstrate that MGlCDG is not essential for growth and photosynthesis in *Synechocystis* under normal conditions with supply of MGDG. Indeed, complemented mutant by *AtMGDI* have healthy thylakoid membranes and moderate pigment content, although I observed slightly swelled membranes. My data indicate that MGlCDG has important roles under stress conditions. Membrane lipids of cells were exposed to various environmental stresses. Proteins, such as Hik33 (Suzuki et al., 2001) may sense these stresses, which are

embedded in their membranes. Modification of membrane lipids and fatty acid compositions affects the activity of these membrane associated proteins. Although involvement of MGlcDG in heat-shock response was reported (Balogi et al., 2005), MGlcDG deficient mutant was acquired thermal stability which is induced by heat-shock treatment. In case of photosynthetic activity, I conclude that the thermal stability was induced MGlcDG independently. Instead, the growth of MGlcDG deficient mutant was inhibited under low temperature, suggesting that MGlcDG is involved in adaptation to cold stress. MGlcDG deficient mutants showed some notable phenomena. First, in galactolipids, 16:0 and 16:1 fatty acids were increased. Substrate preferences of AtMGD1 and CtMgdA may cause this phenomenon, suggesting that distribution of DAG molecular species between galactolipids and SQDG was modulated by substrate preferences of MGlcDG and SQDG synthases. In low temperature adaptation, polydesaturation of fatty acids in MGDG is important in *Synechocystis*. However, since 16:X/16:X molecular species of MGDG are hardly desaturated, imbalance of DAG supply for subsequent lipid biosynthesis may affect adaptation for cold stress. Second, although growth of MGlcDG deficient mutant was delayed, the delay disappeared late logarithmic growth phase, suggesting that MGlcDG may contribute to primary sensor for rapid cold adaptation. Hik33 is well known as cold stress sensor and regulate gene expression for cold adaptation. However, there are low temperature-inducible genes, including fatty acid desaturases, unaffected by Hik33 (Suzuki et

al., 2001, Zorina et al., 2011). Other pathways sensing cold stress in *Synechocystis* has not yet been clarified.

In summary, according to the results obtained from this study, I illustrated two proposed model for plant and cyanobacterial MGDG synthesis pathways (Fig. II-11 and III-15). These data demonstrated that plant-type MGDG synthesis pathway exists in photosynthetic bacteria. Moreover, the type of MGD is possibly ancestor of the plant-type MGDs. In *Synechocystis*, I demonstrated that this plant-type MGDG synthesis pathway is functional. Resent report about complementation of plant-type MGD with green sulfur bacterial MGD also supports this plant-type MGD has similar function (Masuda et al., 2011). In this study, I focused on MGDG biosynthesis. Further analysis in other glycolipid and phospholipid synthases will be needed to obtain more detail information about the evolution of phototrophs, in particular, focusing on glycolipids which are important photosynthetic membranes. Moreover, physiological functions of MGDG synthesis pathway in each organism, such as MGlcDG, are really important to understand dynamic state for adaptation to different environmental conditions.

References

- Balogi, Z., Török, Z., Balogh, G., Jós vay, K., Shigapova, N., Vierling, E., Vígh, L., and Horváth, I. 2005, Heat shock lipid” in cyanobacteria during heat/light-acclimation, *Arch. Biochem. Biophys.*, 436, 346–354.
- Keeling, P.J., and Palmer, J.D. 2008, Horizontal gene transfer in eukaryotic evolution, *Nat. Rev. Genet.*, 9, 605–618.
- Masuda, S., Harada, J., Yokono, M., Yuzawa, Y., Shimojima, M., Murofushi, K., Tanaka, H., Masuda, H., Murakawa, M., Haraguchi, T., Kondo, M., Nishimura, M., Yuasa, H., Noguchi, M., Oh-Oka, H., Tanaka, A., Tamiaki, H., and Ohta, H. 2011, A Monogalactosyldiacylglycerol Synthase Found in the Green Sulfur Bacterium *Chlorobaculum tepidum* Reveals Important Roles for Galactolipids in Photosynthesis, *Plant Cell*, 23, 2644-2658
- Raymond, J., Zhaxybayeva, O., Gogarten, J.P., Gerdes, S.Y., and Blankenship, R.E. 2002, Whole-genome analysis of photosynthetic prokaryotes, *Science*, 298, 1616–1620.
- Suzuki, I., Kanasaki, Y., Mikami, K., Kanehisa, M., and Murata, N. 2001, Cold-regulated

genes under control of the cold sensor Hik33 in *Synechocystis*, *Mol. Microbiol.*, 40, 235-244.

Zorina, A. A., Mironov, K. S., Stepanchenko, N. S., Sinetova, M. A., Koroban, N. V.,

Zinchenko, V. V., Kupriyanova, E. V., Allakhverdiev, S. I., and Los, D. A.. 2011, Regulation

systems for stress responses in cyanobacteria, *Russian Journal of Plant Physiology*, 58,

749-767.

Acknowledgments

I greatly appreciate Professor Hiroyuki Ohta, Tokyo Institute of Technology, for his invaluable guidance and support in carrying out this study and through my campus life here. I always feel great respect for him.

I deeply appreciate Professor Norihiro Okada, Tokyo Institute of Technology. He and Prof. Ohta gave me the opportunity to start this study in Tokyo Institute of Technology.

I would like to thank Associate professor Shinji Masuda, Tokyo Institute of Technology. I was always helped by his great technical advice and objective suggestion. He showed me his attitude and mind as a scientist.

I am very grateful to Assistant professor Mie Shimojima, Tokyo Institute of Technology, for her kind guidance and encouragement. Especially, I learned the skill and knowledge about lipid analysis from her.

I also express my acknowledgment to Assistant professor Hidenori Nishihara, Tokyo Institute of Technology. I am grateful for his warm support and kind advice while I performed this study.

I would like to thank my colleague during my master course, Mr. Hironori Tanaka. For his hospitality, I could quickly adapt myself to my new life in graduate school. I always felt stimulated by his thinking-method when we discussed about our study.

During my master course, I went overseas education in Professor Peter Dörmann's

laboratory, University of Bonn in Germany. I give special thanks to him and the members of his laboratory for their heartwarming hospitality. I gave amazing experience at work and in my private with them.

I am thankful to Dr. Robert P. Olinski, who was a member of Prof. Okada's laboratory, for constructing an aligned dataset of MGDG synthases, Professor Keizo Shimada, Tokyo Metropolitan University, for help with the *R. castenholzii*, Mr. Tsuyoshi Haraguchi, who was a graduate school student of Tokyo Institute of Technology, for help on NMR analysis, Associate professor Naoki Mizusawa, Hosei University, for kind advice about measuring oxygen-evolving activity, and Ms. Keiko Yamamichi, Tokyo Institute of Technology, for help on TEM observation.

I am also grateful to the members of my laboratory at Tokyo Institute of Technology for helpful encouragement, warm atmosphere and memorable time. They really helped me to develop as a scientist.

In the end, I want to tell my family my deepest appreciation for all their help.